Special Report 87-9

June 1987

DTIC FILE COPY

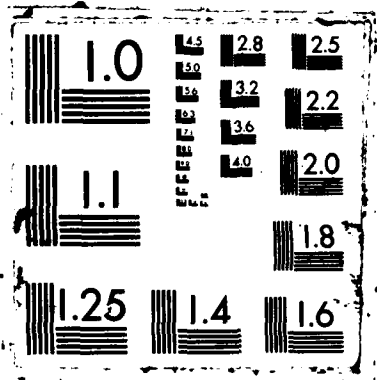**US Army Corps
of Engineers**
Cold Regions Research &
Engineering Laboratory

A nodal domain integration model of two-dimensional heat and soil-water flow coupled by soil-water phase change

Ted Hromadka

DTIC
SELECTED
AUG 1 2 1987
E

87 8 11 011

AD-A183 518

REPORT DOCUMENTATION PAGE

Form Approved
OMB No 0704-0188
Exp Date Jun 30, 1986

1a. REPORT SECURITY CLASSIFICATION	1b. RESTRICTIVE MARKINGS
Unclassified	

2a. SECURITY CLASSIFICATION AUTHORITY	3. DISTRIBUTION/AVAILABILITY OF REPORT
	Approved for public release;
2b. DECLASSIFICATION/DOWNGRADING SCHEDULE	distribution isunlimited.

4. PERFORMING ORGANIZATION REPORT NUMBER(S)	5. MONITORING ORGANIZATION REPORT NUMBER(S)
	Special Report 87-9

6a. NAME OF PERFORMING ORGANIZATION	6b. OFFICE SYMBOL (If applicable)	7a. NAME OF MONITORING ORGANIZATION
Williamson and Schmid		U.S. Army Cold Regions Research and Engineering laboratory

6c. ADDRESS (City, State, and ZIP Code)	7b. ADDRESS (City, State, and ZIP Code)
Irvine, California 92714	Hanover, New Hampshire 03755-1290

8a. NAME OF FUNDING/SPONSORING ORGANIZATION	8b. OFFICE SYMBOL (If applicable)	9. PROCUREMENT INSTRUMENT IDENTIFICATION NUMBER
		P.O. 84-M-1691

8c. ADDRESS (City, State, and ZIP Code)	10. SOURCE OF FUNDING NUMBERS			
	PROGRAM ELEMENT NO.	PROJECT NO	TASK NO	WORK UNIT ACCESSION NO
				CWIS 31711

11. TITLE (Include Security Classification)
A Nodal Domain Integration Model of Two-dimensional Heat and Soil-Water Flow
Coupled by Soil-Water Phase Change

12. PERSONAL AUTHOR(S)
Ted Hromadka

13a. TYPE OF REPORT	13b. TIME COVERED FROM _____ TO _____	14. DATE OF REPORT (Year, Month, Day) June 1987	15. PAGE COUNT 129

16. SUPPLEMENTARY NOTATION

17. COSATI CODES			18. SUBJECT TERMS (Continue on reverse if necessary and identify by block number)
FIELD	GROUP	SUB-GROUP	Computer models Soils
			Frozen soils Soil water
			Heat flux Water

19. ABSTRACT (Continue on reverse if necessary and identify by block number)
A model of phase change in freezing and thawing soils is developed for cold regions engineering problems which require two-dimensional analysis of the thermal regime of soils. These problems include complex boundary conditions such as atmosphere/ground surface thermal interaction and snowpack insulation. Other concerns include complex soil conditions such as the presence of a peaty muskeg or tundra-like soil which may provide thermal insulation for underlying muskeg or tundra-like soil which may provide thermal insulation for underlying ice-rich mineral soil. Although several models have been developed to predict temperatures in freezing and thawing soils, often the key question is simply whether or not the soil is frozen, since soil structural properties are significantly influenced by the soil-water state of phase. In this report, a simple two-dimensional model is developed for use in cold regions engineering studies. A FORTRAN computer program is available which accommodates two-dimensional heat and soil-water flow models as coupled by an isothermal phase change model. The program can be used to analyze two-dimensional freezing-thawing problems which have sufficient known information to supply the necessary modeling parameters, boundary conditions, and initial conditions. Because of the sophistication of the two-dimensional phase change model and the data requirements needed to properly represent inhomogeneity,

20 DISTRIBUTION/AVAILABILITY OF ABSTRACT	21. ABSTRACT SECURITY CLASSIFICATION
☒ UNCLASSIFIED/UNLIMITED ☐ SAME AS RPT ☐ DTIC USERS	Unclassified

22a. NAME OF RESPONSIBLE INDIVIDUAL	22b. TELEPHONE (Include Area Code)	22c. OFFICE SYMBOL
Richard Berg	603-646-4335	CECRL-EE

DD FORM 1473, 84 MAR

83 APR edition may be used until exhausted
All other editions are obsolete

19. Abstract (cont'd)

of the system, boundary conditions, and other complexities, a special data input program is developed in order to aid the model user. This general purpose data preparation program, PROTO∅, develops the data input file to be used directly by the two-dimensional phase change program.

Keywords: soil mechanics

PREFACE

This report was prepared by Ted Hromadka, Director of Water Resources, Williamson and Schmid. The work was performed for CRREL under Contract 84-M-1691 and was funded by the Directorate of Civil Works, Office of the Chief of Engineers, under Civil Works Order No. CWIS 31711, Time Rate and Magnitude of Degradation of Permafrost.

Critical reviews of the report were furnished by Dr. Richard Berg and Francis Sayles, the project monitor.

The contents of this report are not to be used for advertising or promotional purposes. Citation of brand names does not constitute an official endorsement or approval of the use of such commercial products.

Accession For

NTIS GRA&I

DTIC TAB

Unannounced

Justification

By

Distribution/

Availability Codes

Dist   and/or Special

A-1

DTIC COPY INSPECTED

TABLE OF CONTENTS

LIST OF FIGURES

1. INTRODUCTION

1.0 OBJECTIVES OF REPORT

The main objectives of this report are:

(1) provide the theoretical and modeling background used in a two-dimensional model of heat and soil-water flow, coupled by soil-water freezing and thawing (FROST2X series).

(2) present the major modeling assumptions used in the computer program, and the various components of the program in order to aid the user in the use of the model.

(3) present the necessary parameters and data requirements used in the computer model.

(4) discuss the computer model output product, and methods to interpret the results.

(5) present the data input sequence to the computer model.

1.1 REPORT ORGANIZATION

This report is organized into five chapters and one appendix.

CHAPTER 1. Provides an introduction to the report.

CHAPTER 2. Develops the Nodal Domain Integration (NDI) model of two-dimensional soil-water flow in saturated and unsaturated soils.

CHAPTER 3. Develops the NDI model for heat flow in three dimensions. The third dimension is included in this NDI development (an NDI analog for radial coordinates is presented in Appendix A) in order to provide for the extension of the phase change model to other coordinate systems.

CHAPTER 4. Develops the two-dimensional soil-water phase change model used to couple the heat and soil-water flow during soil-water freezing and thawing.

CHAPTER 5. Presents a summary of the two-dimensional freezing/thawing model and the modeling input-output characteristics. Provides documentation to the computer program input requirements.

APPENDIX Expands upon the heat flow modeling approach developed in chapter 3 to radial coordinates. The theory developed in the appendix applies to both heat and soil-water flow in the selection of mass-lumping factors for use in NDI domain models.

1.2 COMPUTER PROGRAM SOURCE CODE

This report presents documentation for the FROST2B version of the FROST2X series of two-dimensional phase change models. Also provided in this report is the documentation for the program PROTO∅ which provides a user-friendly data input capability for subsequent use by program FROST2B.

Both computer programs are written in FORTRAN IV and can be used on most mini-computer class computers.

Computer code for the FROST2B and PROTO∅ can be obtained from the U.S. Army Corps of Engineers, Cold Regions and Research Laboratory (CRREL).

1.3 REPORT AUTHORIZATION

This report was prepared under the direction of Dr. Richard L. Berg and Mr. Francis Sayles of CRREL, Hanover, New Hampshire.

2. UNIFIED NUMERICAL MODEL OF TWO-DIMENSIONAL SOIL-WATER FLOW

2.0 INTRODUCTION

Numeric approximation of two-dimensional non-linear partial differential equations such as occur in the theory of unsaturated ground water flow is generally limited to numeric solution by the finite difference or finite element methods. Finite difference approximations, such as described by Spalding (1972) for a specified control volume, can be determined for rectangular and also for irregular two-dimensional domains. Finite element methods, such as variational principle applications and weighted residuals, can also be applied to irregular two-dimensional domains. Both methods determine numerical algorithms which are often compared to each other for numerical "efficiency" or other descriptions of superiority (Hayhoe, 1978).

Recently, Hromadka and Guymon (1982a,b) have developed a new numerical approach called the nodal domain integration method which has been applied to one and two-dimensional linear and non-linear problems for irregular rectangular domains. From this numerical approach, the finite difference and finite element (Galerkin) methods are "unified" into a single numerical statement.

In this chapter the nodal domain integration method is applied to the two-dimensional triangular finite element. As special cases, the finite element and finite difference numerical analogs are determined by the appropriate specification of a single parameter in the resulting nodal domain integration numerical statement. Thus, all three numerical approaches are unified by one numerical statement similar to the usual finite element matrix system.

The purpose of this effort is two-fold. The first objective is to present a basic description of the nodal domain integration procedure as applied to the class of partial differential equations generally encountered in the

theory of unsaturated groundwater flow. Detailed mathematical derivations of this numerical approach are contained in the literature (Hromadka and Guymon, 1980a,b,c) and will not be repeated here. The theoretical foundations of this numerical method are based on the well-known subdomain technique of the finite element weighted residuals approach.

The second objective is to present a unified numerical statement which represents the finite element Galerkin statement, finite difference integrated control volume statement, and the nodal domain integration statement (for a linear shape function distribution of the state variable) by the specification of a single constant parameter in the resulting triangle element matrix system.

A secondary objective is to briefly discuss the application of the nodal domain integration triangle element statement to reducing computer memory requirements by the technique of approximating a higher order or more complex family of triangle (or global) shape functions by a linear shape function approximation. A detailed mathematical description of this linear shape function approximation technique is given for the one-dimensional case in a previous work (Hromadka and Guymon, 1982a and will not be repeated here.

The main purpose of this chapter is to develop a generalized unified triangle element matrix system which can be used in computer programming efforts. Consequently, a single computer program can be developed which essentially represents the finite difference, finite element (Galerkin), and nodal domain integration numerical approaches. This work does not recommend one numerical approach, (although for the problems tested, the nodal domain integration scheme produced better levels of accuracy, i.e. Hromadka and Guymon, 1980a-c, and generalizes the numerical expressions so that the extension to the three-dimensional case can be made by appropriate integration of the resulting expressions in the third dimension (see Chapter 3).

4

2.1 GOVERNING EQUATIONS

Two-dimensional unsaturated Darcian soil-water flow in a nondeformable soil matrix Ω may be described by the partial differential equation

$$\frac{\partial}{\partial x}(K_x \frac{\partial \phi}{\partial x}) + \frac{\partial}{\partial y}(K_y \frac{\partial \phi}{\partial y}) = \frac{\partial \theta}{\partial t}, \quad (x,y)\epsilon\Omega \tag{1}$$

where (K_x, K_y) are anisotropic hydraulic conductivity values in the (x,y) directions, respectively; ϕ is the total hydraulic energy head ($\phi = \psi + y$); ψ is the soil-water pore pressure head; and θ is the volumetric water content. In (1), water content is assumed to be functionally related to soil-water pore pressure according to the usual soil drying curve, with hysterisis effects neglected. Thus,

$$\theta = \begin{cases} \theta(\psi), & \psi < 0 \\ \theta_o, & \psi \geq 0 \end{cases} \tag{2}$$

where θ_o is the soil porosity, assumed constant.

Guymon and Luthin (1974) define a volumetric water content to pore pressure gradient by

$$\theta^* = \begin{cases} \frac{\partial \theta}{\partial \psi}, & \psi < 0 \\ 0, & \psi \geq 0 \end{cases} \tag{3}$$

Therefore, (1) may be rewritten as

$$\frac{\partial}{\partial x} [K_x \frac{\partial \phi}{\partial x}] + \frac{\partial}{\partial y} [K_y \frac{\partial \phi}{\partial y}] = \theta^* \frac{\partial \phi}{\partial t}; \quad (x,y)\epsilon\Omega \tag{4}$$

5

For ease of presentation, the soil matrix Ω is assumed homogeneous and isotropic with hydraulic conductivity K_h. Therefore, (4) is simplified for discussion purpose as

$$\frac{\partial}{\partial x} [K_h \frac{\partial \phi}{\partial x}] + \frac{\partial}{\partial y} [K_h \frac{\partial \phi}{\partial y}] = \theta^* \frac{\partial \phi}{\partial t} \quad (x,y) \epsilon \Omega \tag{5}$$

2.2 NUMERICAL SOLUTION

The class of partial differential equations including (5) can be described by an operator relation

$$A(\phi) = 0; \quad (x,y) \epsilon \Omega \tag{6}$$

where $A(\phi)$ is the mathematical relation operating on the state variable, ϕ. The finite element method can be used to approximate (6) by the method of weighted residuals (Pinder and Gray, 1977).

$$\int\int_\Omega A(\hat{\phi}) w_i dx dy = 0 \quad (i = 1,2,\ldots,M) \tag{7}$$

where ϕ is approximated by a linear combination of suitable functions, $\hat{\phi}$, defined by

$$\hat{\phi} = \sum_{j=1}^{M} a_j \phi_j \tag{8}$$

The subdomain version of weighted residuals uses the weighting functions

$$w_j = \begin{cases} 1, (x,y) \epsilon \ \Omega^e_j \\ 0, (x,y) \notin \Omega^e_j \end{cases} \tag{9}$$

where Ω is discretized into two-dimensional nodal domains Ω^e_j (with respect to finite element e)

$$\Omega = U\Omega^e_j \tag{10}$$

6

Thus, the subdomain method is simply an appropriate integration of the governing equations over each finite element.

The nodal domain integration method (Hromadka and Guymon, 1980a,b) is an application of the finite element subdomain approach over appropriately defined nodal domains. These nodal domains are partitions of the finite element such that the resulting nodal domain corresponds to the control volume configuration established by Spalding (1972). For a two-dimensional triangle finite element, the nodal domain partitions are established by the triangle medians as shown in Fig.2.1 allocating one-third of the triangle's area to each respective nodal domain. Detailed mathematical descriptions of the integration process for linear and nonlinear partial differential operators are given in Hromadka and Guymon (1980a,b,c). These derivations result in an expression

$$
\int_{k\Delta t}^{(k+1)\Delta t} \int_{\Omega_j^e(y)} \left\{ K_h(x,y) \frac{\partial \phi}{\partial x} \right\} \Bigg|_{\Gamma_j^e(x)} dydt + \int_{k\Delta t}^{(k+1)\Delta t} \int_{\Omega_j^e(x)} \left\{ K_h(x,y) \frac{\partial \phi}{\partial y} \right\} \Bigg|_{\Gamma_j^e(y)} dxdt
$$

(11)

$$
= \int_{k\Delta t}^{(k+1)\Delta t} \int\int_{\Omega_j^e} \theta^* \frac{\partial \phi}{\partial t} \, dxdydt
$$

where integrations are made on the assumed shape function spatial and temporal distributions of the state variable and nonlinear parameters.

This integration procedure substantially differs from the integrated finite difference control volume approach (Spalding, 1972) due to the finite difference approach assuming the state variable to be constant interior to each control volume (nodal domain) and due to the finite difference approach assuming flux terms as constant (spatially) along each side of the control

7
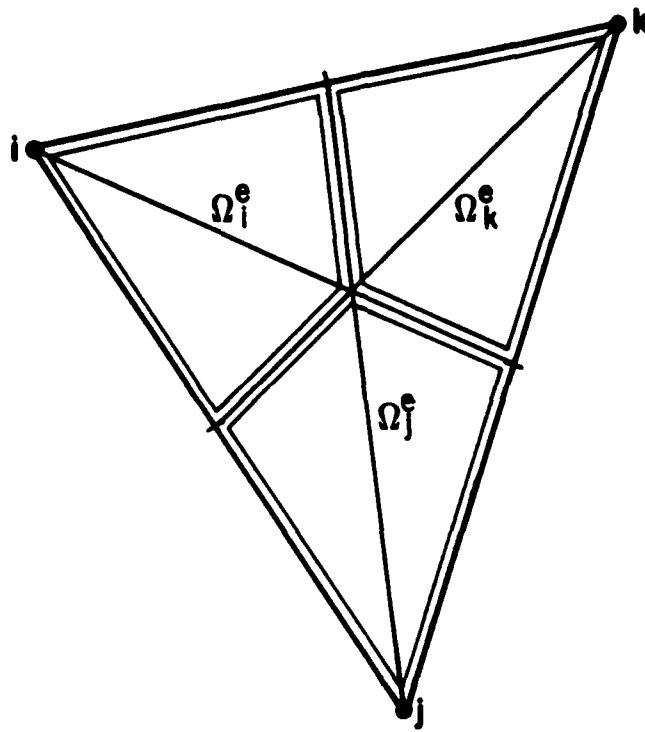
FIG. 2.I.   LINEAR SHAPE FUNCTION TRIANGULAR FINITE ELEMENT
PARTITIONED INTO NODAL DOMAIN CONTRIBUTIONS
BY MEDIANS
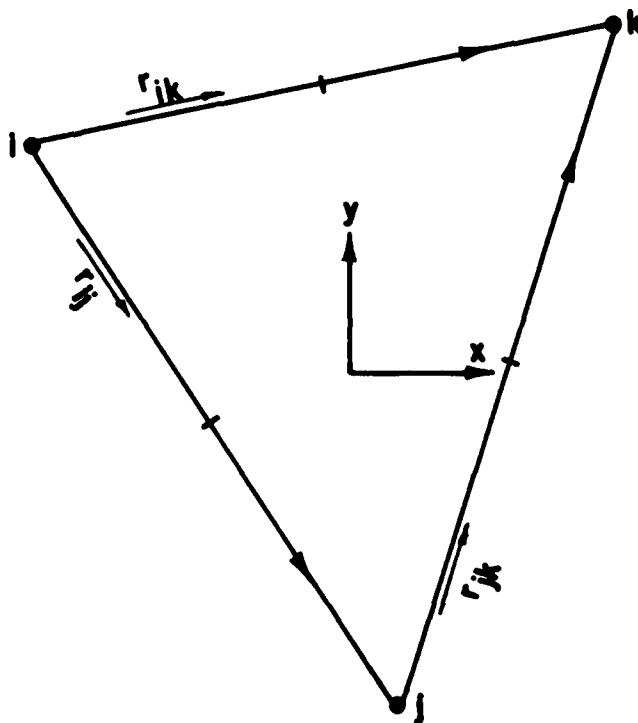
FIG. 2.2.   VECTOR DESCRIPTION OF TRIANGLE FINITE ELEMENT
GEOMETRY

volume rather than integrating the spatial variation of the flux terms as defined by the assumed shape function distribution of the state variable. Another major difference of the nodal domain integration method from the usual finite element and finite difference approaches is the use of the resulting linear shape function nodal domain integration numerical statement to approximate higher order or more complex families of shape functions without an increase of computer memory requirements associated to the use of such more complex families of shape functions (Hromadka and Guymon, 1981).

In order to evaluate the spatially integrated flux terms of (11) for each nodal domain partition of a triangular finite element, the triangle geometry is defined by a system of vectors as shown in Fig.2.2. For the assumed linear shape function variation of the state variable, ϕ, in the finite element triangle the spatially integrated flux term contribution to the triangle partition associated to nodal domain Ω_i^e is geometrically determined by Fig.2.3. From Fig.2.3 flux must contribute to Ω_i^e through the boundaries of Ω_i^e and can be calculated by the flux vector through state variable ϕ-values ϕ_i (at node i) and ϕ' as shown in the figure. Thus,

$$\phi' = \frac{1}{L} (\phi_j d_1 + \phi_k d_2) \qquad (12)$$

The integration of the spatial boundary of Ω_i^e normal to the considered flux vector is L/2 as shown in Fig.2.3. Thus, the efflux is geometrically determined to be (constant for linear shape function approximation)

$$- \frac{K_h \, [\phi_j (\frac{d_1}{L}) + \phi_k (\frac{d_2}{L}) - \phi_i]}{h} \qquad (13)$$

9
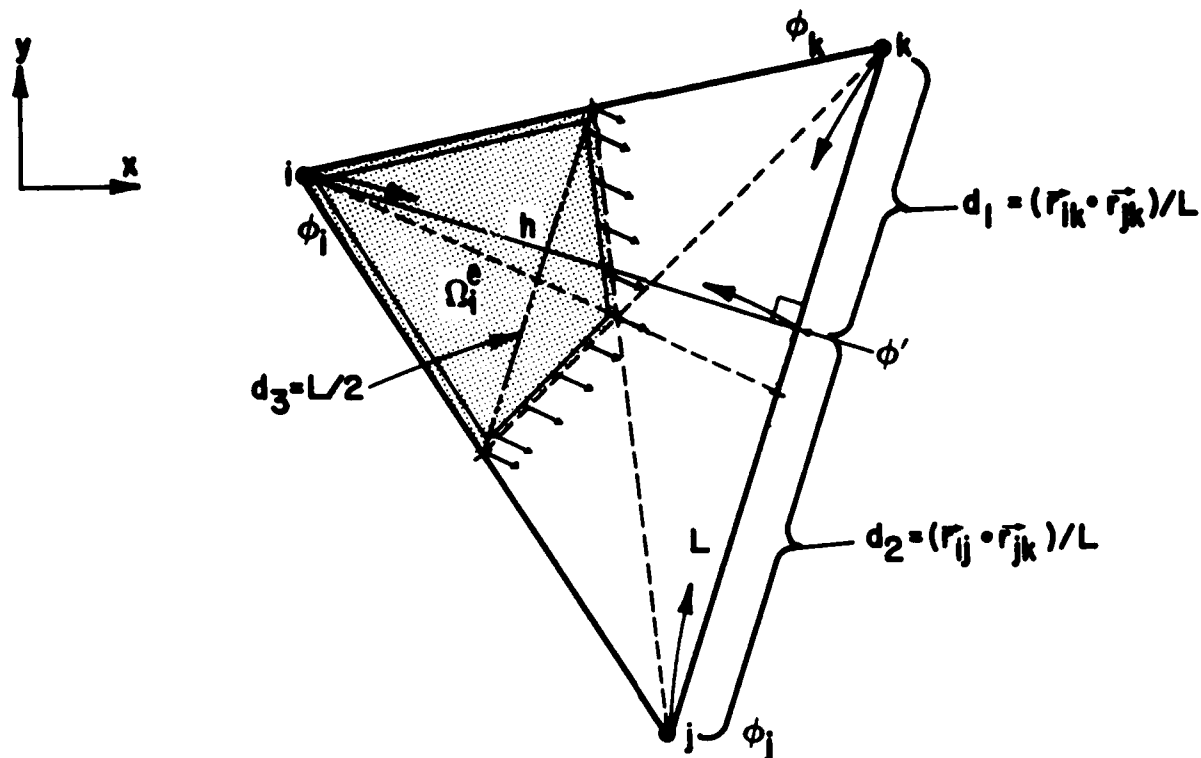
FIG. 2.3. GEOMETRIC SOLUTION OF FLUX DISTRIBUTION (FOR NODAL DOMAIN Ω_i^e) FOR ASSUMED LINEAR SHAPE FUNCTION DISTRIBUTION OF STATE VARIABLE
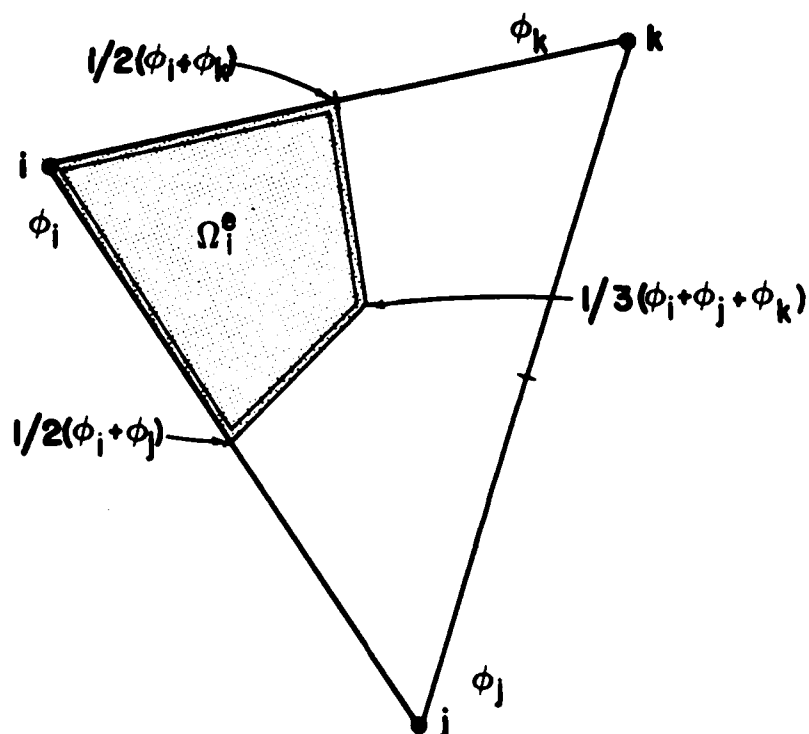
FIG. 2.4. LINEARLY DISTRIBUTED STATE VARIABLE VALUES IN NODAL DOMAIN PARTITION Ω_i^e

and the integrated efflux contribution for Ω_j^e is

$$- \frac{K_h}{2hL} [\phi_j d_1 L + \phi_k d_2 L - L^2 \phi_i] \tag{14}$$

where, from Fig. 2.3,

$$L^2 = \vec{r}_{jk} \cdot \vec{r}_{jk} = x_{jk}^2 + y_{jk}^2 \tag{15}$$

$$d_1 L = \vec{r}_{ik} \cdot \vec{r}_{jk} = x_{ik} x_{jk} + y_{ik} y_{jk} \tag{16}$$

$$d_2 L = \vec{r}_{ij} \cdot \vec{r}_{jk} = - (x_{ij} x_{jk} + y_{ij} y_{jk}) \tag{17}$$

and where $x_{jk} = x_k - x_j$. In vector notation, the integrated efflux contribution for nodal domain partition Ω_i^e of the triangle finite element (assumed linear shape function) is

$$\frac{K_h^{(e)}}{4A^{(e)}} [(x_{jk}^2 + y_{jk}^2) - (x_{ik} x_{jk} + y_{ik} y_{jk})(x_{ij} x_{jk} + y_{ij} y_{jk})] \begin{Bmatrix} \phi_i \\ \phi_j \\ \phi_k \end{Bmatrix} \tag{18}$$

where in (18) $A^{(e)}$ is the area of the finite element triangle, and $K_h^{(e)}$ the uniform value of hydraulic conductivity assumed for a sufficiently small finite element triangle (Hromadka and Guymon, 1980a).

This net efflux contribution to the triangle partition of Ω_i is identical to an integrated finite difference control volume approach as outlined by Spalding. Additionally, the net efflux term of (18) is identical to the Galerkin-determined finite element triangle component of the net efflux for nodal point i (Pinder and Gray, 1977).

11

The above described geometric considerations can be applied for each nodal domain partition of the triangle resulting in an element conduction matrix identical to a Galerkin-determined element conduction matrix (linear shape function)

$$
\underset{\sim}{K}^{(e)} = \frac{K_h^{(e)}}{4A^{(e)}} \begin{bmatrix} (x_{jk}^2 + y_{jk}^2) - (x_{ik}x_{jk} + y_{ik}y_{jk}) & (x_{ij}x_{jk} + y_{ij}y_{jk}) \\ & x_{ik}^2 + y_{ik}^2 & -(x_{ij}x_{ik} + y_{ij}y_{ik}) \\ \text{(symmetric)} & & x_{ij}^2 + y_{ij}^2 \end{bmatrix} \quad (19)
$$

where (e) refers to properties of the finite element triangle element (e). The notation and representation of the element conduction matrix by (19) can be compared to the finite element analog given in Myers (1971).

The nodal domain integration method evaluates the integration of the state variable in the triangle partition for Ω_i^e as

$$
\iint\limits_{\Omega_i^e} \phi \, dxdy = \frac{A^{(e)}}{108} [22\phi_i + 7\phi_j + 7\phi_k] \quad (20)
$$

where (20) represents the integrated variation of a linearly distributed state variable in Ω_i^e, (Fig. 2.4.)

The integrated finite difference control volume contribution of the state variable integrated or Ω_i^e (as described by Spalding) would be

$$
\iint\limits_{\Omega_i^e} \phi \, dxdy = \frac{A}{3} [\phi_i] \quad (21)
$$

The Galerkin-approach finite element so-called capacitance contribution is given by (Myers, 1971)

$$
\frac{A^{(e)}}{12} [2\phi_i + \phi_j + \phi_k] \quad (22)
$$

In matrix notation, the nodal domain integration numerical analog is represented by the element capacitance matrix for $\theta^*(e)$ a uniform value of θ^* within a sufficiently small finite element triangle (e)

$$P_{(\eta)}^{(e)} = \frac{A^{(e)}\theta^*(e)}{3(\eta+2)} \begin{bmatrix} \eta & 1 & 1 \\ 1 & \eta & 1 \\ 1 & 1 & \eta \end{bmatrix} \tag{23}$$

where ($\eta = \frac{22}{7}$) corresponds to a linear shape function distribution of the state variable in the finite element triangle, and other values of η correspond to other shape function approximations as estimated by a linear shape function approximation (for example, the alternation theorem; Hromadka and Guymon, 1981).

From (21) and (22), the element matrix of (23) also represents the Galerkin-version of the finite element method as well as the finite difference analog for $\eta = (2,\infty)$, respectively. Thus, the various numerical approaches are "unified" by the nodal domain integration procedure where the finite element and finite difference approaches are given by a specified constant parameter, η.

The resulting nodal domain integration numerical approximation of (5) is given by the cumulative triangle element contributions

$$\underset{\sim}{K}^{(e)} \left\{ \begin{array}{c} \phi_i \\ \phi_j \\ \phi_k \end{array} \right\} + P_{(\eta)}^{(e)} \left\{ \begin{array}{c} \dot{\phi}_i \\ \dot{\phi}_j \\ \dot{\phi}_k \end{array} \right\} = 0 \tag{24}$$

where dots represent time derivatives of nodal point values of the state variable, ϕ, and $\eta = (2, \frac{22}{7}, \infty)$ correspond to a linear shape function numerical approximation by the Galerkin finite element, nodal domain integration, and finite difference methods, respectively.

From the above, the popular domain numerical methods of finite element and finite difference are unified into an overall numerical approach which is

13

a subset of the nodal domain integration approach. Consequently, a computer program based on a finite element approach may be modified into the unified approach of the nodal domain integration method.

Nodal domain integration numerical statements for irregular rectangular domains (and one-dimensional domains) are contained in other recent papers (Hromadka and Guymon, 1982a,b). Extension to three-dimensional problems is provided in Chapter 3. Additionally radial, cylindrical and spherical coordinate systems are considered in Appendix A.

2.3 CONCLUSIONS

The nodal domain integration numerical approach has been used to determine a numerical analog which incorporates the finite element (Galerkin) and integrated finite difference methods as special cases. The resulting numerical statements involve the same computational requirements as does the finite element procedure. Therefore, the nodal domain integration procedure unifies the finite element and finite difference approaches by a single numerical statement as a function of a single constant parameter. Thus, computer programs may be prepared based on the nodal domain integration procedure which inherently contains both the finite element (Galerkin) and finite difference techniques.

REFERENCES

1. Hayhoe, H. N., Study of Relative Efficiency of Finite Difference and Galerkin Techniques for Modeling Soil-Water Transfer, Water Resources Research, 14(1), 1978, 97-102.

2. Guymon, G. L., and J. N. Luthin, A Coupled Heat and Moisture Transport Model for Arctic Soils, Water Resources Research, 10(5), 1974, 995-1001.

3. Hromadka II, T. V., and G. L. Guymon, Some Effects in Linearizing the Unsaturated Soil-Moisture Transfer Diffusion Model, Water Resources Research, (16), 1980a, 643-650.

4. Hromadka II, T. V., and G. L. Guymon, Numerical Mass Balance for Soil-Moisture Transport Problems, Water Resources Research, (3), 1980b, 107.

5. Hromadka II, T. V., and G. L. Guymon, A Note on Time Integration of Soil-Water Diffusivity Problems, Advances in Water Resources, (3), 1980c, 181-186.

6. Hromadka II, T. V., and G. L. Guymon, Improved Linear Shape Function Model of Soil Moisture Transport, Water Resources Research, (3), 1981, 504-512.

7. Hromadka II, T. V., and G. L. Guymon, Nodal Domain Integration Model of One-Dimensional Advection-Diffusion, Advances in Water Resources, (5), 1982a, 9-16.

8. Hromadka II, T. V., and G. L. Guymon, A Note on Numerical Approximation of Advection-Diffusion Processes in Rectangular Domains, Advances in Water Resources, (5), 1982b, 56-60.

9. Myers, G. E., Analytical Methods in Conduction Heat Transfer, McGraw-Hill, New York, 1971.

10. Pinder, G. F., and W. G. Gray, Finite Element Simulation in Surface and Subsurface Hydrology, Academic Press, 1977.

3. UNIFIED MODEL OF THREE-DIMENSIONAL HEAT TRANSFER
3.0 INTRODUCTION

A two-dimensional integrated finite difference method is presented by
Patankar (1980). This triangle element model can be extended to a three-dimensional
tetrahedron element model, and both the two- and three-dimensional finite
element models can be compared in the solution of linear heat conduction problems.

First, the integrated finite difference method is applied to a three-dimensional
heat conduction process where the global domain is discretized into tetrahedra-
shaped finite elements. By integrating the governing partial differential
equations on subsets of the finite elements (nodal domains), an extension
of the integrated finite difference (Spalding, 1972) analog is developed.
By using the subdomain integration version of the method of weighted residuals,
another numerical analog is developed which is similar to the integrated
finite difference approach. Comparison of the integrated finite difference
and subdomain integration numerical analogs to one determined by the Galerkin
finite element method of the weighted residuals process indicates that all
three analogs determine similar finite element matrix systems which when com-
bined into a global matrix system satisfy both Dirichlet and Neumann
boundary conditions.

Hromadka and Guymon(1981a,b) have examined the finite difference, sub-
domain integration, and Galerkin finite element methods for solution of
partial differential equations in one- and two-dimensional problems. They
combine these numerical approaches into a single numerical statement which
can represent any of the considered numerical methods by the specification
of a single constant parameter, η, in the element matrix systems. Examinations
of model approximation error in comparison to analytical solutions for linear
heat and mass conduction problems indicate that the element matrix mass
lumping η must be variable between elements and with respect to time in

16

order to reduce approximation error. That is, to minimize numerical approximation error, the method of numerical solution generally must vary through the entire range of domain numerical techniques including the Galerkin finite element, subdomain integration, integrated finite difference, (control volume, or mass lumped finite element) and numerous versions of finite element mass-weighting schemes. Extensive computer simulations of one- and two-dimensional problems indicate that sometimes a single numerical analog will minimize the approximation error for only a particular region of the solution domain or only for a certain duration of the simulation, and that continued use of the particular numerical analog will produce approximation errors greater than errors generated by switching the method of numerical solution to another technique.

The reduction of the Galerkin finite element mass matrix into a diagonal mass lumped matrix is well known (Zienkiewicz,1977). However, it is important to note that the so-called mass lumped diagonal matrix is analogous to the integrated finite difference capacitance matrix as developed by Spalding (1972). An infinity of mass weightings of element nodal contributions can be determined directly by introducing an improved linear trial function in the finite element, where the element-boundary trial function continuity requirements are relaxed, and then using the usual subdomain integration version of the weighted residual process. The fact that certain mass lumping patterns may improve computational results (Ramadhyani and Patankar, 1980) indicates that a unified model may be developed which utilizes a variable mass matrix and yet can still represent the well known Galerkin, subdomain integration, and integrated finite difference analogs.

In this chapter, the general form of the three-dimensional nodal domain integration finite element matrix system will be developed. The resulting element matrix system will be shown to represent an extension of the integrated

17

finite difference method, subdomain integration version of the finite element method of weighted residuals, and the Galerkin finite element method by the specification of a single constant parameter. The finite element used is a three-dimensional tetrahedron with a linear trial function used to approximate the governing transport equation's state variable within each element. Although the main consideration of this work is towards diffusion processes, an advection component is included in the model development for generalization purposes.

The main objectives in this chapter are as follows:

(1) develop a three-dimensional integrated finite difference analog for a diffusion (or advection-diffusion process) using a tetrahedron finite element discretization. This objective is an extension of the two-dimensional triangle element analog recently presented by Baliga and Patankar (1980), and includes the development of a three-dimensional model and the representation of the model in finite element matrix form. An integrated finite difference approach is seen to result in a node-centered control volume analog or, as it is usually referred to in finite element models, the "diagonal mass-lumping" finite element approach.

(2) develop a subdomain integration model for the tetrahedron finite element using a linear trial function in each finite element. The subdomain integration method is also referred to as a control volume approach and has been shown to result in numerical models which may give better approximation results than the often used Galerkin finite element method. The subdomain integration analog will also be developed into a finite element matrix form in a manner such that the integrated finite difference and subdomain integration models can be readily compared to the well known Galerkin finite element analog.

18

(3) develop a variable "mass-lumping" finite element analog.

(4) show that Dirichlet and Neuman boundary conditions are satisfied in the global matrix systems for each of the above determined analogs. This is significant due to the misconception that the finite difference and subdomain integration analogs need special formulae to approximate a Neumann boundary condition (e.g., Bear, 1979).

(5) develop a unified three-dimensional domain numerical analog which represents all of the above numerical-models by the specification of a single parameter in the resulting unified matrix system.

(6) since the various domain approaches determined above can be unified into one numerical statement, use the unified model to examine model approximation error by allowing the unified model to vary between the infinity of available domain models. This objective is achieved by determining the optimum capacitance matrix nodal mass weightings in the finite element for two transient linear heat conduction problems. Both two- and three-dimensional nodal mass weighting factors are determined for comparison purposes. Methods to determine an optimum element nodal mass weighting factor, η, is the subject of current research; however, a method for estimating a mass-lumping factor, η, for radial coordinates is given in Appendix A, and in Hromadka and Guymon(1981).

3.1 GOVERNING EQUATIONS AND SET DEFINITIONS

A three-dimensional advection-diffusion process in an inhomogeneous aniso-tropic nondeformable medium without sources or sinks may be macroscopically described by the nonlinear partial differential equation

$$\frac{\partial}{\partial x}\left[K_x \frac{\partial T}{\partial x} - UT\right] + \frac{\partial}{\partial y}\left[K_y \frac{\partial T}{\partial y} - VT\right] + \frac{\partial}{\partial z}\left[K_z \frac{\partial T}{\partial z} - WT\right] = C\frac{\partial T}{\partial t} \qquad (1)$$

19

where (x,y,z) are spatial coordinates; t is time; $(K_x = K_{xx}, K_y = K_{yy}, K_z = K_{zz})$ are principal axis values of conductivity (e.g. Fickian diffusivity or thermal conductivity); C is a capacitance coefficient; T is the state variable (e.g. temperature); and (U,V,W) are (x,y,z)-axis advection components (e.g. fluid velocity). It is assumed that (1) described the governing flow process in the nondeformable global domain of spatial definition Ω with global boundary Γ. All parameters defined in (1) are assumed variable with respect to both space and time

$$\zeta = \zeta(x,y,z,t) \text{ for } \zeta \in \{K_x, K_y, K_z, U, V, W, C\} \qquad (2)$$

In vector notation, (1) may be written as

$$\int_{\Gamma} \vec{q} \cdot \overrightarrow{d\Gamma} = \int_{\Omega} C \frac{\partial T}{\partial t} dV \qquad (3)$$

where $\overrightarrow{d\Gamma}$ is the outward unit normal vector to surface Γ, $\|\overrightarrow{d\Gamma}\| = dA$; and

$$\vec{q} \equiv (K_x \frac{\partial T}{\partial x} - UT) \vec{i} + (K_y \frac{\partial T}{\partial y} - VT) \vec{j} + (K_z \frac{\partial T}{\partial z} - WT) \vec{k} \qquad (4)$$

The numerical approximation of (4) requires a discretization of the problem domain, Ω. The subdomain (control volume) and finite element discretization processes differ. However by overlapping the two main discretization patterns, the intersection of subdomains with the finite elements result in a third discretization composed of smaller "nodal domains" which are common to both of the main discretizations. For an n-nodal point distribution in Ω with associated subdomains R_j and boundaries B_j

$$\Omega \equiv \overset{n}{\underset{j=1}{U}} R_j \tag{5}$$

$$R_j \equiv \overline{R_j} = R_j \cup B_j \tag{6}$$

$$R_j \cap R_k \equiv B_j \cap B_k \tag{7}$$

$$(x_j, y_j) \in R_j; \quad (x_j, y_j) \notin R_k, \quad j \neq k \tag{8}$$

Combining (3) with (5) and (6),

$$\int_\Gamma \vec{q} \cdot \overrightarrow{d\Gamma} = \int_{UB_j} \vec{q} \cdot \overrightarrow{d\Gamma} \tag{9}$$

$$\int_\Omega C \frac{\partial T}{\partial t} dV = \int_{UR_j} C \frac{\partial T}{\partial t} dV \tag{10}$$

A finite element discretization of Ω is defined by

$$\Omega = U\Omega^e \tag{11}$$

where each finite element Ω^e has a boundary Γ^e where

$$\Omega^e \equiv \overline{\Omega^e} = \Omega^e \cup \Gamma^e \tag{12}$$

A set of nodal domains Ω_j^e can be defined for each finite element as the intersection with associated subdomains

$$\Omega_j^e \equiv R_j \cap \Omega^e \tag{13}$$

This set of nodal domains is defined for each finite element Ω^e by the index of element nodal numbers(see Fig. 3.1 for the one-dimensional case; the two-dimensional case is illustrated for triangles in Fig. 3.2)

$$\Omega^e = U\Omega_j^e, \quad j \in S^e \tag{14}$$

21
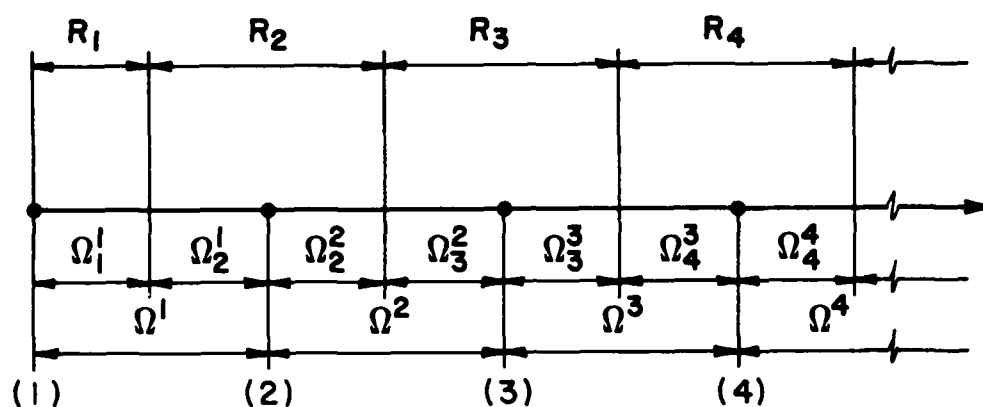
FIG. 3.1. ONE DIMENSIONAL DISCRETIZATION OF GLOBAL DOMAIN Ω SHOWING NODAL POINTS (I), FINITE ELEMENTS Ω^e, SUBDOMAINS R_j, NODAL DOMAINS Ω_j^e, AND NODES •
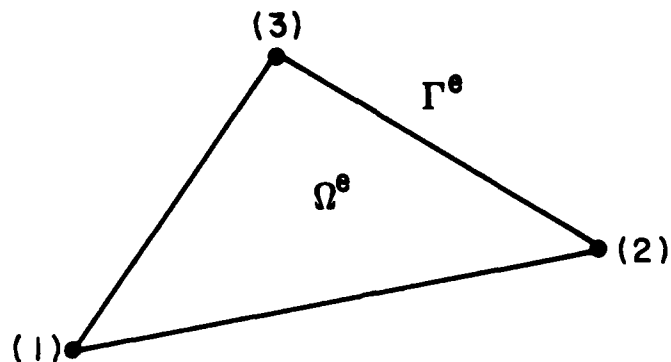
FIG. 3.2a. FINITE ELEMENT Ω^e WITH THREE VERTEX
LOCATED NODAL POINTS
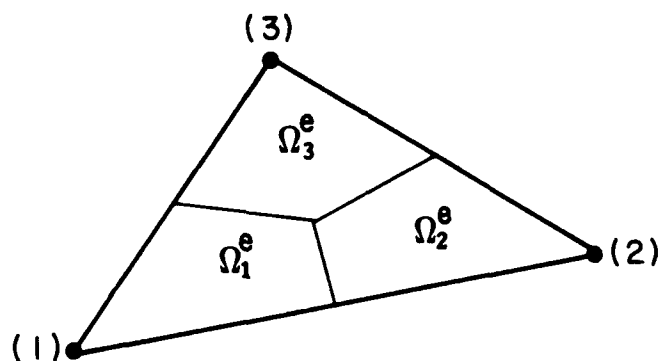
FIG. 3.2b. FINITE ELEMENT PARTITIONED INTO NODAL DOMAINS
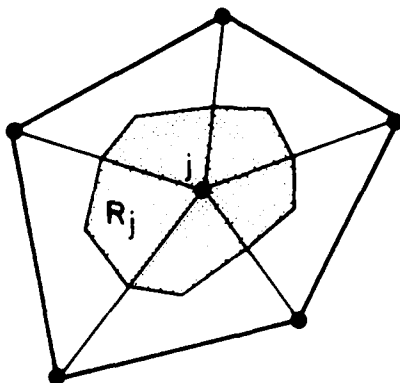
FIG. 3.2c. SUBDOMAIN R_j AS THE UNION OF ALL NODAL
DOMAINS ASSOCIATED TO NODAL POINT j.

23

where

$$S^e \equiv \left\{ j \,\middle|\, \Omega_j^e \cap \Omega^e \neq \{\emptyset\} \right\} \tag{15}$$

From (15) S^e is simply the set of nodes associated to element Ω^e. A finite element matrix system equivalent to the governing domain equation (1) is generated for local finite element Ω^e by

$$\left\{ \int_{\Gamma_j^e} \vec{q} \cdot \overrightarrow{d\Gamma} - \int_{\Omega_j^e} C \frac{\partial T}{\partial t} \, dV \right\} = \{0\} \ , \ j \in S^e \tag{16}$$

Likewise, a subdomain integration statement for (1) is generated for local subdomain R_j by

$$\left\{ \int_{B_j} \vec{q} \cdot \overrightarrow{d\Gamma} - \int_{R_j} C \frac{\partial T}{\partial t} \, dV \right\} = \{0\} \tag{17}$$

Expanding the transport integral of (16) gives

$$\int_{\Gamma_j^e} \vec{q} \cdot \overrightarrow{d\Gamma} = \int_{\Gamma_j^e} \left[K_x \frac{\partial T}{\partial x} \ell_x + K_y \frac{\partial T}{\partial y} \ell_y + K_z \frac{\partial T}{\partial z} \ell_z - UT\ell_x - VT\ell_y - WT\ell_z \right] dA \ , \ j \in S^e \tag{18}$$

where (ℓ_x, ℓ_y, ℓ_z) are the direction cosines of $\overrightarrow{d\Gamma}$, and dA is the differential surface area. Equation (18) can be rewritten as

$$\int_{\Gamma_j^e} \vec{q} \cdot \overrightarrow{d\Gamma} = \int_{\Gamma_j^e \cap \Gamma^e} \left[K_x \frac{\partial T}{\partial x} \ell_x + K_x \frac{\partial T}{\partial y} \ell_y + K_x \frac{\partial T}{\partial y} \ell_z \right] dA$$

$$\tag{19}$$

$$- \int_{\Gamma_j^e \cap \Gamma^e} \left[UT\ell_x + VT\ell_y + WT\ell_z \right] dA + \int_{\Gamma_j^e - \Gamma_j^e \cap \Gamma^e} \vec{q} \cdot \overrightarrow{d\Gamma} \ , \ j \in S^e$$

24

where $\Gamma^e \equiv$ boundary of finite element Ω^e. The first integral in the expansion of (19) satisfies Neumann boundary conditions on Γ^e or preserves flux continuity (due to conduction processes) between finite elements, Ω^e. In the global assemblage of $U\Omega^e$, the first integral in the expansion of (19) also satisfies Neumann boundary conditions on the discretized approximation of global boundary Γ by Γ^e. From (19), the element matrix system of (16) is given by

$$\left\{ \int_{\Gamma_j^e - \Gamma_j^e \cap \Gamma^e} \vec{q} \cdot \vec{d\Gamma} - \int_{\Gamma_j^e \cap \Gamma^e} [UT\vec{i} + VT\vec{j} + WT\vec{k}] \cdot \vec{d\Gamma} - \int_{\Omega_j^e} C \frac{\partial T}{\partial t} dv \right\} = \{0\} \ , \ j \ \epsilon \ S^e \qquad (20)$$

where it is assumed that boundary conditions of Neumann or Dirichlet are specified on global boundary Γ.

3.2 NUMERICAL SOLUTIONS

In the derivation of the finite element integration statement of (20) for Ω^e, no specification of the character of the state variable is assumed. In the following, the state variable T is assumed to be adequately approximated by a linear trial function T^e in each finite element Ω^e. Additionally, each Ω^e is assumed to be a tetrahedron finite element with four vertex-located nodal points. Therefore

$$T \simeq T^e = \Sigma L_j T_j^e \qquad (21)$$

where the L_j are the usual tetrahedra volume local coordinates in Ω^e; and T_j^e are nodal point values of the trial function estimate T^e in Ω^e. Due to the linear definition of T^e in Ω^e, all spatial gradients of T^e are constant. Consequently, several well known domain numerical solutions of (1) in Ω embodied in the finite element method of weighted residuals result in similar numerical approximations in Ω^e except for slight variations in the element mass matrix.

In the following, a Galerkin finite element (linear trial function), subdomain integration (linear trial function), and integrated finite difference analogs will be determined and combined into a single expression. For the finite difference and subdomain analogs, the integrations of (1) on a nodal domain cover Ω_j^e of each finite element Ω^e will be used to determine a finite element matrix system for Ω^e. For all three numerical methods, the following description variable is defined:

$$\Phi \equiv \frac{\partial}{\partial x}\left[K_x \frac{\partial T}{\partial x} - UT\right] + \frac{\partial}{\partial y}\left[K_y \frac{\partial T}{\partial y} - VT\right] + \frac{\partial}{\partial z}\left[K_z \frac{\partial T}{\partial z} - WT\right] - C \frac{\partial T}{\partial t}, \quad (x,y,z) \in \Omega$$

$$(22)$$

Although the Galerkin method of weighted residuals used to solve (1) in each Ω^e is well known, its derivation of a finite element matrix system is presented in order to develop some of the notation and simplifications used in the subsequent determinations of the subdomain integration and integrated finite difference analogs.

Galerkin Method of Weighted Residuals

In local element Ω^e,

$$\int_{\Omega^e} \Phi L_j dV \equiv 0$$

$$(23)$$

generates a Galerkin finite element matrix system for approximation of (1) on Ω^e. Equation (23) is linearized by assuming all parameters quasi-constant during a small timestep Δt (e.g., Bear, 1979)

$$\zeta \equiv \zeta^e + \zeta^*, \qquad \zeta^e \gg \zeta^*; \; (x,y,z) \in \Omega^e$$

$$(24)$$

For the linear trial function T^e definition of the state variable T in Ω^e, the x-direction terms of (23) are given by

26

$$\int_{\Omega^e} (K_x^e \frac{\partial^2 T^e}{\partial x^2} - U^e \frac{\partial T^e}{\partial x}) \, L_j dV \tag{25}$$

$$= \int_{\Gamma^e} K_x^e \frac{\partial T^e}{\partial x} \, dA_x - \int_{\Omega^e} (K_x^e \frac{\partial T^e}{\partial x} \frac{\partial L_j}{\partial x} - U^e \frac{\partial T^e}{\partial x} L_j) \, dV$$

where the first integral of (25) satisfies Neumann type boundary conditions on global boundary Γ or conduction flux continuity between Ω^e.

For a linear trial function T^e in Ω^e and Neumann boundary conditions on Γ,

$$\int_{\Omega^e} (K_x^e \frac{\partial^2 T^e}{\partial x^2} - U^e \frac{\partial T^e}{\partial x}) \, L_j dV = - \int_{\Omega^e} (K_x^e \frac{\partial T^e}{\partial x} \frac{\partial L_j}{\partial x} - U^e \frac{\partial T^e}{\partial x} L_j) \, dV \tag{26}$$

$$= - K_x^e \frac{\partial T^e}{\partial x} \frac{\partial L_j}{\partial x} \int_{\Omega^e} dV - U^e \frac{\partial T^e}{\partial x} \int_{\Omega^e} L_j dV \tag{27}$$

where

$$\frac{\partial T^e}{\partial x} = \frac{\Sigma b_j \, T_j^e}{6V^e} \tag{28}$$

where T_j^e are nodal values of T^e at nodal points j; $V^e \equiv$ volume of the tetrahedron element; and b_j are vertex coordinate co-factors. Substituting (28) into (27) gives

$$\int_{\Omega^e} (K_x^e \frac{\partial^2 T^e}{\partial x^2} - U^e \frac{\partial T^e}{\partial x}) \, L_j dV = - K_x^e \frac{\Sigma b_i T_i^e}{6V^e} \frac{\partial L_j}{\partial x} V^e - U^e \frac{\Sigma b_i T_i^e}{6V^e} \frac{V^e}{4} \tag{29}$$

From Figs. 3.3 and 3.4 the shape function gradient in (29) can be determined geometrically as (see chapter 2, equation 13 for two-dimensions)

$$\frac{\partial L_j}{\partial x} = \frac{\partial}{\partial x} \left(\frac{V_j}{V^e} \right) = \frac{1}{V^e} \frac{\partial V_j}{\partial x} = - \frac{1}{(h_j, x)} \tag{30}$$

27
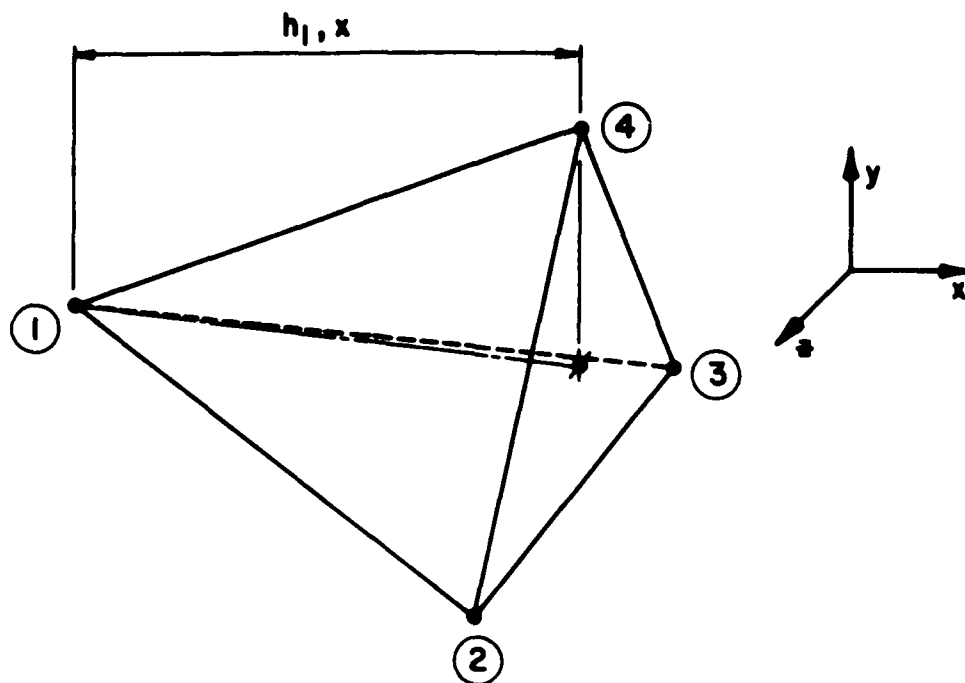
FIG. 3.3. PROJECTION IN THE x DIRECTION OF NODAL POINT I
ONTO THE TRIANGLE [2, 3, 4]
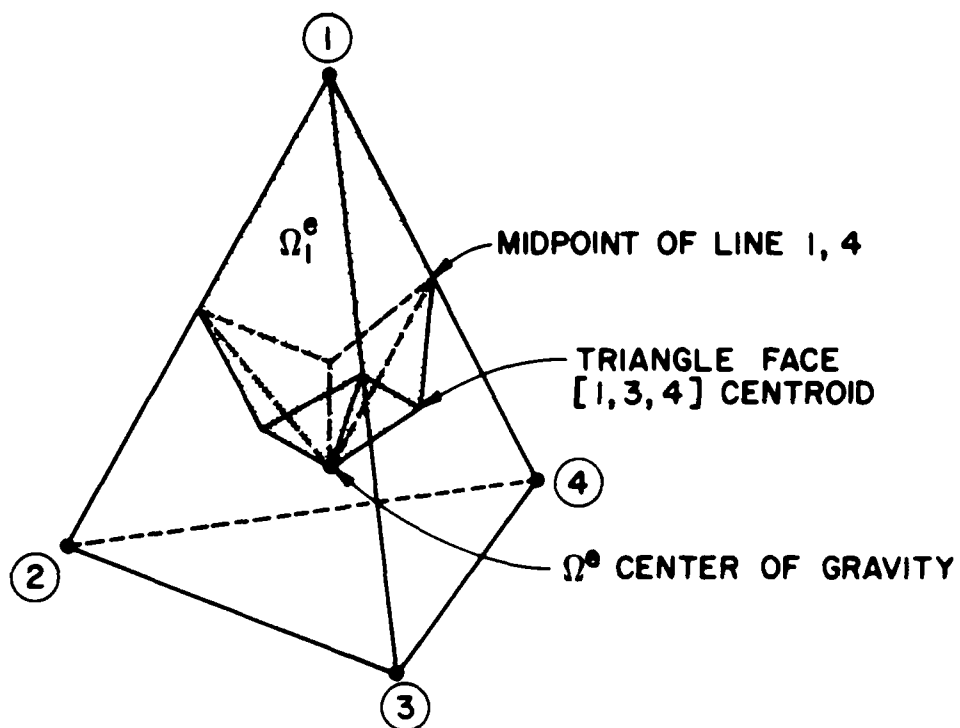
FIG. 3.4. NODAL DOMAIN Ω_I^e : GEOMETRIC DEFINITION

Thus,

$$\frac{\partial L_1}{\partial x} \, V^e = - \frac{1}{(h_1,x)} \left(\frac{1}{3} h_1,x \right) (A_1,x) \tag{31}$$

where (A_1,x) is the projection of the triangle face $[2,3,4]$ onto the (y,z) coordinate plane.

Simplifying (31) and substituting into (29) gives

$$\int_{\Omega^e} \left(K_x^e \frac{\partial^2 T^e}{\partial x^2} - U^e \frac{\partial T^e}{\partial x} \right) L_j dV = K_x^e \frac{\Sigma b_i T_i^e}{6V^e} \frac{(A_1,x)}{3} - U^e \frac{\Sigma b_i T_i^e}{6V^e} \frac{V^e}{4} \tag{32}$$

The (y,z) direction terms are determined analogous to the above. The time derivative term of (23) is modeled by

$$\int_{\Omega^e} C^e \frac{\partial T^e}{\partial t} L_j dV = C^e \int_{\Omega^e} L_i L_j \frac{\partial T_i^e}{\partial t} dV \tag{33}$$

Solution of (33) determines the Galerkin finite element capacitance matrix for local element Ω^e

$$P^e(2) \, \dot{\underline{T}}^e \equiv \frac{C^e V^e}{20} \begin{bmatrix} 2 & 1 & 1 & 1 \\ 1 & 2 & 1 & 1 \\ 1 & 1 & 2 & 1 \\ 1 & 1 & 1 & 2 \end{bmatrix} \begin{Bmatrix} \dot{T}_1^e \\ \dot{T}_2^e \\ \dot{T}_3^e \\ \dot{T}_4^e \end{Bmatrix} \tag{34}$$

where $\dot{T}_j^e \equiv \frac{\partial T_i^e}{\partial t}, \{j = (1,2,3,4)\}$.

Subdomain Integration

A cover of finite element Ω^e is given by the union of nodal domains $\hat{\Omega}_j^e$ where $j \in S^e$. For a tetrahedron finite element, local nodal domain $\hat{\Omega}_1^e$ in $\hat{\Omega}^e$ is assumed defined by Fig. 3.4.

29

The subdomain integration method solves (1) in Ω^e by

$$\int_{\Omega^e_j} \Phi dV = 0 \ , \ j \ \epsilon \ S^e \tag{35}$$

For the x-term transport components of (1),

$$\int_{\Omega^e_j} \left\{ \frac{\partial}{\partial x} \left[K_x^e \frac{\partial T^e}{\partial x} \right] - \frac{\partial}{\partial x} \left[U^e \ T^e \right] \right\} dV = \dot{M}^e_j \ , \ j \ \epsilon \ S^e \tag{36}$$

where $\dot{M}^e_j \equiv \int_{\Omega^e_j} C^e \frac{\partial T^e}{\partial t} dV$

Expanding (36) gives

$$\int_{\Gamma^e_j \cap \Gamma^e} K_x^e \frac{\partial T^e}{\partial x} dA_x + \int_{\Gamma^e_j - \Gamma^e_j \cap \Gamma^e} K_x^e \frac{\partial T^e}{\partial x} dA_x - \int_{\Omega^e_j} U^e \frac{\partial T^e}{\partial x} dV = \dot{M}^e_j \tag{37}$$

The first integral in (37) satisfies Neumann boundary conditions on Γ and conduction flux continuity between Ω^e similar to the Galerkin formulation. Thus, (36) reduces to

$$\int_{\Gamma^e_j - \Gamma^e_j \cap \Gamma^e} K_x^e \frac{\partial T^e}{\partial x} dA_x - \int_{\Omega^e_j} U^e \frac{\partial T^e}{\partial x} dV = \dot{M}^e_j \tag{38}$$

For a linear trial function T^e in Ω^e, (38) simplifies to

$$K_x^e \frac{\partial T^e}{\partial x} \int_{\Gamma^e_j - \Gamma^e_j \cap \Gamma^e} dA_x - U^e \frac{\partial T^e}{\partial x} \int_{\Omega^e_j} dV = \dot{M}^e_j \tag{39}$$

30

The surface $\Gamma_j^e - \Gamma_{j'}^e \cap \Gamma^e$ projection onto the (y,z) plane is given by the integral with respect to dA_x in (39). From Fig. 3.4,

$$\int_{\Gamma_j^e - \Gamma_{j'}^e \cap \Gamma^e} dA_x = \frac{1}{3}(A_1,x) \tag{40}$$

where (A_1,x) is the projection of triangle face onto the (y,z) plane. Additionally, from Fig. 3.4

$$\int_{\Omega_j^e} dV = \frac{V^e}{4} \tag{41}$$

Combining (28), (39), (40) and (41) gives for Ω^e

$$K_x^e \frac{\partial T^e}{\partial x} \int_{\Gamma_j^e - \Gamma_{j'}^e \cap \Gamma^e} dA_x - U^e \frac{\partial T^e}{\partial x} \int_{\Omega_j^e} dV = \tag{42}$$

$$K_x^e \frac{\Sigma b_i T_i^{\;e}}{6V^e} \frac{(A_1,x)}{3} - U^e \frac{\Sigma b_i T_i^{\;e}}{6V^e} \frac{V^e}{4}$$

Comparison of (32) to (42) indicates that the Galerkin finite element and subdomain integration method of weighted residuals determine identical transport system matrices for the assumed linear trial function T^e in Ω^e.

For the time derivative component of (36),

$$\dot{M}_j^e = \int_{\Omega_j^e} C^e \frac{\partial T^e}{\partial t} dV = C^e \frac{\partial}{\partial t} \int_{\Omega_j^e} T^e dV \; , \; j \in S^e \tag{43}$$

which in matrix form gives

31

$$\underset{\sim}{P^e} \left(\frac{75}{23}\right) \underset{\sim}{\dot{T}^e} \equiv \frac{c^e \, v^e}{576} \begin{bmatrix} 75 & 23 & 23 & 23 \\ 23 & 75 & 23 & 23 \\ 23 & 23 & 75 & 23 \\ 23 & 23 & 23 & 75 \end{bmatrix} \begin{Bmatrix} \dot{T}^e_1 \\ \dot{T}^e_2 \\ \dot{T}^e_3 \\ \dot{T}^e_4 \end{Bmatrix} \qquad (44)$$

Integrated Finite Difference

Spalding (1972) developed an integrated finite difference numerical solution for partial differential equations such as (1) defined on rectangular-shaped control volumes (subdomains). In this version of the subdomain integration method, it is assumed that

$$\int_{R_j} T^e \, dV = T_j^{\ e} \int_{R_j} dV \qquad (45)$$

that is, the nodal value of T^e at node j is assumed equal to the spatial distribution of T in subdomain R_j.

For a linear trial function T^e in each Ω^e, the transport terms of (1) evaluated on each B_j determines a conduction matrix identical to the Galerkin and subdomain integration approaches previously derived. From (45), the capacitance matrix from an integrated finite difference approach differs from both the Galerkin and subdomain integration approaches and is given in matrix form by the so-called lumped mass diagonal matrix

$$\underset{\sim}{P^e} (\infty) \underset{\sim}{\dot{T}^e} \equiv \frac{c^e \, v^e}{4} \begin{bmatrix} 1 & 0 & 0 & 0 \\ 0 & 1 & 0 & 0 \\ 0 & 0 & 1 & 0 \\ 0 & 0 & 0 & 1 \end{bmatrix} \begin{Bmatrix} \dot{T}^e_1 \\ \dot{T}^e_2 \\ \dot{T}^e_3 \\ \dot{T}^e_4 \end{Bmatrix} \qquad (46)$$

32

Nodal Domain Integration

Hromadka and Guymon (1981) examined the one-dimensional form of (1) and developed a modification of the subdomain integration method of weighted residuals which improved numerical modeling accuracy by the approach of approximating a higher order trial function $\hat{T}^e$ estimate of the state variable T by using a linear trial function T^e. Using this approach, a significant increase in modeling accuracy was achieved while preserving matrix symmetry and the reduced matrix sizes associated to a linear trial function. By integrating the governing equations on suitably defined nodal domains, a variable symmetric element capacitance matrix was defined which represented the Galerkin finite element, subdomain integration and finite difference methods as special cases.

The nodal domain integration numerical statement for solution of (1) on Ω^e using a linear trial function is found to be similar to the one-dimensional case and is given in element matrix form for Ω^e by

$$\underset{\sim}{K}^e \ \underset{\sim}{T}^e + \underset{\sim}{P}^e \ (\eta) \ \dot{\underset{\sim}{T}}^e = \{0\} \tag{47}$$

where $\underset{\sim}{K}^e \equiv$ sum of element Ω^e conduction and convection matrices given (for the x-term) by (32) and (42);

$$\underset{\sim}{P}^e \ (\eta) \equiv \frac{c^e \ v^e}{4(\eta+3)} \begin{bmatrix} \eta & 1 & 1 & 1 \\ 1 & \eta & 1 & 1 \\ 1 & 1 & \eta & 1 \\ 1 & 1 & 1 & \eta \end{bmatrix} , \tag{48}$$

and $\underset{\sim}{T}^e$, $\dot{\underset{\sim}{T}}^e$ = vectors of element Ω^e nodal values and time-derivative of nodal values.

In (48), the Galerkin finite element, subdomain integration, and integrated finite difference numerical statements for a linear trial function in Ω^e is given by $\eta = (2, \frac{75}{23}, \infty)$, respectively.

33

Consequently, a single computer code can be prepared which readily represents each of the more popular domain numerical methods by the specification of single parameter. Additionally it should be noted that (47) accommodates both Dirichlet and Neumann boundary conditions on Γ similar to the Galerkin finite element approach

For the one-dimensional nodal domain integration approach the corresponding η parameter was determined to be a function of time and variable between finite elements (Hromadka and Guymon, 1981b),

$$\eta \equiv \eta \ (\Omega^e, t) \tag{49}$$

As an aid in selecting the mass-lumping factor, a procedure for calculating the factor as a function of timestep and element size is given in Appendix A for the case of radial coordinates.

3.3 APPLICATION

As an application of the above methods, two linear heat conduction problems (Figs. 3.5 and 3.6) are modeled to examine approximation error for various values of mass lumping. For both problems, a two- and three-dimensional nodal domain integration model are used to approximate the temperature fields.

Using mean relative error as the measurement, the finite element mass matrix was varied by trial and error until a value of η was determined such that the timestep advancement (Crank-Nicolson approach) resulted in a minimum error. In all simulations, the finite element mass-lumping factor (η) is assumed constant throughout the solution domain for the time advancement timestep. Consequently, mean relative error is minimized as a function of one mass-lumping variable. The plots of η during the simulation are given in Fig 3.7 where both two- and three-dimensional (triangle and tetrahedron elements) models are used to solve the test problems.
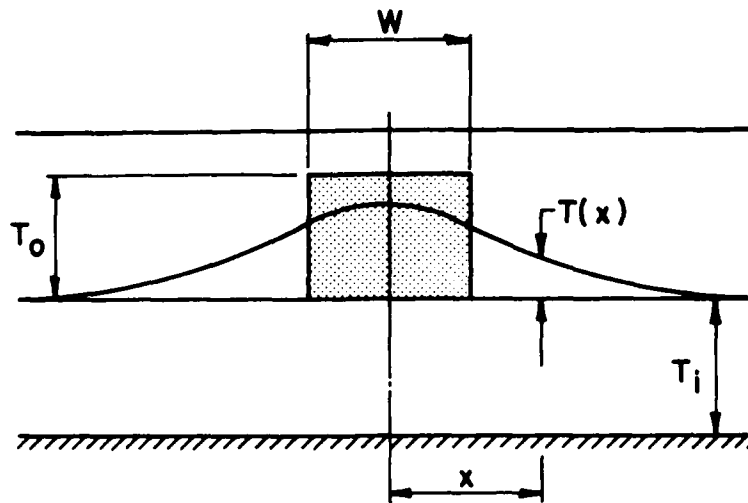
FIG. 3.5.   THE THERMAL DIFFUSION FROM A LONG HEAT SOURCE STRIP
OF   WIDTH   W   (STEP   CHANGE   IN   TEMPERATURE).
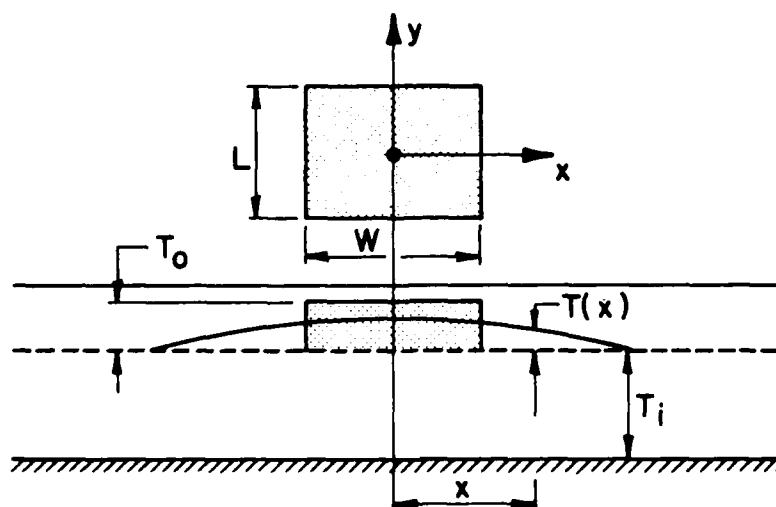
FIG. 3.6.   THERMAL   DIFFUSION   FROM   A   RECTANGULAR   SOURCE
(STEP CHANGE IN   TEMPERATURE).

From Fig. 3.7, both two- and three-dimensional solutions indicate that for the initial portion of the numerical solutions, an integrated finite difference analog minimizes the error measurement. As the solution progresses with time, however, the numerical analog approaches a subdomain integration numerical model. This variation in numerical approach was found similar to other test problem results for one- and two-dimensional problems. Apparently, the integrated finite difference approach reduces mean relative error when the state variable gradient is severe within a finite element, and a subdomain integration analog best serves a milder variation of the state variable in a finite element.

Use of different timesteps and element sizes altered the shape of the η curves in Fig. 3.7, but the scan of numerical analogs from integrated finite difference to subdomain integration is still evident.

As suggested by (49), the η factor was found to vary both between finite elements and with respect to time for one-dimensional problems. The extension of such an approach to multidimensional problems may follow based on the selection of a rule to determine η for each finite element. One approach is to approximate a higher order. or more complex trial function within a finite element by a linear trial function, and then use the improved linear trial function to determine an appropriate η mass-lumping factor. As η varies, a global matrix regeneration is required which increases computational effort. However for highly nonlinear problems, global matrix regeneration may already be frequently necessary which helps offset the η factor complications. Appendix A presents an approach for selecting the mass-lumping factor, and the approach tested for the case of a radial coordinate system.
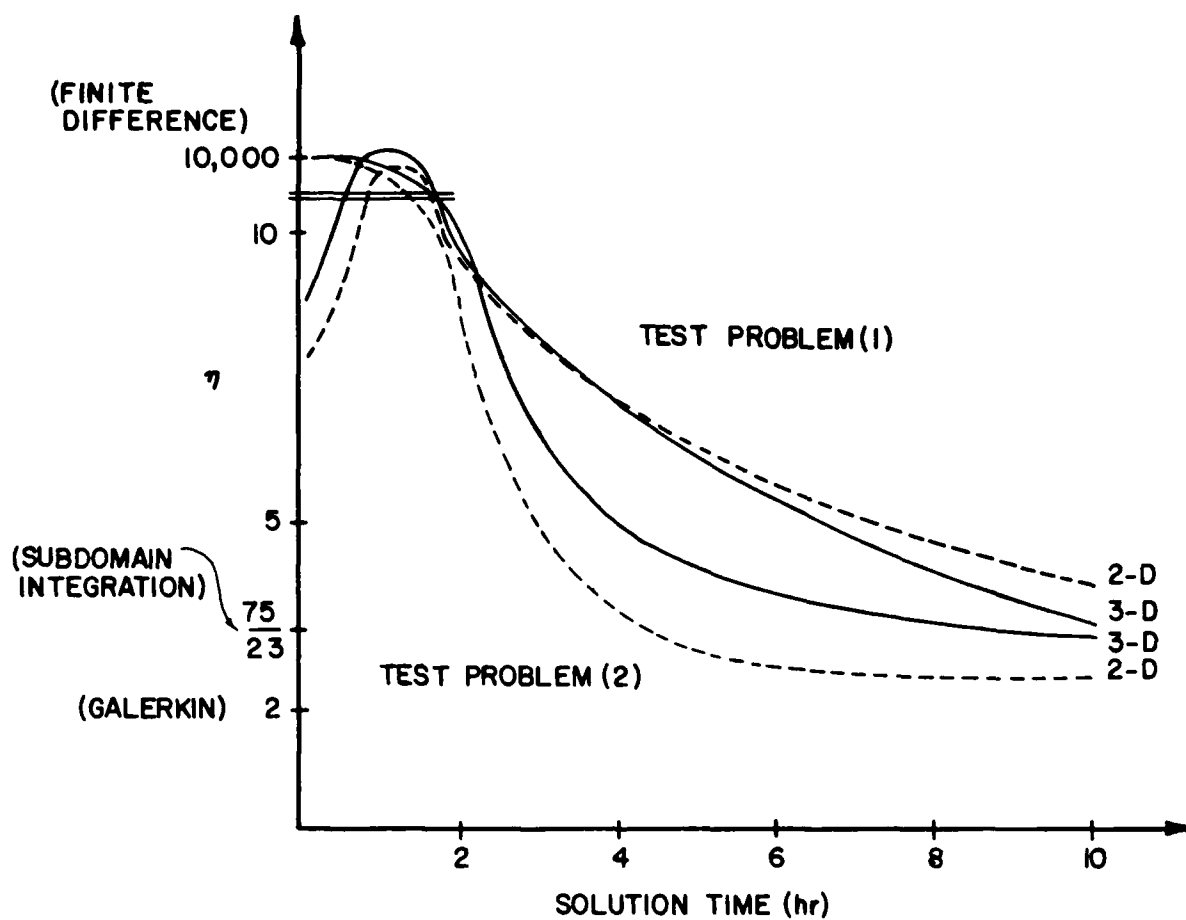
FIG. 3.7 OPTIMUM MASS WEIGHTING η-FACTORS FOR TWO AND THREE-DIMENSIONAL FINITE-ELEMENT SOLUTION OF TEST PROBLEMS

37

The results of the two test problems presented in this chapter are typical of the overall results obtained by numerous other computer simulations of problems where analytical solutions exist. Generally speaking, holding the mass-weighting factor η uniform and constant in each finite element results in a numerical method which provides varying degrees of approximation error. That is for some problems, a constant mass-weighting numerical model (such as Galerkin, finite difference, subdomain integration, or some other selected mass-weighting model) may provide a "best" overall numerical approximation. For other problems, the same selected mass-weighting model may provide a "best" numerical approximation for only a certain interval of the simulation or for only a certain region of the total problem domain. This generality applies to one-, two- and three-dimensional problems when using the well known rectangle, triangle and, as presented in this chapter, tetrahedron finite elements.

Although the test problems considered here only indicate the necessary variation in uniform finite element mass-weightings to minimize a measure of error (while holding the mass-weighting factor constant between finite elements), similar variations in mass-weightings were found evident when holding finite element mass-weighting's constant with respect to time and yet variable between finite elements. That is, if the finite element mass-weighting factor were allowed to be variable between finite elements but held constant during the entire simulation, different distributions of η throughout the problem domain resulted in various levels of approximation accuracy.

Methods for determining mass-weighting factors for each finite element are presented for one-dimensional problems in Hromadka and Guymon (1981). Two techniques of improving a linear trial function in each finite element are considered. Each improved trial function approach results in a variable mass-weighting factor for each finite element.

It is noted from the extensive computer simulations prepared during this research, that there is a strong correlation between the minimization of overall approximation error and the use of a large η factor distribution (e.g. a finite difference analog) in regions of large or fast variations of the problems' governing state variable. Additionally, use of a sub-domain integration η distribution in regions of mild or slow variations of the state variable also tends to reduce overall approximation error. Surprisingly, the various optimized η curves, such as shown in Fig. 3.7, did not include the often used Galerkin finite element numerical model.

3.4 CONCLUSIONS

A nodal domain integration numerical model is derived for approximating a three-dimensional anisotropic heat conduction process in an inhomogeneous continuum. The nonlinear partial differential equation is linearized in each tetrahedron-shaped finite element by assuming all parameters quasi-constant for small durations of time. A linear trial function is assumed to adequately describe the governing state variable in each finite element.

The resulting nodal domain integration model is found to represent the Galerkin finite element, subdomain integration, and finite difference methods as special cases. Additionally, both Dirichlet and Neumann boundary conditions are accommodated similar to a Galerkin finite element numerical model.

Application of the nodal domain integration model to linear heat conduction problems indicate that the finite element mass matrix must vary with time in order to provide an optimum numerical solution for the entire simulation. The mass matrix is defined as a function of a single variable, η, and allows a good representation of the required mass-lumping necessary to minimize numerical solution error. Use of the numerical model allows a unified computer code to be developed which offers the capability to represent a Galerkin, sub-

domain integration, integrated finite difference, and an infinity of different mass-lumped matrix models, as well as provide the capability to vary between these numerical analogs according to some specified model-selection rule.

From the complete NDI development of Chapter 3 for three-dimensional flow problems and the two-dimensional development of Chapter 2, it is seen that both heat and soil-water NDI models can be prepared which represent the Galerkin finite element, integrated finite difference and subdomain integration methods by the specification of a single mass-lumping factor. This NDI approach is used in program FROST2B to model both the heat and soil-water flow regimes. Consequently, the program user can specify a particular domain analog by the use of the appropriate mass-lumping factor.

REFERENCES

1. Patankar, S. V., Numerical Heat Transfer and Fluid Flow, McGraw-Hill, 1980.

2. Spalding, D. B., A Novel finite-difference formulation for differential expressions involving both first and second derivations, 1st Journal for Num. Methods in Eng., (4), 551, 1972.

3. Hromadka II, T. V., G. L. Guymon, G. C. Pardoen, Nodal Domain Integration Model of Unsaturated Two-Dimensional Soil-Water Flow: Development, Water Resources Research, Vol. 17, No. 5, 1425-1430, 1981a.

4. Hromadka II, T. V., and G. L. Guymon, Nodal Domain Integration Model of One-Dimensional Advection-Diffusion, Advances in Water Resources, Vol. 5, 9-16, 1981b.

5. Hromadka II, T. V., and G. L. Guymon, A Note on Numerical Approximation of Advection-Diffusion Processes in Rectangular Spatial Domains, Advances in Water Resources, Vol. 5, 56-60, 1982.

6. Zienkiewicz, O. C., The Finite Element Method in Engineering Science, McGraw-Hill, 1977.

7. Ramadhyani, S. and S. V. Patankar, Solution of the Poisson Equation: Comparison of the Galerkin and Control-Volume Methods, 1st Journal for Num. Methods in Eng., (15), 1395-1418, 1980.

8. Baliga, B. R., and W. V. Patankar, A New Finite-Element Formulation for Convection-Diffusion Problems, Numerical Heat Transfer, Vol. 3, 393-409, 1980.

9. Bear, Jacob, Hydraulics of Groundwater Flow, McGraw-Hill, 1979.

10. Hromadka II, T. V., and G. L. Guymon, Improved Linear Trial Function Finite Element Model of Soil Moisture Transport, Water Resources Research, Vol. 17, No. 3, 504-512, 1981.

4. ISOTHERMAL PHASE CHANGE MODEL

4.0 INTRODUCTION

A model of phase change in freezing and thawing soils is developed for cold regions engineering problems which require two-dimensional analysis of the thermal regime of soils. Such problems include complex boundary conditions such as atmosphere-ground surface thermal interaction and snowpack-insulation. Other concerns include complex soil conditions such as the presence of a peaty muskeg or tundra-like soil which may provide thermal insulation for underlying ice-rich mineral soil. Although several models have been developed to predict temperatures in freezing and thawing soils, oftentimes the key question is simply whether or not the soil is frozen since soil structural properties are significantly influenced by the soil-water state of phase.

The history of modeling the coupled heat and moisture transfer process with phase change in freezing (and thawing) soils seems to begin with the work of Stefan in 1890. By assuming that water freezes in the soil at a constant temperature ($0^{o}C$) the equations of conduction heat transfer can be solved exactly. The resulting solution is known as the moving boundary problem, and is inadequate for soils where moisture is retained in the thawed condition (for freezing temperatures), or when moisture transfer occurs.

Neumann expanded on Stefan's analysis by including a partial differential equation system to describe the thermal profile on both sides of the moving boundary. Although inadequate for real world systems, the Neumann problem can be used to verify numerical models of soil freezing wherein moisture transfer and residual unfrozen moisture contents are neglected. Such applications of Neumann's anaylsis were used in Berggren (1943) and Aldrich(1956). Further exact solutions are available for soil freezing problems. These mathematical developments (Goodman, 1964; Sikarskie and

42

Boley, 1965) are valid, however, only for special case studies.

For problems of soil freezing where an unfrozen moisture content exists below the freezing temperatures, a moisture transport process is generally also occuring. Williams(1972) concluded that this moisture transfer effect is usually of the magnitude that ignoring its contribution can lead to unacceptable errors. The presence of moisture below freezing temperatures negates the assumptions used in the moving boundary problems. Thus, an entirely new approach to fine-grained soil freezing analysis was required. Lukianov and Golovko (1957) introduced the "apparent specific heat capacity" approach whereby the latent heat effects of freezing water are lumped into the transient heat capacity term of the heat transport equation.

With the advent of computer simulation capability, the past two decades have witnessed considerable effort in freezing soil analysis developments. These recent numerical modeling efforts can be divided into two groups depending on whether soil moisture transfer effects are included.

Nakano and Brown (1971) modeled the heat transfer process while Harlan (1973) approached the coupled heat and moisture transport problem with a finite difference numerical algorithm, which is based on the assumption of an analogy between moisture transport processes in unsaturated soil and a freezing soil. Guymon and Luthin (1974) included vertical soil-water flow in a finite element model of a one-dimensional vertical soil column. Sheppard (1978) and Taylor and Luthin (1978) also presented mathematical models for the coupled heat and moisture transfer process. These models use the assumption that water content of the soil is a function of temperature during phase change. Jame (1978) expanded on Harlan's model to compare numerically simulated results to experimental data. It is noted that these later models require spatial and temporal magnitudes on the order of 1.18 in. (3 cm) and 0.5 hours, respectively. A method to extend the above models to

43

economically model large-scale, long duration two-dimensional problems has not been advanced. These models and numerical models of frost heave are reviewed by Guymon, et al. (1980) and Hopke (1980) among others. It is noted that while one-dimensional models of soil freezing or thawing are adequate for a large number of applications,at least two-dimensional models are required for many problems such as buried pipelines, roadway berm problems, and embankments on permafrost.

Geothermal models (i.e., soil-water flow effects are neglected) often provide a thermal analysis capability which is sufficient for many problems. Examples of geothermal models which are reported in the literature include the isothermal phase change model of Bafus and Guymon (1976), the two- and three-dimensional isothermal phase change model of Guymon and Hromadka (1977), and more recently the sophisticated two-dimensional, moving-mesh, finite element model of Albert (1984).

An advantage of the continuously deforming grid system is that the freezing front is tracked sharply, and requires negligible interpretation of nodal value estimates of ice content to locate the interface between frozen and unfrozen soil. An earlier one-dimensional version of a finite element continuously deforming coordinate system model is presented in detail in O'Niell and Lynch (1981). Currently, both of these models are restricted to homogeneous soil systems. Additionally, the mathematical modeling approach results in a type of convection term due to the precise handling of the mesh movement. The mesh moving algorithm requires additional computational effort in order to provide a freezing front coordinate-movement approximation coupled with an interior domain nodal point transformation and finite element regeneration capability. Such a modeling approach may be inadequate, however, for soil-water freezing/thawing

44

problems which involve soil-water flow effects and a nonhomogeneous soil system.

The main objective of this chapter is to present the soil-water phase change modeling approach used to couple the heat and soil-water flows described in chapters 2 and 3, respectively. The ultimate goal of this effort is to develop a computer model capable of determining the thermal and moisture states of a two-dimensional soil system subjected to the freezing and thawing processes experienced in cold climate regions. A major factor influencing the choice of the modeling approach is that not only should the computer model be accurate, it should also be economical to use, without the need to obtain parameter data which is costly to evaluate. Additionally, it is desirable that the computer code be prepared such that it can be accomodated on small computers such as the PDP 11/34 or Data General "Eclipse" computer systems.

4.1 HEAT AND SOIL-WATER FLOW

The theory of heat transport in freezing soils and their thermal pro-perties have been the subject of several recent publications such as Lunardini (1981) and Farouki (1981). For two-dimensional heat flow in isotropic soils, the governing partial differential equation is

$$\frac{\partial}{\partial x}\left[K_T \frac{\partial T}{\partial x}\right] + \frac{\partial}{\partial y}\left[K_T \frac{\partial T}{\partial y}\right] = C_m \frac{\partial T}{\partial t} - L \frac{\rho_i}{\rho_w} \frac{\partial \theta_i}{\partial t} + C_w U \frac{\partial T}{\partial x} + C_w V \frac{\partial T}{\partial x} \quad (1)$$

where x and y = cartesian coordinates, t=time, T=soil-water-air-ice mixture temperature, θ_i=volume of ice per unit total volume of soil, K_T=thermal

45

conductivity of soil-water-air-ice mixture, C_m=volumetric heat capacity of soil-water-air-ice mixture, L=volumetric latent heat of fusion of bulk water, ρ_i = ρ_w = density of ice and water, respectively, C_w=volumetric heat capacity of water, and U and V =the x and y velocity flux components. In (1), the latent heat parameter, L, may be assumed to be constant for temperatures less than -20°C (Anderson, et al, 1973). The thermal parameters, K_T and C_m, are assumed to be functions of the volumetric content of each material constituent over the nodal point control surface and control volume (chapter 3). To reduce computational effort, the convection terms in (1) are approximated as an average value estimated from the previous timestep solution, and then included in the load vector term of the numerical analog. Figure 4.1 illustrates the heat flow conservation model used for each nodal point. For example, DeVries (1966) uses a volumetric fraction proportion

$$C_m = \Sigma\, C_j\, \theta_j \qquad (2)$$

where C_j=volumetric heat capacity of the jth constituent and θ_j =volumetric fraction of the jth constituent. The heat flow equation is nonlinear due to the K_T and C_m parameters being functions of ice and water content in a freezing and thawing soil. Other considerations include relationships between temperature and soil-water undergoing phase change such as discussed by Anderson, et al (1973). A mathematical model of soil-water flow in unfrozen, isotropic soils given in nondeformable saturated or unsaturated porous media is (e.g., Bear, 1979)

$$\frac{\partial}{\partial x}\left[K_H \frac{\partial\phi}{\partial x}\right] + \frac{\partial}{\partial y}\left[K_H \frac{\partial\phi}{\partial y}\right] = \frac{\partial\theta}{\partial t} + S \qquad (3)$$

where ϕ =total hydraulic head, K_H=Darcy hydraulic conductivity,

ALGORITHM STEP NUMBER

ALGORITHM PROCEDURE

(1) Estimate area-averaged thermal parameters of heat capacity over the control volume R_i, and thermal conductivity on the control surface B_i.

(2) Estimate nodal values of temperature at time $t+\Delta t$ given the temperatures at time t. (See Chapter 3).

(3) If nodal temperature values at time t or $t+\Delta t$ indicate phase change of soil-water, modify nodal temperature values and thermal parameters according to the isothermal phase change model.

(4) Return to Step (1) to model next timestep advancement.

FIG. 4.1. HEAT FLOW MODEL

● = NODE

TRIANGLE ELEMENTS SURROUNDING NODE i

- = BISECTOR
+ = CENTROID

TRIANGLE ELEMENTS SUBDIVIDED INTO NODAL DOMAINS

→ = HEAT FLUX

B_i

R_i

CONTROL VOLUME R_i AND CONTROL SURFACE B_i ASSOCIATED TO NODE i
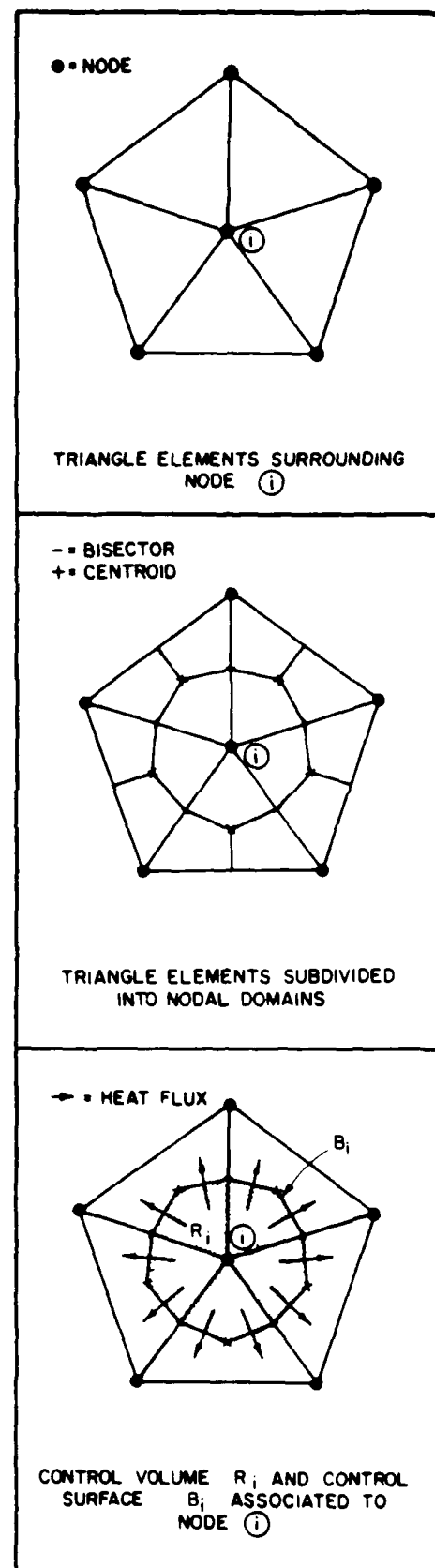
θ_u =volumetric water content, and S=moisture sink. Figure 4.2 illustrates the soil-water flow conservation model used for each nodal point. In unsaturated soils K_H may be assumed to be a function of soil-water pore pressures (soil-water tension). The moisture sink term for a freezing soil accounts for the phase change of liquid water to ice by

$$S = L \frac{\rho_i}{\rho_w} \frac{\partial \theta_i}{\partial t} \qquad (4)$$

Application of (3) in a freezing/thawing problem requires the incorporation of special considerations in order to describe soil-water flow in a frozen soil. For example, the presence of ice in soil significantly affects the rate of soil-water flow (Nakano, 1982). This impact may be interpreted as a reduction in the Darcian hydraulic conductivity (assuming a Darcian soil-water flow model). In studies by Jame (1978) and Taylor and Luthin (1978), the soil-water flow model hydraulic conductivity had to be significantly reduced in a freezing zone in order to adequately reproduce measured thermal and soil-water data in freezing horizontal columns. From these studies, a general hydraulic conductivity relationship was proposed

$$K = K_H 10^{-E\theta_i} \qquad (5)$$

where K=soil-water hydraulic conductivity, K_H=unfrozen soil-water hydraulic conductivity, θ_i=volumetric ice content, and E=a calibration factor evaluated from one-dimensional vertical column soil freezing laboratory models. In the computer model, the hydraulic conductivity in (5) is assumed to be zero for completely frozen soils. Soil-water freezing characteristic curves indicate that soil-water exists even at very cold temperatures. This "residual" water content is used as a lower bound for water content in the model.

ALGORITHM   ALGORITHM PROCEDURE
STEP NUMBER

(1) Estimate area-averaged soil-water flow parameters of Θ^* over the control volume R_i, hydraulic conductivity on the control surface B_i.

(2) Estimate nodal values of soil-water energy head at time $t + \Delta t$ given the values at time t. (See Chapter 2.)

(3) If phase change is predicted from the HEAT FLOW MODEL, modify nodal values of water content, pore pressure and energy head according to isothermal phase change model. Adjust soil-water flow parameters to accommodate soil-water-ice mixture.

(4) Return to Step (1) to model next timestep advancement.

FIG. 4.2. SOIL-WATER FLOW MODEL

● = NODE

TRIANGLE ELEMENTS SURROUNDING NODE ⓘ

– = BISECTOR
+ = CENTROID

TRIANGLE ELEMENTS SUBDIVIDED INTO NODAL DOMAINS

→ = SOIL-WATER FLUX

B_i

R_i

CONTROL VOLUME R_i AND CONTROL SURFACE B_i ASSOCIATED TO NODE ⓘ

49
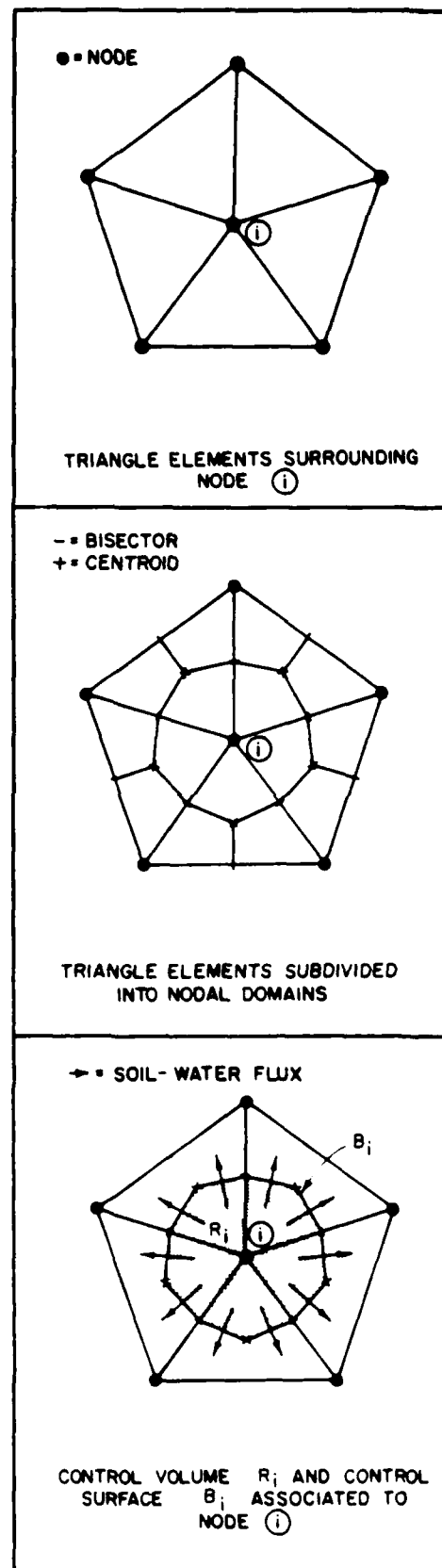
Soil-water content is assumed a function of pore pressure head by

$$\theta = \frac{\theta_o}{A|\psi|^n + 1} \qquad (6)$$

where θ_o =porosity, ψ =soil-water pore pressure head, and A and n =regression fit coefficients.

4.2 PHASE CHANGE

The two-dimensional phase change model has been under continual development since 1979. The primary effort has been under the direction of Dr. Richard L. Berg of the U.S. Army Research and Engineering Laboratory in Hanover, New Hampshire. The main objective of this effort is to develop a computer model which provides analysis capability for geotechnical engineers involved in cold regions engineering project. The program is designed to be comprehensive, and yet easy to use with a minimum of field data requirements. Development of this model has been reported upon as follows (Guymon, et al. 1984): Guymon, et al. (1980) and Berg, et al. (1980) represented the concepts of a modeling approach and presented early verification and sensitivity results. Subsequently, Guymon, et al. (1981a) presented additional verification results, and Hromadka, et al. (1982) presented a detailed evaluation of model sensitivity to the choice of numerical analog. Guymon, et al. (1981b) evaluate parameter sensitivity and develop a probabilistic model which is cascaded with the deterministic one-dimensional model. Finally, Guymon, et al. (1984) present applications of the two-dimensional model applied to pipeline studies and roadway embankments.

A summary of the key assumptions used in the two-dimensional model are as follows:

50

1. Soil-water flow occurs in unfrozen zones by liquid water film driven by hydraulic gradients such as described by Darcy's law.

2. Soil-water flow in frozen zones is negligible.

3. Heat flow is mathematically described by (1).

4. Soil-water flow is mathematically described by (3).

5. Soil-water phase change may be approximated as an isothermal process.

6. Unfrozen zones are nondeformable, and in freezing zones or frozen zones, deformation is due to ice segregation or lens thawing only.

7. Soil water pore pressures in freezing zones are governed by a residual water content determined from soil freezing tests.

8. Hysteresis effects are negligible.

9. Salt exclusion processes are negligible.

10. Constant parameters (e.g., porosity) remain constant with respect to time; i.e., freeze-thaw cycles do not modify parameters.

11. Freezing and thawing processes in a two-dimensional medium occur in such a way that there are no internal shear or stress forces developed between different zones.

The phase change model which couples the heat and soil-water flow models is based upon the simple control volume approach where freezing/thawing occurs isothermally (Guymon and Hromadka, 1977). The algorithm is based on a control volume generated by the nodal integration method. A volume of freezing soil is retained at $0^{o}C$ until the latent heat of fusion of all available soil-water for freezing has been evolved.

Figure 4.3 illustrates the phase change model logic, and indicates how the entire nodal point control volume is lumped during phase change.

51

FIG. 4.3 ISOTHERMAL SOIL-WATER FREEZING MODEL

OBTAIN Nodal Temperature Value for Time $(t+\Delta t)$: $T_i^{t+\Delta t}$

IS $T_i^{t+\Delta t} \geq 0^\circ C$?

yes → no freezing

no

IS $T_i^{t} < 0^\circ C$?

yes → no freezing

no

Soil-water available for freezing (S_i) is estimated from nodal water content $(\Theta_i^{t+\Delta t})$ and residual water content (Θ_{RES}) by

$$S_i = \underset{R_i}{\int} (\Theta_i^{t+\Delta t} - \Theta_{RES})\, dA$$

IS $S_i > 0$?

no → no freezing

yes

Heat evolution (ΔQ_i) during timestep Δt is estimated using the heat capacity C_m by $\Delta Q_i = C_m (0^\circ C - T_i^{t+\Delta t})_{R_i} \int dA$

EVALUATE

$E = (S_i - \Delta Q_i / L_a):$

$E = 0$

- S_i freezes
- set $T_i^{t+\Delta t} = 0^{\circ}C$
- set $\Theta_i^{t+\Delta t} = \Theta_{RES}$

OUT

$E > 0$

- soil-water volume freezing is $\Delta Q_i / L_a$
- set $T_i^{t+\Delta t} = 0^{\circ}C$
- decrease nodal water content value

  by $\Delta Q_i / L_a$

OUT

$E < 0$

- soil-water volume freezing is S_i
- set $T^{t+\Delta t} = \dfrac{(S_i L_a - \Delta Q_i)}{C_m R_i \int dA}$

OUT

53

4.3 MODEL PARAMETER RELATIONSHIPS

Because the soil-water flow model is based on energy head, solution of (3) requires that the relationship between soil-water pressure head and soil-water content be defined where the time-derivative term is replaced by

$$\frac{\partial \theta}{\partial t} = \frac{\partial \theta}{\partial \psi} \frac{\partial \phi}{\partial t} \tag{7}$$

The partial derivative, $\frac{\partial \theta}{\partial \psi}$ is determined from Gardner's (1958) relationship of (6). Hydraulic conductivity is defined as a function of ψ by

$$K_H(\psi) = \frac{K_o}{A_k |\psi|^m + 1} \tag{8}$$

where K_o=saturated hydraulic conductivity, and A_K and m are calibrated parameters. Hydraulic conductivity in soil-freezing zones is estimated by the exponential relationship of (5).

Soil-water pore pressures at freezing fronts are defined by

$$\psi(\text{at freezing front}) = \psi (\theta_{RES})$$

where θ_{RES} is a residual soil-water content.

Additional data required for use with the model are boundary conditions for the heat and soil-water flow models, and initial conditions of temperature, water content and ice content. Boundary conditions are modeled as constants or sinusoidal functions specified by the program user as to amplitude and wave period. Modeling data input requirements are discussed in detail in Chapter 5.

REFERENCES

1. Albert, M. R., "Modeling Two-Dimensional Freezing Using Transfinite Mappings and a Moving-Mesh Finite Element Technique," Cold Regions Research and Engineering Laboratory, CRREL Report 84-10, 1984.

2. Anderson, D. M., A. R. Tice and H. L. McKim, "The Unfrozen Water and the Apparent Specific Heat Capacity of Frozen Soils," Proceedings, Second International Permafrost Conference (North American Contribution), National Academy of Science, 1973.

3. Bafus, G. R. and G. L. Guymon, "Thermal Analysis of Frozen Embankment Islands," J. of Water, Harbors, and Coastal Engineering Div., ASCE, V 102, No. WW2, pp. 123-139, 1976.

4. Bear, J., "Hydraulics of Groundwater," McGraw-Hill International Book Co., 1979.

5. Berg, R. L., Guymon, G. L., and Johnson, T. C., "Mathematical Model to Correlate Frost Heave of Pavements with Laboratory Predictions,: U. S. Army, CRREL, Report 80-10, 1980.

6. Berggren, W. P., "Prediction of Temperature Distribution in Frozen Soils," Transactions of American Geophysical Union, part 3, pp 71-77, 1943.

7. Desai, C. S. and J. F. Abel, "Introduction to the Finite Element Method," Van Nostrand Reinhold Co., 1979.

8. DeVries, D. A., "Thermal Properties of Soils," Physics of Plant Environment, Edited by W. R. van Wijk, North-Holland Pub. Co., p. 383, 1963.

9. DeVries, D. A., "Thermal Properties of Soils," Physics of Plant Environment, Edited by W. R. Van Wijk, North-Holland Pub. Co., pp. 210-235, 1963.

10. Eagelson, P. S., "Dynamic Hydrology," McGraw-Hill, 1970.

11. Farouki, O. T., "Thermal Properties of Soil," U. S. Army, CRREL, Monograph 81-1, 1981.

12. Guymon, G. L. and J. N. Luthin, "A Coupled Heat and Moisture Transport Model for Arctic Soils," Water Resources Research 10(5), 995-1001, 1974.

13. Guymon, G. L. and T. V. Hromadka, II, "Finite Element Model of Transient Heat Conduction with Isothermal Phase Change (two- and three-dimensional)," U. S. Army Cold Regions Research and Engineering Laboratory, Special Report 77-38, 1977.

14. Guymon, G. L., Hromadka II, T. V., and Berg, R. L, "A One-Dimensional Frost Heave Model Based Upon Simulation of Simultaneous Heat and Water Flux," Cold Regions Science and Technology, 3, pp. 253-262, 1980.

15. Guymon, G. L., Harr, M. E., Berg, R. L., and Hromadka II, T. V., "A Probabilistic-Deterministic Analysis of One-Dimensional Ice Segregation in a Freezing Soil Column," Cold Regions Science and Technology, 4, pp. 127-140, 1981.

16. Harlan, R. L., "Analysis of Coupled Heat-Fluid Transport in Partially Frozen Soil," Water Resources Res., 9(5), 1314-1323, 1973.

17. Hopke, S. W., "A Model for Frost Heave Including Overburden," Cold Regions Science and Technology, 3, pp. 111-147, 1980.

18. Hromadka II, T. V., Guymon, G. L., and Berg, R. L., "Sensitivity of a Frost Heave Model to the Method of Numerical Simulation," Cold Regions Science and Technology, 6, pp. 1-10, 1982.

19. Jame, Y. W., and E. I. Norum, "Heat and Mass Transfer in Freezing Unsaturated Soil in a Closed System," Proceedings of Second Conf. on Soil Water Problems in Cold Regions Edmonton, Alberta, Canada, 1976.

20 Jame, Y. W., "Heat and Mass Transfer in Freezing Unsaturated Soil," Ph.D. Dissertation, Univ. of Saskatchewan, Saskatoon, Canada, 1978.

21. Lukianov, V. S. and M. D. Golovko, "Calculation of the Depth of Freeze in Soils," (in Russian), Bul. 23, Union of Transp. Constr., Moscow, (English Translation, Nat. Technical Information Service, Springfield, Va., 1957.

22. Lunardini, B. J., "Heat Transfer in Cold Climates, : Van Nostrand Reinhold Co., New York, 1981.

23. Myers, G. E., "Analytical Methods in Conduction Heat Transfer,: McGraw-Hill New York, 1971.

24. Nakano, Y. and J. Brown, "Effects of a Freezing Zone of Finite Width on the Thermal Regime of Soils," Water Resources Res., 7(5), 1226-1233, 1971.

25. Nakano, Y., Tice, A., Oliphant, J., and Jenkins, T., "Transport of Water in Frozen Soil, II. Effects of Ice on the Transport of Water Under Isothermal Conditions," Advance in Water Resources, 6, pp. 15-26, 1983.

26. O'Neill, K. and D. R. Lynch, "A Finite Element Solution for Freezing Problems. Using a Continuously Deforming Coordinate System", Numerical Methods in Heat Transfer, Edited by R. Lewis, K. Morgan, and O. C. Zienkiewicz, New York, 1981.

27. Sheppard, Marsha, I., B. O. Kay and J. P. G. Loch, "Development and Testing of a Computer Model for Heat and Mass Flow in Freezing Soils," Dept. of Land Resource Science, Univ. of Guelph, Guelph, Ontario, Canada, 1978.

28. Sikarskie, D. L. and B. A. Boley, "Solution of a Class of Two-Dimensional Melting and Solidification Problems," Int'l. J. Solids Structure, V.1, pp. 207-234, 1965.

29. Stefan, J., "Uber die Theorie der Eisbildung, Insbesandere Uber die Eisbildung im Polarmeere," Sitzungsberichte de Mathematisch-Naturwissenschaft-lichen Classe der Kaiserlichen Akademie der Wissenschaften, Wien., pp. 965-983, 1890.

30. Taylor, George S. and J. N. Luthin, "A Model for Coupled Heat and Moisture Transfer During Soil Freezing," Canadian Geotechnical Journal, (15), 548-555, 1978.

31. Williams, P. J., "Thermal Properties of Frozen Soils: Their Importance and Assessment," Proc., Seminar on the Thermal Regime and Measurements in Permafrost, Tech, Memorandum No. 108, NRC Canada, pp. 47-50, 1972.

5. PROGRAM PROTOØ

5.0 INTRODUCTION

A FORTRAN computer program is available which accomodates two-dimensional heat and soil-water flow models (Chapters 2 and 3) as coupled by an isothermal phase change model (Chapter 4). The program can be used to analyze two-dimensional freezing/thawing problems which have sufficient known information to supply the necessary modeling parameters, boundary conditions, and initial conditions.

Because of the sophistication of the two-dimensional phase change model and the data requirements needed to properly represent inhomogeneity of the system, boundary conditions, and other complexities, a special data input program is developed in order to aid the model user. This general purpose data preparation program, PROTOØ, develops the data input file to be used directly by the two-dimensional phase change program.

In this chapter, the PROTOØ program will be reviewed in detail. The actual CRT screen pages will be displayed which show the data entry prompts in their respective order of appearance. Also shown on the CRT screen pages are the computer program variable names associated to each prompt in order to aid in understanding the FORTRAN code.

5.1 MODELING APPROACH

Heat and Soil-Water Flow

Chapters 2 and 3 provide the details of the mathematical models used to approximate the thermal and soil-water effects in two-dimensional problems. The analyst initially discretizes the problem geometry (two-dimensional domain) into a collection of triangle finite elements (Fig. 5.1). The computer model further subdivides these triangles into nodal domains such as shown in Fig. 5.2. The collection of nodal domains forms a control volume for each nodal point (Fig. 5.3). The computer model then balances the

58
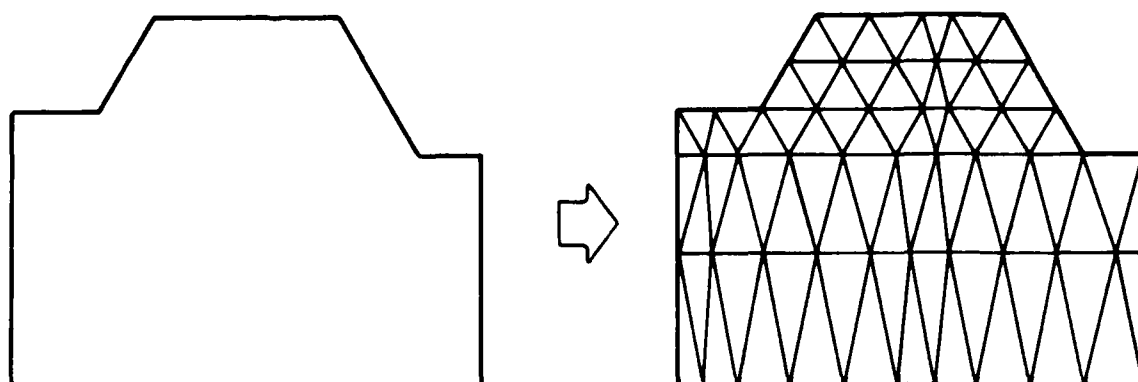
FIG. 5.1. DISCRETIZING THE DOMAIN Ω INTO FINITE ELEMENTS
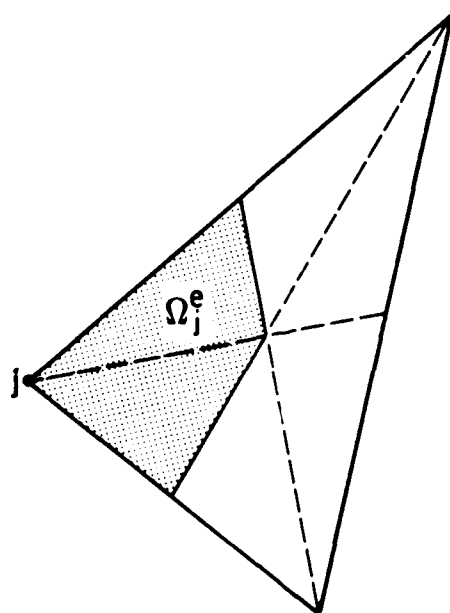
FIG. 5.2. NODAL DOMAIN OF TRIANGLE ELEMENT ASSIGNED TO NODE j
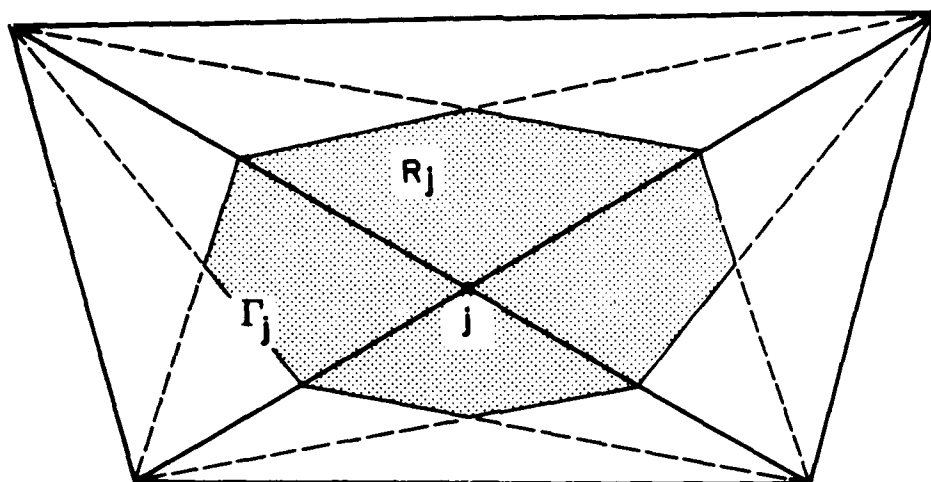
FIG. 5.3. THE AREA OF FLOW-BALANCE FOR NODE j
(FOR HEAT AND SOIL-WATER FLOW)
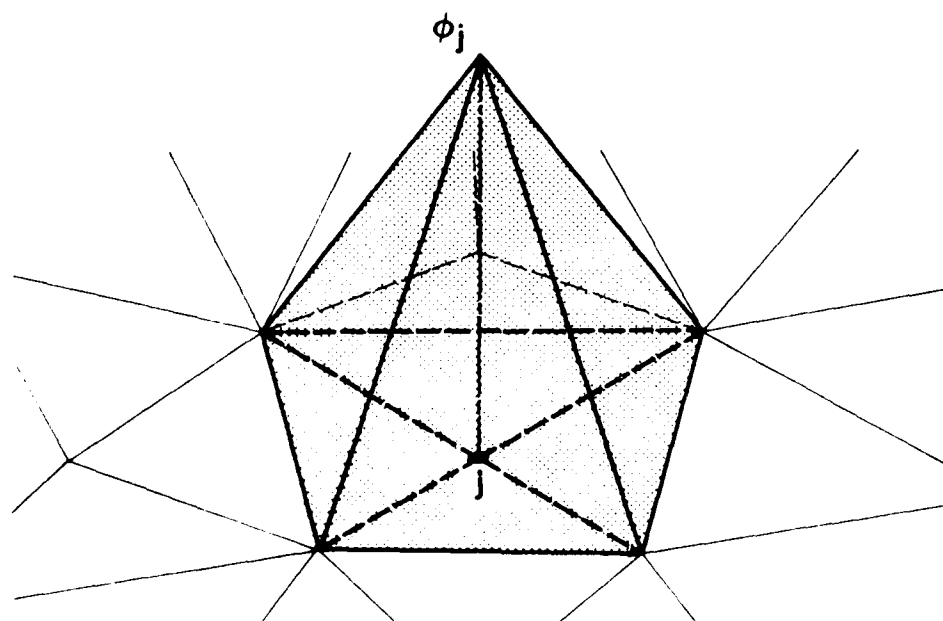
FIG. 5.4. LINEAR DISTRIBUTION OF STATE VARIABLE ϕ_j
(e.g. TEMPERATURE) FROM NODE j VALUE

heat and soil-water flow over each nodal control volume using straight-line interpolation of temperature and soil-water energy head to compute the corresponding rates of flow. This straight-line interpolation function is shown graphically in Fig. 5.4.

Phase Change

Chapter 4 describes the isothermal phase change algorithm used to approximate the freezing and thawing of soil-water. This algorithm is based upon the "lumped-mass" control volume shown in Fig. 5.5 (which conforms geometrically to the control volume used to balance heat and soil-water flow). Figure 5.6 illustrates the budget used for each nodal control volume which accounts for the residual water content (unavailable for freezing), the remaining water content available for freezing, and the ice content. During phase change, the nodal temperature is defined to equal the freezing point depression (usually $0^{\circ}C$).

5.2 MODELING PARAMETERS

The parameters needed for the computer model fall into 3 categories:

    (i)   heat flow parameters

    (ii) soil-water flow parameters

    (iii) phase change parameters

Heat Flow Parameters

Thermal conductivities and heat capacities are required to model heat flow. These parameters can be usually developed from published formulas, or obtained from charts and tables.

Soil-Water Flow Parameters

The soil-water flow model requires information regarding the coefficient and exponent used in the Gardner's function (see chapter 4) relationships for hydraulic conductivity and water content as related to pore pressure.
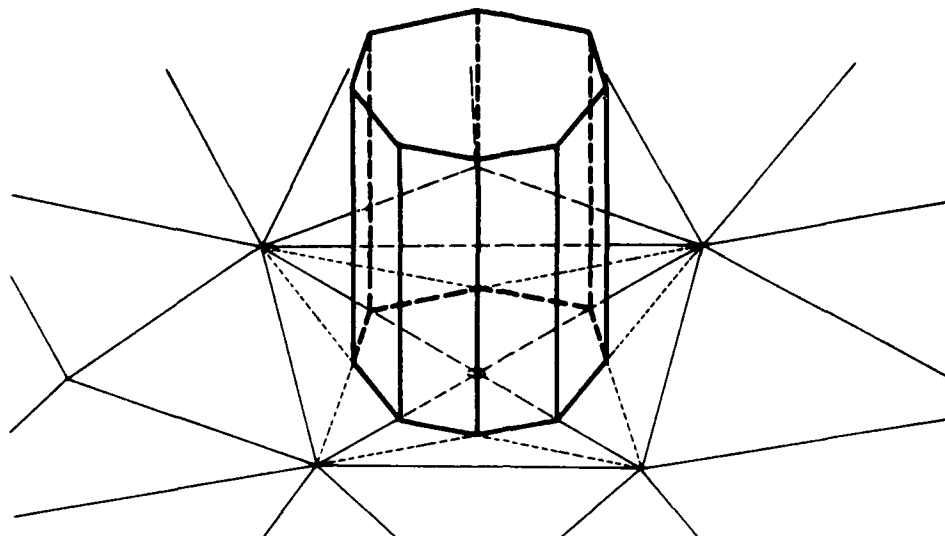
FIG. 5.5. LUMPED MASS CONTROL VOLUME
(USED FOR ICE CONTENT BALANCE)

WATER CONTENT AVAILABLE
FOR FREEZING

ICE CONTENT

RESIDUAL WATER CONTENT,
θ_{RES} (UNAVAILABLE FOR
FREEZING)
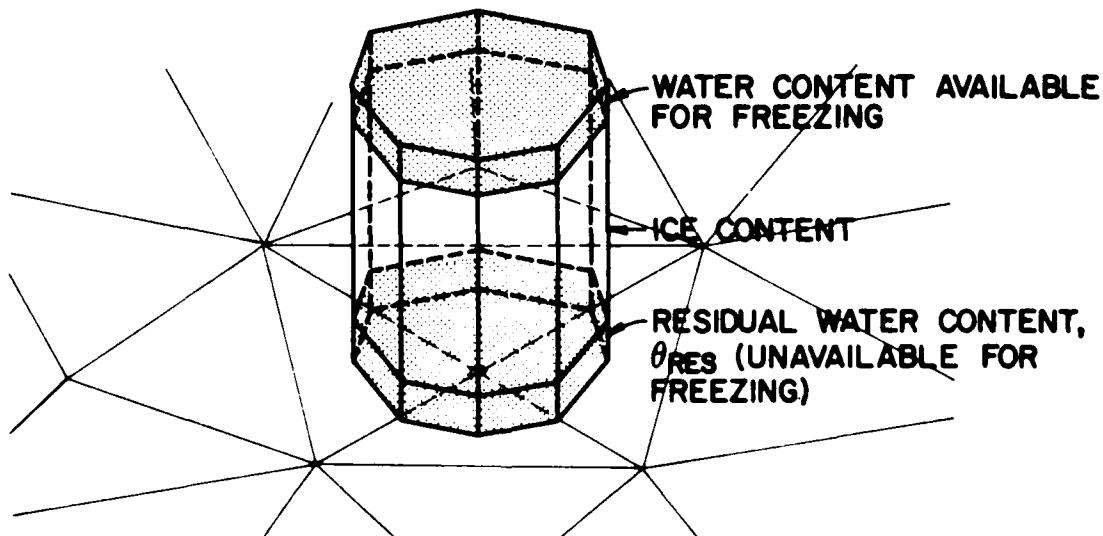
FIG. 5.6. WATER CONTENT BUDGET FOR NODE j
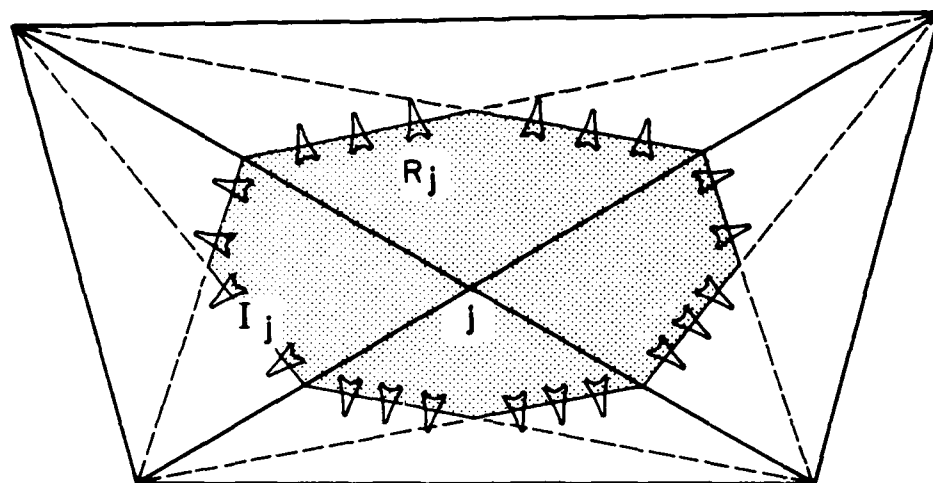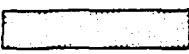
62

Phase Change Parameters

The volumetric latent heat of fusion and freezing point depression are defined by the program user.

Parameter Groups

Rather than enter the several parameters for each finite element, parameter groupings are used to combine similar properties. Two types of groupings are used; namely, element parameter groups and nodal parameter groups.

-Element parameter groups include the conduction parameter data. This enables a better description of conduction values used to compute flow rates across control volume boundaries.

-Nodal parameter groups include the capacitance parameter data. This enables the program user to best define those parameters which are averaged over the control volume area (e.g., heat capacity).

Figure 5.7 demonstrates the flow balance models used, and where the conduction and capacitance parameters are assumed to apply.

5.3 MODELING RESULTS

Nodal Values

The computed results provide nodal point values of temperature, volumetric water content, and volumetric ice content produced at time intervals specified by the program user. A special feature afforded by the program is the ability to also print the previous timestep computed results (along with the current modeling results) in order to compare the change in nodal values of several variables during the recent timestep advancement.

Freezing Front Interpretation

Because the ice content values are specified at nodal points, and due to the mass-lumping budget used for the phase change algorithm (see Fig. 5.6), interpretation of the nodal ice content values are required in order to locate the freezing front (i.e., the line separating the frozen soil from unfrozen soil). Similarly, the temperature values require interpretation in order to locate the $0^{\circ}C$ isotherm (freezing front) at the boundary between the frozen and unfrozen soil regions. The interpretation effort required is directly related to the size of the finite elements used. Large triangular elements necessarily result in large control volume dimensions associated to each nodal point (see Figs. 5.2 and 5.3).

The usual interpretation procedure is to simply assume that the volume of ice estimated to exist in a nodal control volume exists as a single piece, and is located to the side of the control volume which has frozen.

This interpretation can be illustrated in terms of a one-dimensional problem involving rectangular-shaped finite elements. Figure 5.8a shows a nodal point control volume which is initiating freezing of available soil-water. The most recent timestep only evolved enough heat to freeze 10-percent of the soil-water available for phase change. Due to the lumped-mass model, the entire nodal control volume is associated with the nodal point value; hence, the nodal values of temperature and ice content indicate the freezing point depression and 10-percent frozen soil-water, respectively. Thus this information must be interpreted to indicate that the 10-percent frozen available soil-water is in one-piece and located as shown in Fig. 5.8a. Figure 5.8b illustrates the same control volume with 60-percent of the available soil-water frozen. Figure 5.8c illustrates a two-dimensional control volume with 60-percent of the available soil-water frozen.
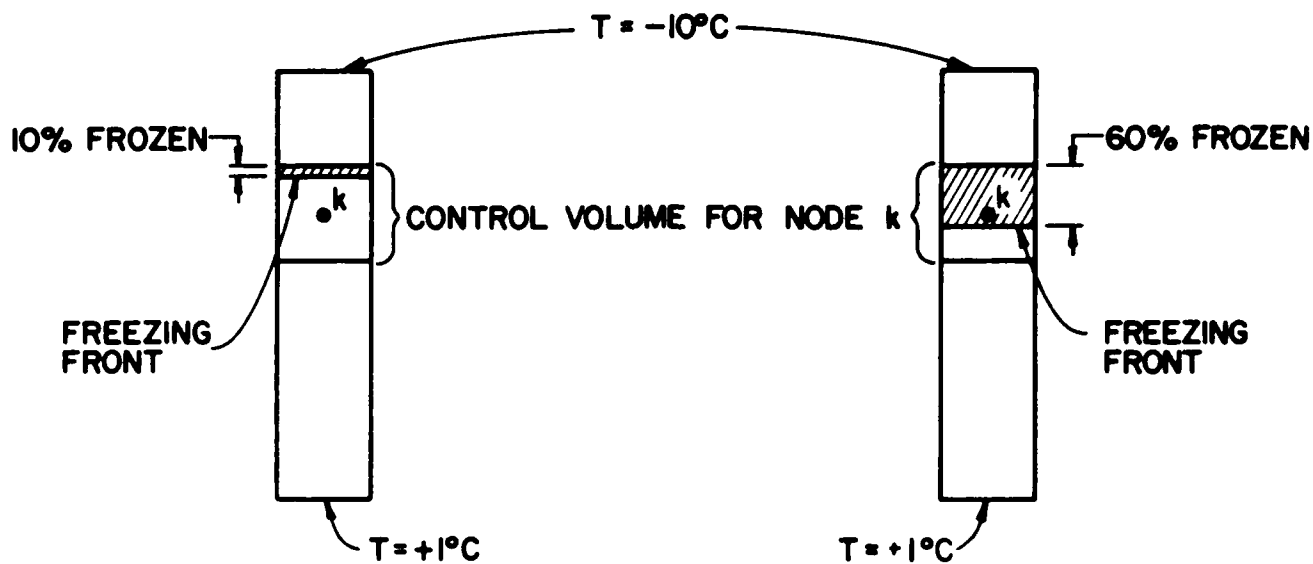
FIG. 5.8a. 10-PERCENT FROZEN
CONTROL VOLUME

FIG. 5.8b. 60-PERCENT FROZEN
CONTROL VOLUME
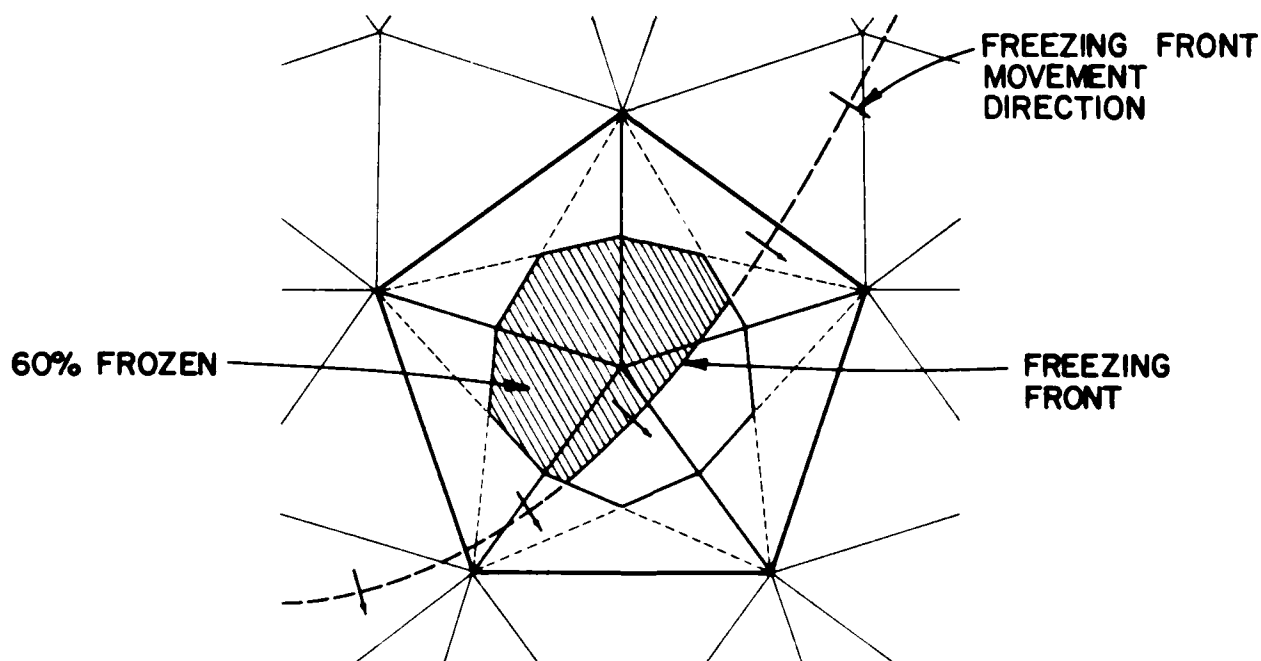
FIG. 5.8c. 60-PERCENT FROZEN CONTROL VOLUME (TRIANGLE ELEMENTS)

5.4 THE TWO-DIMENSIONAL, PHASE CHANGE PROGRAM SYSTEM

The two-dimensional, coupled heat and soil-water flow, with an isothermal phase change approximation computer model is available as the FROST2X series of programs where currently four versions are available (Table 5.1).

Similarly, the PROTO∅ program has been extended to serve special purpose problems where the problem geometry is of a typical character. For example, PROTO1 enables for a quick data file preparation for roadway embankment problems where the interior nodal points and finite elements are developed by the program based on the entry of a few critical geometric coordinates of the problem boundary and locations of regional homogeneity (i.e., identical parameters for heat and soil-water flow).

It is noted that by considering the data entry requirements used in PROTO∅, the engineer can prepare special purpose data file preparation codes which are compatible with the FROST2X series, significantly reducing the data entry requirements associated with the PROTO∅ general purpose code.

5.5 PROTO∅ DATA REQUIREMENTS

The data entry requirements associated with PROTO∅ fall into four broad categories. These data groupings are illustrated in Fig. 5.9.

TABLE 5.1   PROGRAM FROST2X DESCRIPTIONS

PROGRAM	DESCRIPTION
FROST2A	Base Development Version of FROST2X Series.
FROST2B	Two-Dimensional Heat and Soil-Water Flow Model With Isothermal Phase Change Model. Accomodates Heterogeneous But Isotropic Soil Systems. Includes an Apparent Heat Capacity During Phase Change Compatible With PROTO∅ For Data File Preparation.
FROST2C	Extends FROST2B To Include Anisotropic Soil-Water Flow.
FROST2D	Extends FROST2C To Include Vertical Frost Heave and Overburden Effects. Compatible With PROTO1 For Data File Preparation of Roadway Embankment Problems

TABLE 5.2   SUBROUTINE TABULATION

PROGRAM	
FROST2B	Main, Indata, Bcsine, Trans, Phase, Output, Presol, Comb, Finsol.
FROST2D	Main, Indata, Bcsine, Trans, Phase, Output, Presol, Comb, Finsol, Over.

Note: The PROTO∅ program presented in this chapter is compatible with FROST2B.

68

- MODEL CONTROL DATA
    - nodal domain integration mass lumping factor
    - timestep
    - time between global matrix regeneration
    - time of simulation
    - time between output of results
    - model selection:
        - heat and soil-water flow
        - heat flow
        - soil-water flow
        - include isothermal phase change
    - thermal parameters of water and ice
    - number of nodes
    - number of temperature boundary condition nodes
    - number of pore pressure boundary condition nodes
    - number of triangle finite elements

- FINITE ELEMENT PARAMETER GROUPS
    - thermal conductivity of soil
    - heat capacity of soil
    - saturated hydraulic conductivity of soil
    - exponent in Gardner's hydraulic conductivity
    - coefficient in Gardner's hydraulic conductivity
    - hydraulic conductivity ice content correction factor (exponent)

- NODAL POINT PARAMETER GROUPS
    - soil porosity
    - exponent in Gardner's water content
    - coefficient in Gardner's water content
    - frozen soil residual water content
    - heat capacity of control volume

- FINITE ELEMENT NODE NUMBERS AND (x,y) COORDINATE DATA

  NODAL POINT INITIAL CONDITIONS
    - temperature
    - soil-water pore pressure head
    - ice content

- TEMPERATURE BOUNDARY CONDITIONS
    - node number
    - maximum temperature
    - minimum temperature
    - sine period
    - phase shift

- SOIL-WATER PORE PRESSURE BOUNDARY CONDITIONS
    - node number
    - maximum pore pressure head
    - minimum pore pressure head
    - sine period
    - phase shift

FIG. 5.9.   PROGRAM FROST2B DATA REQUIREMENTS

69

5.6 PROTO∅ DATA ENTRY

Program PROTO∅ prompts the model user for all data entries. In the following, the data entry prompts are shown in their order of appearance. Included with the prompts are the associated PROTO∅ variable names. It is noted that several of the prompts include suggested parameter values (for typical soil-water phase change problems), and the range of values allowed for use with program FROST2B.

```
****************************************************************
                        TWO-DIMENSIONAL
                HEAT AND SOIL WATER FLOW MODEL
                 WITH AND WITHOUT PHASE CHANGE
================================================================
                               .
                               .
                         DEVELOPED AT
              UNIVERSITY OF CALIFORNIA, IRVINE.




           PRINCIPAL INVESTIGATOR: GARY L. GUYMON
           PROGRAM DEVELOPMENT: TED V. HROMADKA




                  VERSION DATE: APRIL, 1982
:::::ENTER A [1] TO CONTINUE::::::::::::::::::::::::::::::::::::::::::::
```

```
****************************************************************
              *PROGRAM  PROCESS  SELECTION*
****************************************************************




ENTER PROGRAM PROCESS NUMBER:                          KOPT
     1 = CREATE A NEW DATA BANK
     2 = CONTINUE CREATING A DATA BANK
     3 = EDIT AN EXISTING DATA BANK
     4 = EXIT PROGRAM [PROTOOA]
```

INTRODUCTION:(PROTO0A)
  THIS GENERAL PURPOSE DATA FILE PREPARATION PROGRAM
  REQUIRES:
   1.NO MORE THAN 90 NODAL POINTS.
   2.NO MORE THAN 150 TRIANGULAR FINITE ELEMENTS.
     (THREE VERTEX-LOCATED NODES TO EACH ELEMENT)
   3.ALL COORDINATES ARE IN FIRST QUADRANT.
   4.ALL NODAL POINTS ARE NUMBERED SEQUENTIALLY
     FROM NUMBER 1.
   5.ALL ELEMENTS ARE NUMBERED SEQUENTIALLY FROM
     NUMBER 1.
   6.MATRIX BANDWIDTH MUST NOT EXCEED 18
     (BANDWIDTH = MAXIMUM ARITHMETIC DIFFERENCE BETWEEN
     ANY FINITE ELEMENT NODAL NUMBERS, + 1)

:::::ENTER A [1] TO CONTINUE:::
:::

ENTER NODAL DOMAIN INTEGRATION(NDI) MASS-LUMPING FACTOR: **XNETA**
NOTE:MASS-LUMPING FACTORS FOR NUMERICAL METHODS ARE:
          2 = GALERKIN
          3 = SUBDOMAIN INTEGRATION
       1000 = INTEGRATED FINITE DIFFERENCE
(ALLOWABLE VALUES ARE BETWEEN [1] AND [100000])
:::

ENTER TIMESTEP MAGNITUDE (HOURS):   **DELT**
(CRANK-NICOLSON TIME ADVANCEMENT METHOD IS USED FOR
HEAT TRANSPORT MODEL, FULLY-IMPLICIT TIME ADVANCEMENT
METHOD IS USED FOR SOIL-MOISTURE TRANSPORT MODEL)
:::

DEFINITION OF 'UPDATE' :
IN THIS COMPUTER MODEL ALL THERMAL AND SOIL-MOISTURE
PARAMETERS ARE HELD CONSTANT FOR A USER-SPECIFIED
DURATION OF TIME. THIS DURATION OF TIME IS CALLED THE
THE 'UPDATE PERIOD' AND IS EXPRESSED IN UNITS OF HOURS

ENTER UPDATE PERIOD (HOURS):   **UPDAT**
  (SMALLEST ALLOWABLE VALUE IS [0.100000])
:::

```
-----------------------------------------------------------------
  THE TOTAL COMPUTER MODEL SIMULATION TIME IS
      EXPRESSED IN UNITS OF DAYS
-----------------------------------------------------------------
  ENTER LENGTH OF SIMULATION (DAYS):                      ENSIM
   (SMALLEST ALLOWABLE VALUE IS [      0.004167])



  ::::::::::::::::::::::::::::::::::::::::::::::::::::::::::::::::::::::::::::::



-----------------------------------------------------------------
    COMPUTER SOLUTIONS ARE PRINTED ACCORDING TO A USER
    SPECIFIED SIMULATION INTERVAL.THIS OUTPUT TIME
    INTERVAL IS EXPRESSED IN UNITS OF DAYS
-----------------------------------------------------------------
  ENTER TIME INTERVAL BETWEEN COMPUTER OUTPUTS (DAYS):     OUT
   (SMALLEST ALLOWABLE VALUE IS [     0.004167])
   (LARGEST ALLOWABLE VALUE IS [   2.0000])
```

```
=================================================================
 NDI MASS LUMPING FACTOR =     1000.000         (INPUT EXAMPLE)
 TIME STEP MAGNITUDE =     0.100000 HOURS
 UPDATE PERIOD =    0.100000 HOURS
 LENGTH OF SIMULATION =    2.000000 DAYS
 TIME INTERVAL BETWEEN COMPUTER OUTPUTS =     1.000000 DAYS
-----------------------------------------------------------------




:::SELECT DATA OPTION NUMBER:::::::::::::::::::::::::::::::::::::::::::::::::::
    1 = ACCEPT DATA AND CONTINUE
    2 = DATA IS UNACCEPTABLE; REINPUT LAST SEQUENCE
    3 = ACCEPT DATA AND TERMINATE PROCESS
```

```
*************************************************************************
                    PROGRAM MODEL SELECTIONS
*************************************************************************




========================================================================
ENTER PROGRAM MODEL OPTION NUMBER:                              NPATHI
      0 = HEAT AND MOISTURE TRANSPORT
      1 = HEAT TRANSPORT ONLY
      2 = MOISTURE TRANSPORT ONLY
========================================================================
::::::::::::::::::::::::::::::::::::::::::::::::::::::::::::::::::::::::::::
```

```
::::::::::::::::::::::::::::::::::::::::::::::::::::::::::::::::::::::::::::


-------------------------------------------------------------------------
IN THIS MODEL, SOIL WATER PHASE CHANGE IS ASSUMED
TO OCCUR ISOTHERMALLY. SOIL-WATER AND ICE CONTENTS
ARE ACCOUNTED FOR BY A SIMPLE CONTROL VOLUME
BUDGET KEEPING. A CONTROL VOLUME IS DEFINED FOR
EACH NODAL POINT BY THE SUMMATION OF EACH
TRIANGLE ELEMENT NODAL DOMAIN ASSOCIATED TO
EACH NODE.

ENTER PROGRAM SOIL-MOISTURE FREEZING/THAWING MODEL      IPHASE
OPTION NUMBER:
      0 = EXCLUDE ISOTHERMAL FREEZING/THAWING MODEL.
      1 = INCLUDE ISOTHERMAL FREEZING/THAWING MODEL.
```

```
================================================================
 USER SPECIFIED MODEL SELECTIONS:                  (INPUT EXAMPLE)
 HEAT AND MOISTURE TRANSPORT
 INCLUDE FREEZING/THAWING MODEL
----------------------------------------------------------------



:::SELECT DATA OPTION NUMBER:::::::::::::::::::::::::::::::::::::::::::
    1 = ACCEPT DATA AND CONTINUE
    2 = DATA IS UNACCEPTABLE; REINPUT LAST SEQUENCE
    3 = ACCEPT DATA AND TERMINATE PROCESS
```

```
================================================================
                 *SPECIFIED THERMAL INFORMATION*
================================================================



ENTER FREEZING POINT DEPRESSION OF WATER (C DEGREES):          TFPD
NOTE:
     ENTER [0] FOR METRIC SYSTEM
(ALLOWABLE VALUES ARE BETWEEN [-100] AND [100])



::::::::::::::::::::::::::::::::::::::::::::::::::::::::::::::::::::::::
```

VOLUMETRIC HEAT CAPACITY OF WATER:(cal/cm**3)
NOTE:ENTER [1.00] FOR METRIC SYSTEM   **CW**

::

ENTER VOLUMETRIC HEAT CAPACITY OF ICE:(cal/cm**3)
NOTE:ENTER [0.46] FOR METRIC SYSTEM   **CI**

::

ENTER THERMAL CONDUCTIVITY OF WATER:(cal/hr.cm.c)   **TKW**
NOTE:ENTER [4.8] FOR METRIC SYSTEM

::

ENTER THERMAL CONDUCTIVITY OF ICE:(cal/hr.cm.c)   **TKI**
NOTE:ENTER [19.0] FOR METRIC SYSTEM

::

ENTER VOLUMETRIC LATENT HEAT OF FUSION:(cal/cm**3)   **XL**
NOTE:ENTER [80.] FOR METRIC SYSTEM

```
================================================================
                *SPECIFIED THERMAL INFORMATION*   (INPUT EXAMPLE)
THE THERMAL FREEZING POINT DEPRESSION OF WATER =    0.000000
HEAT CAPACITY OF WATER =  1.0000
HEAT CAPACITY OF ICE =  0.4600
THERMAL CONDUCTIVITY OF WATER =  4.8000
THERMAL CONDUCTIVITY OF ICE = 19.0000
LATENT HEAT OF FUSION =   80.000000
----------------------------------------------------------------



:::SELECT DATA OPTION NUMBER:::::::::::::::::::::::::::::::::::::::::::::::
    1 = ACCEPT DATA AND CONTINUE
    2 = DATA IS UNACCEPTABLE; REINPUT LAST SEQUENCE
    3 = ACCEPT DATA AND TERMINATE PROCESS
```

```
----------------------------------------------------------------
                    NODAL DOMAIN INTEGRATION
             MODEL PROBLEM-DEFINITION INFORMATION
----------------------------------------------------------------




::::::::::::::::::::::::::::::::::::::::::::::::::::::::::::::::::::::::::


ENTER NUMBER OF NODAL POINTS IN THE MODEL:                      NNOD
 ALLOWABLE VALUES ARE BETWEEN [4] AND [90])
    ::::::::::::::::::::::::::::::::::::::::::::::::::::::::::::::::::::::
```

ENTER NUMBER OF NODAL POINTS WITH SPECIFIED TEMPERATURE   **NNBCT**
BOUNDARY CONDITIONS:
    (ALLOWABLE VALUES ARE BETWEEN [1] AND [42])
::

ENTER NUMBER OF NODAL POINTS WITH SPECIFIED   **NNBCP**
SOIL-WATER PORE PRESSURE HEAD BOUNDARY CONDITIONS:
    (ALLOWABLE VALUES ARE BETWEEN [1] AND [42])
::

ENTER NUMBER OF TRIANGLE FINITE ELEMENTS IN THE MODEL: **NEL**
(ALLOWABLE VALUES ARE BETWEEN [2] AND [150])

==
NUMBER OF FINITE ELEMENTS IN THE MODEL = 40   **(INPUT EXAMPLE)**
NUMBER OF NODAL POINTS IN THE MODEL = 42
NUMBER OF NODES WITH SPECIFIED TEMPERATURE =   4
NUMBER OF NODES WITH SPECIFIED PORE PRESSURE HEAD =   2

:::SELECT DATA OPTION NUMBER:::
    1 = ACCEPT DATA AND CONTINUE
    2 = DATA IS UNACCEPTABLE; REINPUT LAST SEQUENCE
    3 = ACCEPT DATA AND TERMINATE PROCESS

```
*****************************************************************************
                   *ELEMENT PARAMETER GROUPING INFORMATION*
*****************************************************************************


----------------------------------------------------------------------------
        IN THIS COMPUTER MODEL,FINITE ELEMENT PARAMETER
   INFORMATION IS GROUPED INTO 'PARAMETER GROUPINGS' WHEREBY
   THE APPROPRIATE GROUPING NUMBER IS USED TO SPECIFY
   PARAMETER INFORMATION FOR EACH FINITE ELEMENT.THEREFORE,
   THE USER SPECIFIES A GROUPING NUMBER RATHER THAN ENTERING
   OFTEN-REPETATIVE PARAMETER DATA FOR EACH ELEMENT. UP TO
   [10] ELEMENT-PARAMETER GROUPINGS MAY BE DEFINED.
----------------------------------------------------------------------------

   ENTER THE NUMBER OF ELEMENT-PARAMETER GROUPINGS:            NEPG
   (ALLOWABLE VALUES ARE BETWEEN [1] AND [10])
   :::::::::::::::::::::::::::::::::::::::::::::::::::::::::::::::::::::::::::
```

```
----------------------------------------------------------------------------
      ENTER ELEMENT-PARAMETER GROUPING #[ 1 ]INFORMATION :
----------------------------------------------------------------------------
   :::::::::::::::::::::::::::::::::::::::::::::::::::::::::::::::::::::::::::


   ENTER THERMAL CONDUCTIVITY OF SOIL (cal/hr.cm.c):          PARELE(J,1)
   :::::::::::::::::::::::::::::::::::::::::::::::::::::::::::::::::::::::::::


   ENTER VOLUMETRIC HEAT CAPACITY OF SOIL (cal/cm**3):        PARELE(J,2)
   :::::::::::::::::::::::::::::::::::::::::::::::::::::::::::::::::::::::::::


   ENTER THE SATURATED HYDRAULIC CONDUCTIVITY OF SOIL(cm/hr): PARELE(J,3)
   :::::::::::::::::::::::::::::::::::::::::::::::::::::::::::::::::::::::::::
```

ENTER EXPONENT OF PORE PRESSURE HEAD IN GARDNERS   **PARELE(J,4)**
HYDRAULIC CONDUCTIVITY FUNCTION:
::

ENTER MULTIPLIER OF PORE PRESSURE HEAD IN GARDNERS   **PARELE(J,5)**
HYDRAULIC CONDUCTIVITY FUNCTION:
::

ENTER HYDRAULIC CONDUCTIVITY EXPONENT ADJUSTMENT   **PARELE(J,6)**
FACTOR 'E':
NOTE:
     ADJUSTMENT FACTOR = 10.**(-E * ICE CONTENT)

===
 ELEMENT-PARAMETER GROUPING # 1   **(INPUT EXAMPLE)**
 THERMAL CONDUCTIVITY OF SOIL = 14.0000
 VOLUMETRIC HEAT CAPACITY OF SOIL = 0.5000
 SATURATED HYDRAULIC CONDUCTIVITY OF SOIL = 0.1000
 EXPONENT OF PORE PRESSURE HEAD IN GARDNERS CONDUCTIVITY FUNCTION = 1.2000
 MULTIPLIER OF PORE PRESSURE HEAD IN GARDNERS CONDUCTIVITY FUNCTION = 0.4000
 HYDRAULIC CONDUCTIVITY EXPONENT ADJUSTMENT FACTOR =   1.000

:::SELECT DATA OPTION NUMBER::
     1 = ACCEPT DATA AND CONTINUE
     2 = DATA IS UNACCEPTABLE; REINPUT LAST SEQUENCE
     3 = ACCEPT DATA AND TERMINATE PROCESS

```
          ------------------------------------------------------------------
              SIMILAR TO THE 'ELEMENT PARAMETER GROUPINGS',FURTHER
          PARAMETER INFORMATION IS DEFINED FOR NODAL POINTS.
          THIS 'NODAL POINT PARAMETER GROUPING' INFORMATION IS
          IDENTIFIED BY A NODAL-PARAMETER GROUPING NUMBER.
          THESE SETS OF PARAMETERS ARE USED TO MORE PRECISELY
          DEFINE ASSUMED CONSTANT PARAMETERS ON A CONTROL
          VOLUME BASIS FOR EACH NODAL POINT RATHER THAN
          SIMPLY AVERAGING FINITE ELEMENT PARAMETERS
          FOR EACH NODAL CONTROL VOLUME.
          UP TO [10] NODAL-PARAMETER GROUPINGS MAY BE DEFINED.
          ------------------------------------------------------------------
          ENTER THE NUMBER OF NODAL-PARAMETER GROUPINGS:              NNPG
          (ALLOWABLE VALUES ARE BETWEEN [1] AND [10])
          :::::::::::::::::::::::::::::::::::::::::::::::::::::::::::::::::::::
```

```
          ------------------------------------------------------------------
              ENTER NODAL-PARAMETER GROUPING #[ 1 ]INFORMATION:
          ------------------------------------------------------------------
          :::::::::::::::::::::::::::::::::::::::::::::::::::::::::::::::::::::


          ENTER THE SATURATED VOLUMETRIC MOISTURE CONTENT OF SOIL:   PARNOD(J,1)
          (ALLOWABLE VALUES ARE BETWEEN [0] AND [1] cm**3/cm**3)
          :::::::::::::::::::::::::::::::::::::::::::::::::::::::::::::::::::::


          ENTER MULTIPLIER OF PORE PRESSURE HEAD IN GARDNERS        PARNOD(J,2)
          VOLUMETRIC MOISTURE CONTENT FUNCTION:
          :::::::::::::::::::::::::::::::::::::::::::::::::::::::::::::::::::::
```

ENTER EXPONENT OF PORE PRESSURE HEAD IN GARDNERS   **PARNOD(J,3)**
VOLUMETRIC MOISTURE CONTENT FUNCTION:
::

IN THIS MODEL, IT IS ASSUMED THAT NOT ALL OF THE
SOIL WATER IS AVAILABLE FOR PHASE CHANGE. THIS
UNAVAILABLE SOIL WATER IS CALLED A VOLUMETRIC
UNFROZEN WATER CONTENT FACTOR.

ENTER THE ASSUMED VOLUMETRIC UNFROZEN WATER CONTENT   **PARNOD(J,4)**
FACTOR OF THE SOIL:
(ALLOWABLE VALUES ARE BETWEEN [0] AND [1])
::

ENTER THE VOLUMETRIC HEAT CAPACITY OF THE SOIL(cal/cm**3): **PARNOD(J,5)**

===
NODAL-PARAMETER GROUPING # 1   **(INPUT EXAMPLE)**
SATURATED VOLUMETRIC MOISTURE CONTENT OF SOIL = 0.4000
MULTIPLER OF PORE PRESSURE IN GARDNERS MOISTURE CONTENT FUNCTION = 0.0040
EXPONENT OF PORE PRESSURE IN GARDNERS MOISTURE CONTENT FUNCTION = 1.2000
VOLUMETRIC UNFROZEN WATER CONTENT FACTOR =   0.1500
VOLUMETRIC HEAT CAPACITY OF THE SOIL = 0.5000

:::SELECT DATA OPTION NUMBER::
    1 = ACCEPT DATA AND CONTINUE
    2 = DATA IS UNACCEPTABLE; REINPUT LAST SEQUENCE
    3 = ACCEPT DATA AND TERMINATE PROCESS

```
====================================================================
********************************************************************
                    *NODAL COORDINATE INFORMATION*
********************************************************************

::::::::::::::::::::::::::::::::::::::::::::::::::::::::::::::::::::::


    ENTER NODE NUMBER [  1] INFORMATION:


  ENTER X-COORDINATE OF THE NODE:                        DATNOD(J,1)
  NOTE: X-COORDINATE MUST BE IN FIRST QUADRANT
  ::::::::::::::::::::::::::::::::::::::::::::::::::::::::::::::::::::::


  ENTER Y-COORDINATE OF THE NODE:                        DATNOD(J,2)
  NOTE: Y-COORDINATE MUST BE IN FIRST QUADRANT
  ::::::::::::::::::::::::::::::::::::::::::::::::::::::::::::::::::::::


  ENTER NODAL-PARAMETER GROUP NUMBER:                    DATNOD(J,3)
     (ALLOWABLE VALUES ARE BETWEEN [1] AND [  1])
```

```
====================================================================
  NODE NUMBER    i                            (INPUT EXAMPLE)
  X-COORDINATE =     0.000
  Y-COORDINATE =  40.000
  NODAL-PARAMETER GROUP NUMBER =    1.000
  ------------------------------------------------------------------


:::SELECT DATA OPTION NUMBER::::::::::::::::::::::::::::::::::::::::::::::::::::
     1 = ACCEPT DATA AND CONTINUE
     2 = DATA IS UNACCEPTABLE; REINPUT LAST SEQUENCE
     3 = ACCEPT DATA AND TERMINATE PROCESS
```

83

```
**********************************************************************
                   *PROGRAM PROCESS SELECTION*
                      (PROGRAM [PROTOOB])
**********************************************************************




ENTER PROGRAM PROCESS NUMBER:                              KOPT
     1 = CREATE A NEW DATA BANK (CONTINUATION OF PROTOOA)
     2 = CONTINUE CREATING A DATA BANK (CONTINUATION OF PROTOOB)
     3 = EDIT AN EXISTING DATA BANK
     4 = EXIT PROGRAM [PROTOOB]
==================================================================
```

```
**********************************************************************
                  *FINITE ELEMENT INFORMATION*
**********************************************************************
                              .
                              .
------------------------------------------------------------------
     THE PROBLEM DOMAIN IS ASSUMED DISCRETIZED INTO
     TRIANGLE-SHAPED FINITE ELEMENTS. SINCE THIS
     DATA PREPARATION PROGRAM IS FOR AN ARBITRARY
     DOMAIN, THE USER MUST ENTER ALL GEOMETRIC
     INFORMATION INCLUDING THE PROBLEM MESH.
     EACH FINITE ELEMENT HAS 3 NODAL POINTS ,THESE
     VERTEX NODAL POINTS MUST BE LISTED IN COUNTER
     CLOCKWISE ORDER.
------------------------------------------------------------------
::::ENTER A [1] TO CONTINUE::::::::::::::::::::::::::::::::::::::::::


::::::::::::::::::::::::::::::::::::::::::::::::::::::::::::::::::::::::
```

```
:::::::::::::::::::::::::::::::::::::::::::::::::::::::::::::::::::::::::::
----------------------------------------------------------------------
    ENTER ELEMENT NUMBER [  1] INFORMATION:
----------------------------------------------------------------------


  ENTER THE NODE NUMBER OF THE FIRST VERTEX:               IDTELE(J,1)
:::::::::::::::::::::::::::::::::::::::::::::::::::::::::::::::::::::::::::


  ENTER THE NODE NUMBER OF THE SECOND VERTEX:              IDTELE(J,2)
:::::::::::::::::::::::::::::::::::::::::::::::::::::::::::::::::::::::::::


  ENTER THE NODE NUMBER OF THE THIRD VERTEX:               IDTELE(J,3)
:::::::::::::::::::::::::::::::::::::::::::::::::::::::::::::::::::::::::::


  ENTER ELEMENT-PARAMETER GROUP NUMBER:                    IDTELE(J,4)
=======================================================================
```

```
=======================================================================
  ELEMENT NUMBER   1:                          (INPUT EXAMPLE)

  NODE NUMBER OF THE FIRST  VERTEX =  1
  NODE NUMBER OF THE SECOND VERTEX =  3
  NODE NUMBER OF THE THIRD VERTEX =  2
  ELEMENT-PARAMETER GROUP NUMBER =  1
----------------------------------------------------------------------




:::SELECT DATA OPTION NUMBER::::::::::::::::::::::::::::::::::::::::::::::
    1 = ACCEPT DATA AND CONTINUE
    2 = DATA IS UNACCEPTABLE; REINPUT LAST SEQUENCE
    3 = ACCEPT DATA AND TERMINATE PROCESS
:::::::::::::::::::::::::::::::::::::::::::::::::::::::::::::::::::::::::::
```

```
****************************************************************************
  ENTER INITIAL TEMPERATURE ,INITIAL PORE PRESSURE HEAD,
  AND INITIAL VOLUMETRIC ICE CONTENT OF EACH NODE AS
  REQUESTED:
****************************************************************************
::::::::::::::::::::::::::::::::::::::::::::::::::::::::::::::::::::::::::::::
```

```
    ENTER INITIAL TEMPERATURE AT NODE :  1                    TOLD(J)
::::::::::::::::::::::::::::::::::::::::::::::::::::::::::::::::::::::::::::::
```

```
    ENTER INITIAL PORE PRESSURE HEAD AT NODE :  1            POLD(J)
::::::::::::::::::::::::::::::::::::::::::::::::::::::::::::::::::::::::::::::
```

```
    ENTER INITIAL VOLUMETRIC ICE CONTENT AT NODE :  1      XICEOL(J)
==========================================================================
```

```
NODE NUMBER   1:                                      (INPUT EXAMPLE)

INITIAL TEMPERATURE OF THE NODE =   1.0000
INITIAL PRESSURE HEAD OF THE NODE =    -10.0000
INITIAL VOLUMETRIC ICE CONTENT OF THE NODE =  0.0000


----------------------------------------------------------------------



:::SELECT DATA OPTION NUMBER::::::::::::::::::::::::::::::::::::::::::::::::::::
    1 = ACCEPT DATA AND CONTINUE
    2 = DATA IS UNACCEPTABLE; REINPUT LAST SEQUENCE
    3 = ACCEPT DATA AND TERMINATE PROCESS
::::::::::::::::::::::::::::::::::::::::::::::::::::::::::::::::::::::::::::::::
```

```
****************************************************************************
            *SPECIFIED BOUNDARY CONDITION INFORMATION*
****************************************************************************




NOTE:ALL SPECIFIED BOUNDARY CONDITION (TEMPERATURE AND
     PORE-PRESSURE HEAD) ARE EXPRESSED IN TERMS OF A
     SINUSOIDAL VARIATION.




::::::::::::::::::::::::::::::::::::::::::::::::::::::::::::::::::::::::::::::


ENTER NODE NUMBER WITH SPECIFIED THERMAL BOUNDARY CONDITION    NBCT(J)
( AND SPECIFY THE TEMPERATURE FUNCTION):
::::::::::::::::::::::::::::::::::::::::::::::::::::::::::::::::::::::::::::::
```

```
ENTER MAXIMUM TEMPERATURE ON THE SINE CURVE DESCRIBING        BCT(J,1)
THE BOUNDARY CONDITION AT NODE : 1
::::::::::::::::::::::::::::::::::::::::::::::::::::::::::::::::::::::::::::::


ENTER MINIMUM TEMPERATURE (IN THE SINE CURVE DESCRIBING       BCT(J,2)
THE BOUNDARY CONDITION AT NODE : 1
::::::::::::::::::::::::::::::::::::::::::::::::::::::::::::::::::::::::::::::


ENTER THE PERIOD(HOURS) OF THE SINE CURVE DESCRIBING          BCT(J,3)
THE TEMPERATURE BOUNDARY CONDITION AT NODE : 1
::::::::::::::::::::::::::::::::::::::::::::::::::::::::::::::::::::::::::::::


ENTER THE PHASE SHIFT(HOURS) OF THE SINE CURVE.               BCT(J,4)
DESCRIBING THE TEMPERATURE BOUNDARY CONDITION AT  NODE :  1
--------------------------------------------------------------------------
THREE POSSIBLE VALUES CAN BE USED TO DESCRIBED THE
SHIFTING SINE CURVE :
   1.ENTERING A "O" VALUE: THIS IS A STANDARD SINE CURVE.
   2.ENTERING A "POSITIVE" VALUE: THIS SINE CURVE IS BEING SHIFTED BACKWARD,
     BY THAT ENTERED VALUE, FROM THE STANDARD SINE CURVE.
   3.ENTERING A "NEGATIVE" VALUE: THIS SINE CURVE IS BEING SHIFTED FORWARD,
     BY THAT ENTERED VALUE, FROM THE STANDARD SINE CURVE.
--------------------------------------------------------------------------
```

87

```
-------------------------------------------------------------------
-------------------------------------------------------------------
NODE NUMBER WITH SPECIFIED TEMPERATURE =  1           (INPUT EXAMPLE)

MAXIMUM TEMPERATURE ON THE SINE CURVE = -5.0000
MINIMUM  TEMPERATURE ON THE SINE CURVE = -5.0000
THE PERIOD OF THE SINE CURVE = 48.0000
THE PHASE SHIFT OF THE SINE CURVE =  0.0000
-------------------------------------------------------------------




:::SELECT DATA OPTION NUMBER:::::::::::::::::::::::::::::::::::::::::::::
    1 = ACCEPT DATA AND CONTINUE
    2 = DATA IS UNACCEPTABLE; REINPUT LAST SEQUENCE
    3 = ACCEPT DATA AND TERMINATE PROCESS
::::::::::::::::::::::::::::::::::::::::::::::::::::::::::::::::::::::::::::
```

```
===================================================================
::::::::::::::::::::::::::::::::::::::::::::::::::::::::::::::::::::::::::::


ENTER NODE NUMBER WITH SPECIFIED SOIL-MOISTURE              NBCP(J)
BOUNDARY CONDITION (AND DEFINE THE PORE-PRESSURE HEAD
FUNCTION AT THAT NODAL POINT):
::::::::::::::::::::::::::::::::::::::::::::::::::::::::::::::::::::::::::::


ENTER MAXIMUM PORE PRESSURE HEAD ON THE SINE CURVE         BCP(J,1)
DESCRIBING THE BOUNDARY CONDITION AT NODE : 41
::::::::::::::::::::::::::::::::::::::::::::::::::::::::::::::::::::::::::::


ENTER MINIMUM PORE PRESSURE HEAD ON THE SINE CURVE         BCP(J,2)
DESCRIBING THE BOUNDARY CONDITION AT NODE : 41
::::::::::::::::::::::::::::::::::::::::::::::::::::::::::::::::::::::::::::
```

ENTER THE PERIOD(HOURS) OF THE SINE CURVE DESCRIBING   **BCP(J,3)**
THE PORE PRESSURE HEAD BOUNDARY CONDITION AT NODE : 41
::

ENTER THE PHASE SHIFT(HOURS) OF THE SINE CURVE
DESCRIBING THE PORE PRESSURE HEAD BOUNDARY CONDITION   AT NODE : 41

THREE POSSIBLE VALUES CAN BE USED TO DESCRIBED THE   **BCP(J,4)**
SHIFTING SINE CURVE :
   1.ENTERING A "0" VALUE: THIS IS A STANDARD SINE CURVE.
   2.ENTERING A "POSITIVE" VALUE: THIS SINE CURVE IS BEING SHIFTED BACKWARD,
     BY THAT ENTERED VALUE, FROM THE STANDARD SINE CURVE.
   3.ENTERING A "NEGATIVE" VALUE: THIS SINE CURVE IS BEING SHIFTED FORWARD,
     BY THAT ENTERED VALUE, FROM THE STANDARD SINE CURVE.

NODE NUMBER WITH SPECIFIED PORE PRESSURE HEAD = 41   **(INPUT EXAMPLE)**

MAXIMUM PORE PRESSURE HEAD ON THE SINE CURVE =-10.0000
MINIMUM PORE PRESSURE HEAD ON THF SINE CURVE =-10.0000
THE PERIOD OF THE SINE CURVE =   48.0000
THE PHASE SHIFT OF THE SINE CURVE =   0.0000

:::SELECT DATA OPTION NUMBER:::
    1 = ACCEPT DATA AND CONTINUE
    2 = DATA IS UNACCEPTABLE; REINPUT LAST SEQUENCE
    3 = ACCEPT DATA AND TERMINATE PROCESS
:::

```
ENTER THE MODEL RESULTS OUTPUT OPTION NUMBER:                      KOLD
    0 = PRINT PREUPDATE TEMPERATURE AND PREUPDATE
        PORE PRESSURE HEAD
    1 = DO NOT PRINT PREUPDATE TEMPERATURE AND PREUPDATE
        PORE PRESSURE HEAD WITH THE OUTPUT.


END OF FROST2B.DATA FILE
```
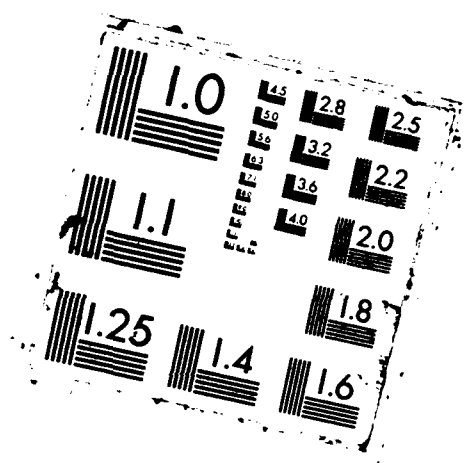
END
9-87
DTIC

5.7 APPLICATIONS

Three example problems are presented which illustrate the data file development by use of PROTO∅, and the performance of the program FROST2B.

Heat Flow Application

A one-dimensional domain of unit length is discretized by 8 triangle finite elements as shown in Fig. 5.10a. At time t=0, the temperature is given by T(x)=1. Boundary conditions are given at x=0 and x=1 by T(x=0)=T(x=1)=0. Using a normalized timestep of t=0.01, the computed results from FROST2B and the exact solution (Myers, 1971) are shown in Fig. 5.10b. The data file prepared by PROTO∅ is shown in Fig. 5.11.

Soil-Water Flow Application

A vertical homogeneous soil column is discretized by triangle finite elements as shown in Fig. 5.12a. A water table forms the base of a steady state 45-degree pore-pressure head profile through the vertical column. The column is insulated on both sides. The top of the column is suddenly flooded at a uniform depth of 2 cm. of water. The FROST2B modeling results are shown in Fig. 5.12b. The data file developed from PROTO∅ is shown in Fig. 5.13.

Phase Change Model Application

The vertical column of Fig. 5.12a is now considered with respect to soil- water freezing. Initially, the column is at a uniform temperature of $+0.1^{O}C$. The top of the column is suddenly set at a constant temperature of $-5^{O}C$. The FROST2B modeling results are shown in Fig. 5.14. The data file developed by PROTO∅ is shown in Fig. 5.15.
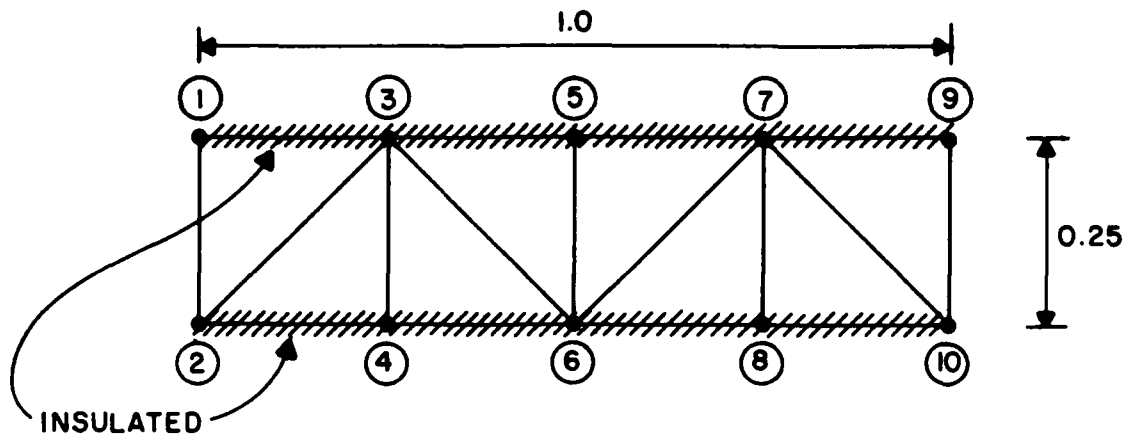
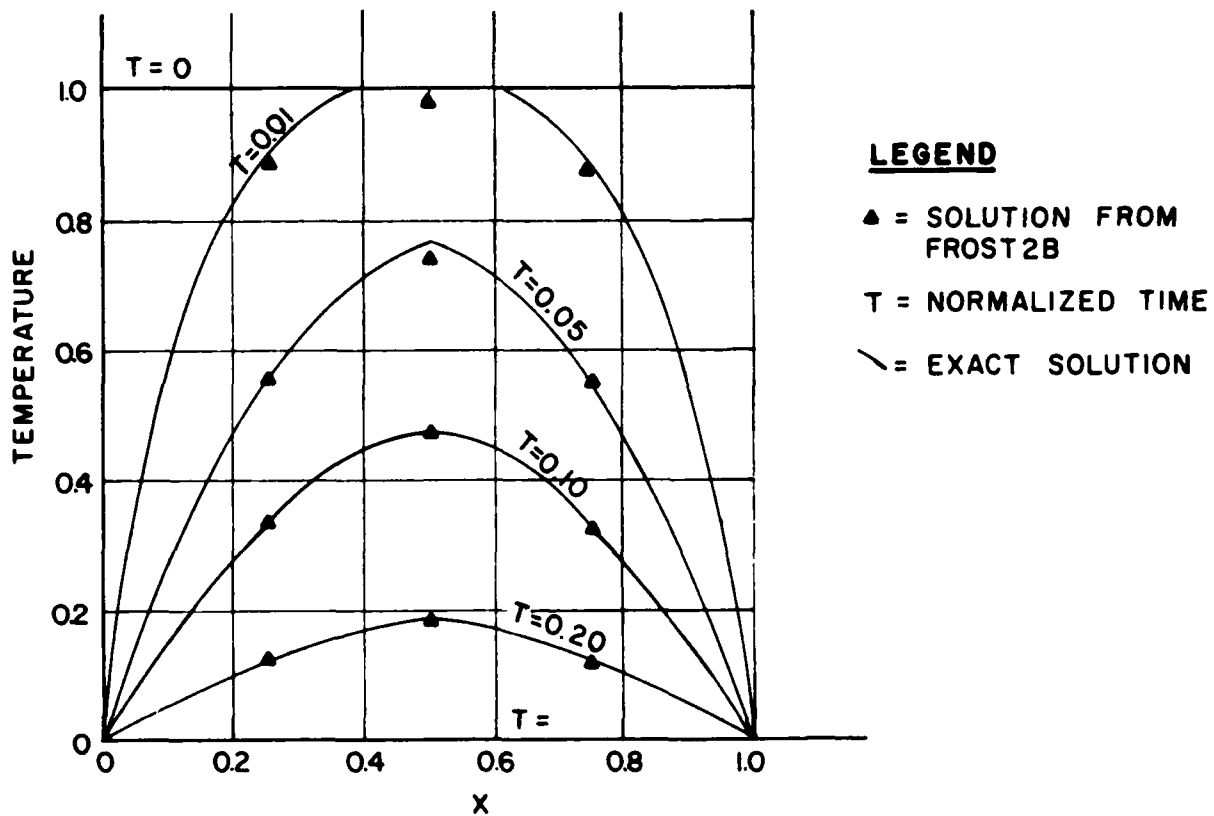FIG. 5.10a HEAT FLOW EXAMPLE PROBLEM

LEGEND

▲ = SOLUTION FROM FROST2B

T = NORMALIZED TIME

╲ = EXACT SOLUTION

FIG. 5.10b HEAT FLOW EXAMPLE PROBLEM SOLUTION

```
1000.000
    0.01000      1   100      10
1   0   1
    0.00000        1.00000        1.00000        1.00000        1.00000        1.00000
     4      0
10      8      1      1
0.40000001    0.00400000    1.20000005    0.15000001    1.00000000
0.00000000    0.00000000    0.00000000    0.00000000    0.00000000


0.00000000    0.00000000    0.00000000    0.00000000    0.00000000
1.00000000    1.00000000    0.10000000    1.20000005    0.40000001    1.00000000
0.00000000    0.00000000    0.00000000    0.00000000    0.00000000    0.00000000
0.00000000    0.00000000    0.00000000    0.00000000    0.00000000    0.00000000
        0.00000        0.25000    1.0
        0.00000        0.00000    1.0
        0.25000        0.25000    1.0
        0.25000        0.00000    1.0
        0.50000        0.25000    1.0
        0.50000        0.00000    1.0
        0.75000        0.25000    1.0
        0.75000        0.00000    1.0
        1.00000        0.25000    1.0
        1.00000        0.00000    1.0
        0.00000        0.00000    0.0
        0.00000        0.00000    0.0
    1       2       3       1
    3       2       4       1
    4       6       3       1
    3       6       5       1
    5       6       7       1
    7       6       8       1
    8      10       7       1
    7      10       9       1
    9      11      10       1
    0       0       0       0

    0       0       0       0
    1.00000     -10.00000        0.00000
    1.00000     -10.00000        0.00000
    1.00000     -10.00000        0.00000
    1.00000     -10.00000        0.00000
    1.00000     -10.00000        0.00000
    1.00000     -10.00000        0.00000
    1.00000     -10.00000        0.00000
    1.00000     -10.00000        0.00000
    1.00000     -10.00000        0.00000
    1.00000     -10.00000        0.00000
    0.00000       0.00000        0.00000
```

FIG. 5.11.   PROTO∅ DATA FILE FOR HEAT FLOW PROBLEM (1 of 2)

```
        0.00000        0.00000        0.00000
  1         0.0000         0.0000        48.0000        0.00000
  2         0.0000         0.0000        48.0000        0.00000
  9         0.0000         0.0000        48.0000        0.00000
 10         0.0000         0.0000        48.0000        0.00000
  0         0.0000         0.0000         0.0000        0.00000
  0         0.0000         0.0000         0.0000        0.00000
  1    1    1    1    1
  1    1    1    1    1
  1    1    0    0    1
  1   10    8   10    4
  0    0    0    0    0
  0    0    0    0    0
  0    0    0    0   10
```
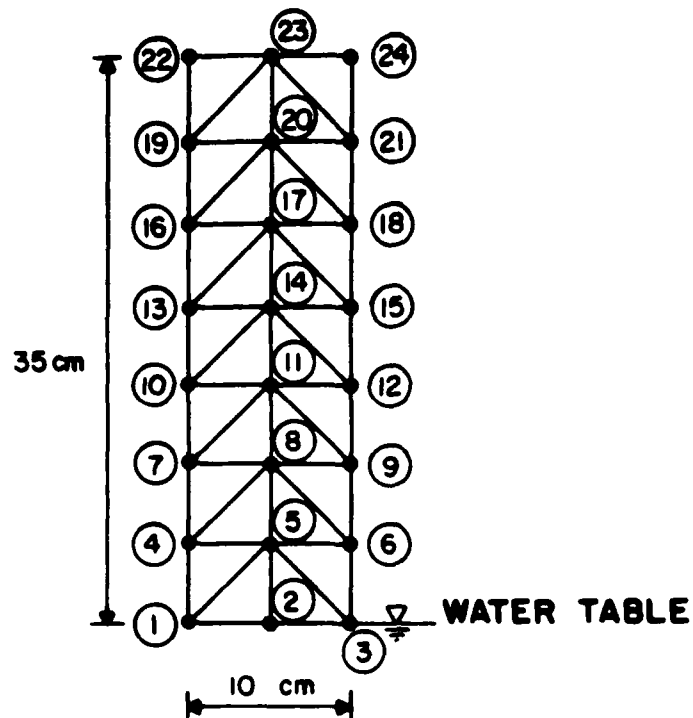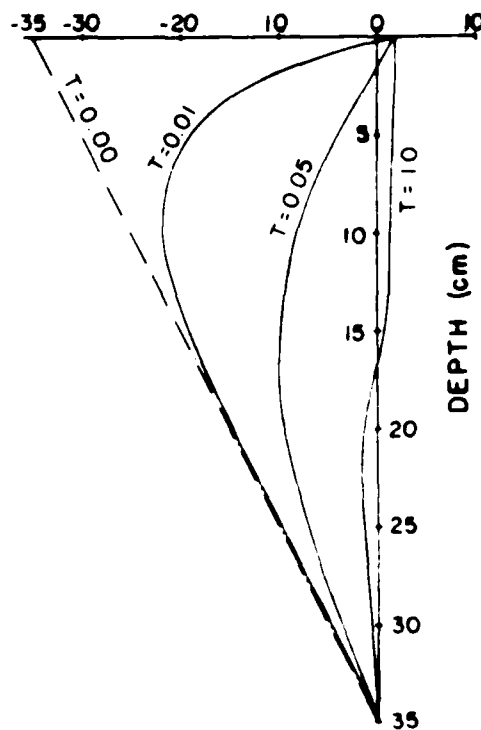
FIG. 5.11.   (2 of 2)

94

FIG. 5.12a SOIL-WATER FLOW EXAMPLE PROBLEM

FIG. 5.12b SOIL-WATER FLOW EXAMPLE PROBLEM SOLUTION

```
1000.000
     0.10000     1   480    60
 2  0  1
     0.00000        1.00000        0.46000        4.80000       19.00000       80.00000
     0     6
 24    28     1     1
0.41600001   0.00000607   1.73600000   0.15000001   0.20000000
0.00000000   0.00000000   0.00000000   0.00000000   0.00000000
0.00000000   0.00000000   0.00000000   0.00000000   0.00000000
5.00000000   0.20000000   0.06250000   2.67400000   0.00000105 12.00000000
0.00000000   0.00000000   0.00000000   0.00000000   0.00000000   0.00000000
0.00000000   0.00000000   0.00000000   0.00000000   0.00000000   0.00000000
       0.00000        0.00000   1.0
       5.00000        0.00000   1.0
      10.00000        0.00000   1.0
       0.00000        5.00000   1.0
       5.00000        5.00000   1.0
      10.00000        5.00000   1.0
       0.00000       10.00000   1.0
       5.00000       10.00000   1.0
      10.00000       10.00000   1.0
       0.00000       15.00000   1.0
       5.00000       15.00000   1.0
      10.00000       15.00000   1.0
       0.00000       20.00000   1.0
       5.00000       20.00000   1.0
      10.00000       20.00000   1.0
       0.00000       25.00000   1.0
       5.00000       25.00000   1.0
      10.00000       25.00000   1.0
       0.00000       30.00000   1.0
       5.00000       30.00000   1.0
      10.00000       30.00000   1.0
       0.00000       35.00000   1.0
       5.00000       35.00000   1.0
      10.00000       35.00000   1.0
       0.00000        0.00000   0.0
       0.00000        0.00000   0.0
      1      5      4      1
      5      4      1      1
      5      2      3      1
      3      6      5      1
      4      5      8      1
      8      7      4      1
      8      5      6      1
      6      9      8      1
      7      8     11      1
     11     10      7      1
     11      8      9      1
      9     12     11      1
     10     11     14      1
```

FIG. 5.13.   PROTOØ DATA FILE FOR SOIL-WATER FLOW PROBLEM
                                                      (1 of 3)

96

14	13	16	1
14	11	12	1
12	15	14	1
13	14	17	1
17	16	13	1
17	14	15	1
15	18	17	1
16	17	20	1
20	19	16	1
20	17	18	1
18	21	20	1
19	20	23	1
23	22	19	1
23	20	21	1
21	24	23	1
0	0	0	0
0	0	0	0

1.00000	0.00000	0.00000
1.00000	0.00000	0.00000
1.00000	0.00000	0.00000
1.00000	-5.00000	0.00000
1.00000	-5.00000	0.00000
1.00000	-5.00000	0.00000
1.00000	-10.00000	0.00000
1.00000	-10.00000	0.00000
1.00000	-10.00000	0.00000
1.00000	-15.00000	0.00000
1.00000	-15.00000	0.00000
1.00000	-15.00000	0.00000
1.00000	-20.00000	0.00000
1.00000	-20.00000	0.00000
1.00000	-20.00000	0.00000
1.00000	-25.00000	0.00000
1.00000	-25.00000	0.00000
1.00000	-25.00000	0.00000
1.00000	-30.00000	0.00000
1.00000	-30.00000	0.00000
1.00000	-30.00000	0.00000
1.00000	-35.00000	0.00000
1.00000	-35.00000	0.00000
1.00000	-35.00000	0.00000
0.00000	0.00000	0.00000
0.00000	0.00000	0.00000

0	0.0000	0.0000	0.0000	0.00000
0	0.0000	0.0000	0.0000	0.00000
1	0.0000	0.0000	48.0000	0.00000
2	0.0000	0.0000	48.0000	0.00000
3	0.0000	0.0000	48.0000	0.00000
22	2.0000	2.0000	48.0000	0.00000
23	2.0000	2.0000	48.0000	0.00000
24	2.0000	2.0000	48.0000	0.00000
0	0.0000	0.0000	0.0000	0.00000

FIG. 5.13. (2 of 3)

```
0        0.0000      0.0000      0.0000      0.00000
1    1    1    1    1
1    1    1    1    1
1    1    0    0    1
1   24   28   24    0
6    0    0    0    0
0    0    0    0    0
0    0    0    0   24
```
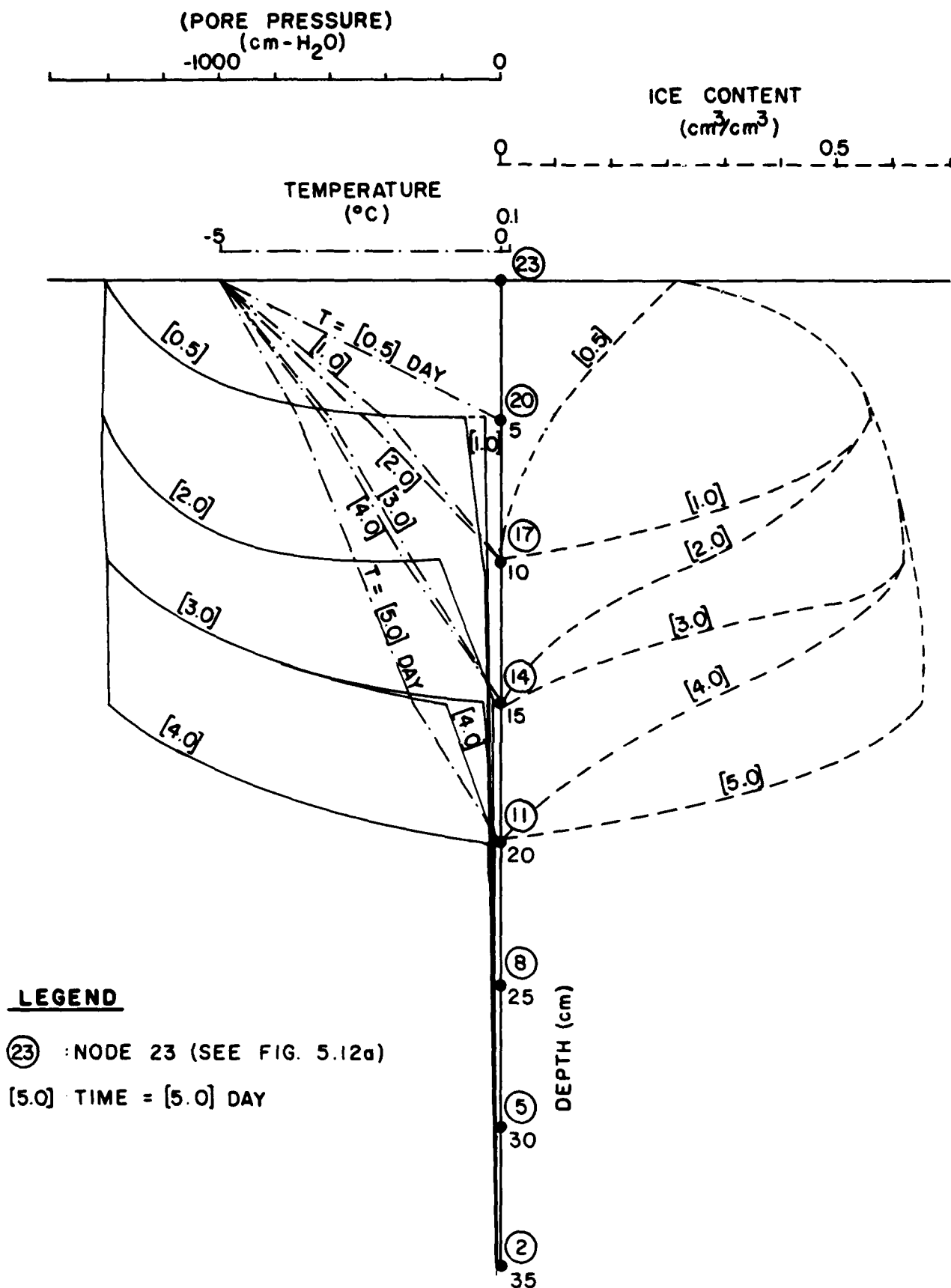
FIG. 5.13. (3 of 3)

FIG. 5.14 PHASE CHANGE PROBLEM SOLUTION

```
1000.000
     0.10000      1   100    10
0   1   1
     0.00000        1.00000       0.46000       4.80000      19.00000     80.00000
     6     3
    24    28     1     1
0.41600001    0.00000607    1.73600000    0.15000001    0.20000000
0.00000000    0.00000000    0.00000000    0.00000000    0.00000000
0.00000000    0.00000000    0.00000000    0.00000000    0.00000000
5.00000000    0.20000000    0.06250000    2.67400000    0.00000105   12.00000000
0.00000000    0.00000000    0.00000000    0.00000000    0.00000000    0.00000000
0.00000000    0.00000000    0.00000000    0.00000000    0.00000000    0.00000000
     0.00000        0.00000    1.0
     5.00000        0.00000    1.0
    10.00000        0.00000    1.0
     0.00000        5.00000    1.0
     5.00000        5.00000    1.0
    10.00000        5.00000    1.0
     0.00000       10.00000    1.0
     5.00000       10.00000    1.0
    10.00000       10.00000    1.0
     0.00000       15.00000    1.0
     5.00000       15.00000    1.0
    10.00000       15.00000    1.0
     0.00000       20.00000    1.0
     5.00000       20.00000    1.0
    10.00000       20.00000    1.0
     0.00000       25.00000    1.0
     5.00000       25.00000    1.0
    10.00000       25.00000    1.0
     0.00000       30.00000    1.0
     5.00000       30.00000    1.0
    10.00000       30.00000    1.0
     0.00000       35.00000    1.0
     5.00000       35.00000    1.0
    10.00000       35.00000    1.0
     0.00000        0.00000    0.0
     0.00000        0.00000    0.0
     1        5        4     1
     5        4        1     1
     5        2        3     1
     3        6        5     1
     4        5        8     1
     8        7        4     1
     8        5        6     1
     6        9        8     1
     7        8       11     1
    11       10        7     1
    11        8        9     1
     9       12       11     1
    10       11       14     1
```

FIG. 5.15.   PROTO0   DATA   FILE   FOR   PHASE   CHANGE   PROBLEM (1 of 3)

```
14    13    16    1
14    11    12    1
12    15    14    1
13    14    17    1
17    16    13    1
17    14    15    1
15    18    17    1
16    17    20    1
20    19    16    1
20    17    18    1
18    21    20    1
19    20    23    1
23    22    19    1
23    20    21    1
21    24    23    1
 0     0     0    0
 0     0     0    0
 0.10000        0.00000       0.00000
 0.10000        0.00000       0.00000
 0.10000        0.00000       0.00000
 0.10000       -5.00000       0.00000
 0.10000       -5.00000       0.00000
 0.10000       -5.00000       0.00000
 0.10000      -10.00000       0.00000
 0.10000      -10.00000       0.00000
 0.10000      -10.00000       0.00000
 0.10000      -15.00000       0.00000
 0.10000      -15.00000       0.00000
 0.10000      -15.00000       0.00000
 0.10000      -20.00000       0.00000
 0.10000      -20.00000       0.00000
 0.10000      -20.00000       0.00000
 0.10000      -25.00000       0.00000
 0.10000      -25.00000       0.00000
 0.10000      -25.00000       0.00000
 0.10000      -30.00000       0.00000
 0.10000      -30.00000       0.00000
 0.10000      -30.00000       0.00000
 0.10000      -35.00000       0.00000
 0.10000      -35.00000       0.00000
 0.10000      -35.00000       0.00000
 0.00000        0.00000       0.00000
 0.00000        0.00000       0.00000
 1     0.1000      0.1000     48.0000     0.00000
 2     0.1000      0.1000     48.0000     0.00000
 3     0.1000      0.1000     48.0000     0.00000
22    -5.0000     -5.0000     48.0000     0.00000
23    -5.0000     -5.0000     48.0000     0.00000
24    -5.0000     -5.0000     48.0000     0.00000
 0     0.0000      0.0000      0.0000     0.00000
 0     0.0000      0.0000      0.0000     0.00000
 1     0.0000      0.0000     48.0000     0.00000
 2     0.0000      0.0000     48.0000     0.00000
 3     0.0000      0.0000     48.0000     0.00000
 0     0.0000      0.0000      0.0000     0.00000
```

FIG. 5.15. (2 of 3)

```
    0           0.0000          0.0000          0.0000          0.00000
    1    1    1    1    1
    1    1    1    1    1
    1    1    0    0    1
    1   24   28   24    6
    3    0    0    0    0
    0    0    0    0    0
    0    0    0    0   24
```

FIG. 5.15. (3 of 3)

APPENDIX A: NDI Model For Radial Coordinates

A.0 INTRODUCTION

In chapter 3 is presented the development of a nodal domain integration (NDI) model of three-dimensional heat conduction based on a tetrahedron finite element. From this numerical model, the finite difference, subdomain integration and Galerkin finite element methods, and an infinity of finite element mass-lumped matrix models are unified into a single numerical statement.

As an extension, the NDI technique is now applied to the radial-coordinate, finite element. It is shown that the Galerkin finite element, subdomain integration, and an integrated finite-difference numerical models are obtained by the appropriate specification of a single parameter in the resulting NDI statement. . Thus, all three numerical approaches are unified into one numerical statement similar in form to a Galerkin finite element matrix system. The extension of the NDI technique to developing unified cylindrical and spherical coordinate models follows from the derived radial coordinate model and the NDI three-dimensional tetrahedron finite element model of chapter 3.

The purpose of this section is three-fold. The first objective is to present a basic description of the NDI technique as applied to the class of partial differential equations generally encountered in the theory of diffusion and heat conduction. Sufficient set definitions and integral manipulations are provided in order that the extensions of the results to cylindrical and spherical coordinate systems are direct. The theoretical foundations of this numerical technique are based on the subdomain version of the finite element weighted residuals approach, and incorporate the mass-lumping techniques used in some finite element approaches. The development closely follows the presentation of Chapters 2 and 3.

103

The second objective is to develop the NDI numerical statement which represents the finite element Galerkin statement, subdomain integration numerical statement, and integrated finite-difference control volume statement, by the specification of a single parameter in the resulting radial element matrix system.

A third objective is to use the unified NDI formulation to gain insight as to the performance of the several well-known domain models in the approximation of radially symmetric heat conduction processes. Since the NDI model represents each of the most popular numerical models as point values of the NDI approximation statement, the same computer code can be used for each numerical analog, as well as an arbitrary finite element mass-lumping scheme.

A.1 NDI MODEL DEVELOPMENT

The partial differential equation describing radially symmetric heat conduction in an isotropic homogeneous medium is given by

$$\frac{\partial}{\partial R}\left[RK\frac{\partial \phi}{\partial R}\right] = RS\frac{\partial \phi}{\partial t} \tag{1}$$

where K is the thermal conductivity; S is the heat capacity; R is the radial coordinate; ϕ is temperature; and t is time.

The finite element technique approximately solves the governing equation on a finite element discretization of the domain (Zienkiewicz, 1977). The integrated finite-difference method uses a control volume discretization (Spalding, 1972).

The nodal domain integration approach partitions a finite element into smaller "nodal domains" which are geometrically defined as the intersection of the finite elements and control volumes. The utility of this further partitioning of the finite element is that an integrated finite-difference or

a subdomain integration analog can be conveniently written in terms of a matrix system similar to the Galerkin finite element matrix system. Additionally, flux type boundary conditions can be accommodated on the problem domain boundary without the need of special equations or finite-difference approximations. The following set definitions of subdomains (control-volumes), finite elements, and nodal domains will be used to develop the NDI finite element matrix system.

Consider the partial differential operator relationship

$$A(\phi) = f; \ (x,y) \ \epsilon \Omega, \ \Omega = \Omega \cup \Gamma \qquad (2)$$

defined on global domain Ω with boundary condition types of Dirichlet or Neumann specified on global boundary Γ. A n-nodal point distribution can be defined in Ω with arbitrary density such that an approximation $\hat{\phi}$ for ϕ is defined in Ω by

$$\hat{\phi} = \sum_{j=1}^{n} N_j(x,y)\phi_j; \ (x,y) \ \epsilon \Omega \qquad (3)$$

where $N_j(x,y)$ are linearly independent global shape functions and ϕ_j are assumed values of the state variable, ϕ, at nodal point j. In (3) it is assumed that except for a set of Lebesque measure zero

$$\lim_{\substack{n \to \infty \\ \max ||(x_j,y_j),(x_k,y_k)|| \to 0}} \hat{\phi} = \lim \hat{\phi} = \phi, \ (x,y) \ \epsilon \Omega \qquad (4)$$

A closed connected spatial subset R_j is defined for each nodal point j such that

$$\Omega = \bigcup_{j=1}^{n} R_j \qquad (5)$$

The sets R_j are generally called control-volumes or subdomains, and usually are accompanied with additional requirements that

$$(x_j, y_j) \in R_j; \ (x_j, y_j) \notin R_k, \ j \neq k \qquad (6)$$

and

$$R_j = R_j \cup B_j \qquad (7)$$

where (x_j, y_j) are the spatial coordinates of node j and B_j is the boundary of R_j. It is assumed that every subdomain is disjoint except along shared boundaries, i.e.

$$R_j \cap R_k = B_j \cap B_k \qquad (8)$$

The subdomain method of the finite element weighted residuals approach approximates (2) by solving the n equations

$$\int_\Omega (A(\phi) - f) \ w_j \ dA = 0, \ j = 1,2,\cdots,n \qquad (9)$$

where

$$w_j = \begin{cases} 1, \ (x,y) \in R_j \\ \\ 0, \ (x,y) \notin R_j \end{cases} \qquad (10)$$

A second cover of Ω is defined by the finite element method with

$$\Omega = \bigcup \Omega^e \qquad (11)$$

where $\bar{\Omega}^e$ is the closure of finite element domain Ω^e and its boundary Γ^e.

106

Let S_e be the set of subscripts defined by

$$S_e \equiv \{j | \Omega^e \cap R_j \neq \{\phi\}\} \qquad (12)$$

that is, S_e is simply the set of nodes associated to Ω^e.

Then a set of nodal domains Ω_j^e is defined for each finite element domain Ω^e by (Fig. A.1)

$$\Omega_j^e = \Omega^e \cap R_j, \quad j \in S_e \qquad (13)$$

The subdomain method of weighted residuals as expressed by (9) can be rewritten in terms of the subdomain cover of Ω by

$$\int_{\Omega} (A(\phi) - f) \, w_j \, dA = \int_{R_j} (A(\phi) - f) \, dA \qquad (14)$$

With respect to the finite element discretization of Ω,

$$\int_{R_j} (A(\phi) - f) \, dA = \int_{R_j \cap \Omega^e} (A(\phi) - f) \, dA \qquad (15)$$

where for each finite element Ω^e a matrix system is given by generating for each nodal point $j \in S_e$

$$\int_{\Omega^e \cap R_j} (A(\phi) - f) \, dA = \int_{\Omega_j^e} (A(\phi) - f) \, dA, \quad j \in S_e \qquad (16)$$

From the above subset definitions and set covers of Ω, application of the usual subdomain method to the governing partial differential operation of (2) is accomplished by an integration of the governing equations over the nodal domains interior of each finite element, resulting in a finite element matrix system similar to that determined by the Galerkin finite element method.

107

A.2 NDI INTEGRATION

In this section, the governing heat flow equation is integrated over the several nodal domains associated to a finite element Ω^e. This approach is simply the subdomain integration weighted residual method as applied to a subdomain or control volume, except that the approximation error is averaged over the nodal domains interior of the subdomain. These nodal domain contributions can then be reassembled into matrix form for each element Ω^e. Using the previous set notation, the operator relationship for the radially-symmetric heat conduction model of (1) is

$$A(\phi) - f = \frac{\partial}{\partial R}\left[RK\,\frac{\partial\phi}{\partial R}\right] - RS\,\frac{\partial\phi}{\partial t} \qquad (17)$$

whereby substituting (17) into (16) gives an element matrix system for Ω^e

$$\left\{\int_{\Omega_j^e}\left(\frac{\partial}{\partial R}\left[RK\,\frac{\partial\phi}{\partial R}\right] - RS\,\frac{\partial\phi}{\partial t}\right)dA\right\} = \{0\}, j \in S_e \qquad (18)$$

Expanding (18),

$$\left\{\int_{\Gamma_j^e \cap \Gamma^e}\left[RK\,\frac{\partial\phi}{\partial n}\right]\Big|_{\Gamma_j^e}ds\right\} + \left\{\int_{\Gamma_j^e-\Gamma_j^e \cap \Gamma^e}\left[RK\,\frac{\partial\phi}{\partial n}\right]\Big|_{\Gamma_j^e}ds\right\}$$

$$= \left\{\int_{\Omega_j^e}RS\,\frac{\partial\phi}{\partial t}\,dA\right\}, j \in S_e \qquad (19)$$

where the first term of (19) cancels due to flux contributions from contiguous finite elements or satisfies Neumann boundary conditions on global boundary Γ; and where (n,s) are normal and tangential vector components on B_j, Γ_j^e, and Γ^e.

108

In order to evaluate the integration expressions of (19), definitions of the finite element and subdomain covers of global domain Ω are necessary. The finite element cover Ω^e of Ω is assumed defined by the

$$\Omega^1 \equiv \{(x,y)\,|\,0 = r_1 \leq R \leq r_2\}$$

$$\Omega^2 \equiv \{(x,y)\,|\,r_2 \leq R \leq r_3\}$$

$$\vdots \tag{20}$$

$$\Omega^{n-1} \equiv \{(x,y)\,|\,r_{n-1} \leq R \leq r_n = L\}$$

where r_i is the radial coordinate of node i; and

$$\Omega \equiv \{(x,y)\,|\,0 \leq R \leq L\}.$$

The subdomain cover R_j of Ω is assumed defined by

$$R_1 \equiv \{(x,y)\,|\,0 = 2r_1 \leq 2R \leq (r_1 + r_2)\}$$

$$R_2 \equiv \{(x,y)\,|\,(r_1 + r_2) \leq 2R \leq (r_2 + r_3)\}$$

$$\vdots \tag{21}$$

$$R_n \equiv \{(x,y)\,|\,(r_{n-1} + r_n) \leq 2R \leq 2L\}$$

Therefore, the nodal domain cover Ω_j^e of finite element Ω^e is defined by

$$\Omega^e = \Omega_e^e \bigcup \Omega_{e+1}^e \tag{22}$$

where (Fig. A.1)

$$\Omega_e^e \equiv \{(x,y)\,|\,r_e \leq R \leq (r_e + r_{e+1})/2\}$$

$$\tag{23}$$

$$\Omega_{e+1}^e \equiv \{(x,y)\,|\,(r_e + r_{e+1})/2 \leq R \leq r_{e+1}\}$$
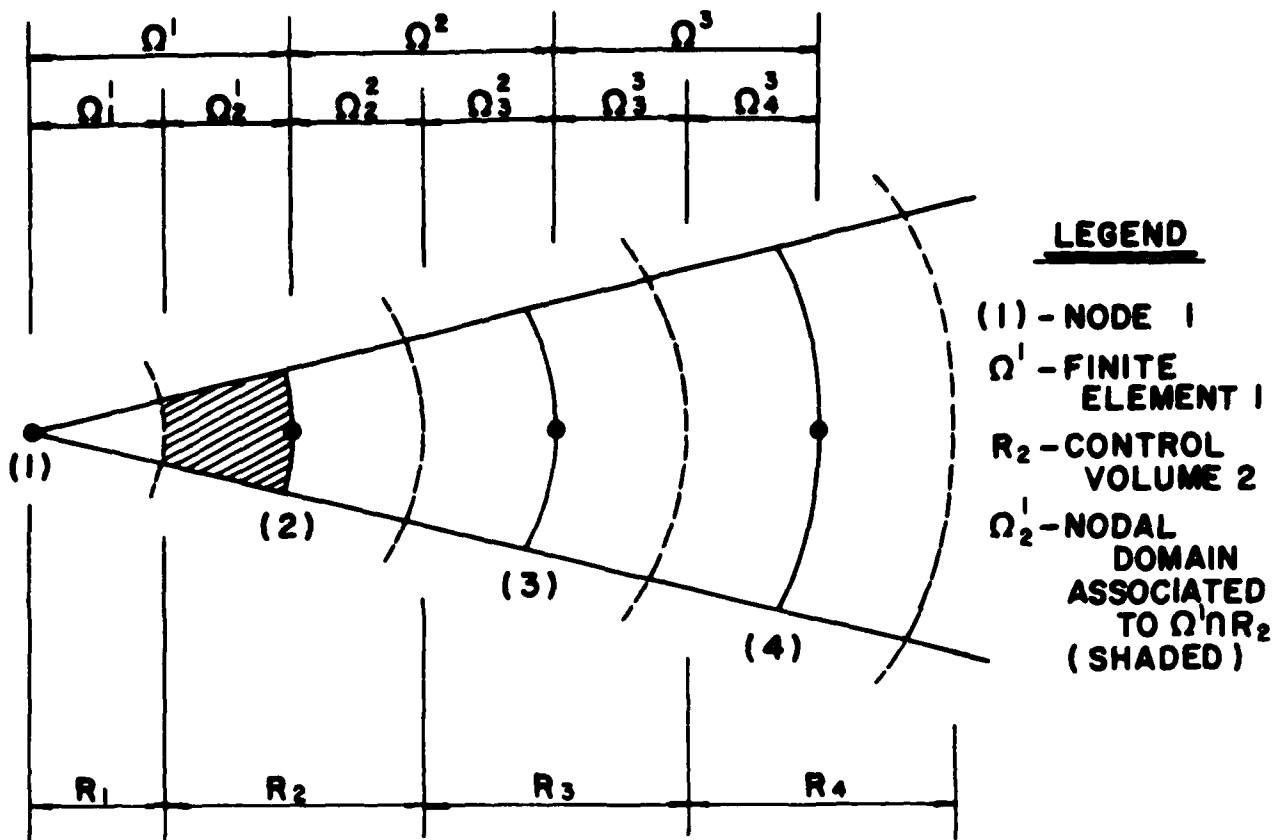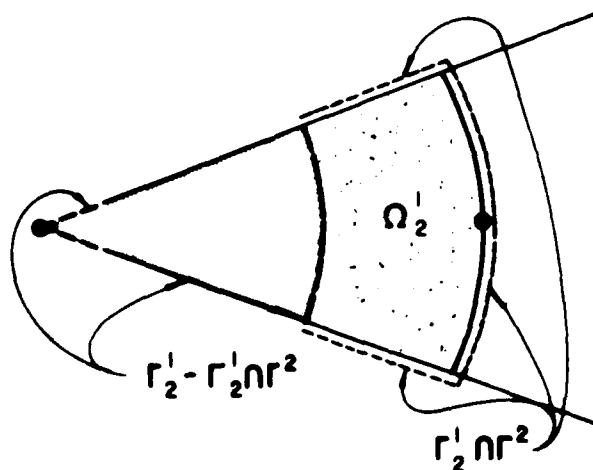
Fig. 1.   Nodal Domain Geometry

Fig. 2.   NDI Boundary Definitions

Integration of the governing flow equation on each Ω_j^e involves the definition and integration of the thermal conductivity, K. An approach to handling the nonlinearity problem is to approximately linearize the governing flow equation by assuming the various parameters to be constant for small timesteps, Δt. For K set to a quasi-constant value K^e in Ω^e during timestep Δt, (19) may be rewritten for the nodal domain Ω_j^e contribution to subdomain R_j

$$\left\{ \int_{\Gamma_j^e - \Gamma_j^e \cap \Gamma^e} \left(RK^e \frac{\partial \phi}{\partial n} \right) \Bigg|_{\Gamma_j^e} ds \right\} = \left\{ \int_{\Omega_j^e} RS \frac{\partial \phi}{\partial t} dA \right\}, \ j \in S_e \qquad (24)$$

Since the governing heat flow equation is radially symmetric, (24) simplifies to (see Fig. A.2)

$$\left\{ \left(RK^e \frac{\partial \phi}{\partial R} \right) \Bigg|_{\Gamma_j^e - \Gamma_j^e \cap \Gamma^e} \right\} = \left\{ \int_{\Omega_j^e} RS \frac{\partial \phi}{\partial t} dR \right\}, \ j \in S_e \qquad (25)$$

This integrated relationship will be used to develop a subdomain integration model in the following section.

A.3 NUMERICAL SOLUTIONS

In the derivation of the finite element integration statement of (25) for Ω^e, no specification of the character of the state variable is assumed. In the following, the state variable ϕ is assumed to be adequately approximated by linear trial function ϕ^e in each finite element Ω^e. Therefore it is assumed that $\phi = \phi^e = \Sigma L_j \phi_j^e$ in each Ω^e where the L_j are the usual linear local coordinates in Ω^e; and ϕ_j^e are nodal point values of the temperature trial function estimate in Ω^e. Due to the linear definition of ϕ^e in Ω^e, all spatial

gradients of ϕ^e are constant. Consequently, several well known domain numerical solutions of (1) in Ω embodied in the finite element method of weighted residuals result in similar numerical approximations of (1) in each Ω^e. To develop these domain numerical solutions, the following description variable is defined:

$$\Phi \equiv \frac{\partial}{\partial R} \left[RK \frac{\partial\phi}{\partial R} \right] - RS \frac{\partial\phi}{\partial t} \qquad (26)$$

Although the Galerkin method of weighted residuals used to solve (1) in each Ω^e is well known, its derivation of a finite element matrix system is presented in order to develop some of the notation and simplifications used in the subsequent determinations of the subdomain integration and integrated finite difference analogs, and to demonstrate the use of flux-type boundary conditions on global boundary Γ.

Galerkin Method of Weighted Residuals

In Ω^e,

$$\int_{\Omega^e} \Phi \, L_j \, dR \equiv 0 \qquad (27)$$

generates a Galerkin finite element matrix system for approximation of (1) on Ω^e.

Integrating by parts reduces (27) to

$$\int_{\Omega^e} \Phi \, L_j \, dR = RK \frac{\partial\phi}{\partial R} L_j \bigg|_{\Gamma^e} - \int_{\Omega^e} \left(RK \frac{\partial\phi}{\partial R} \frac{dL_j}{dR} + SR \frac{\partial\phi}{\partial t} L_j \right) dR \qquad (28)$$

The first term in the expansion of (28) satisfies flux continuity between finite elements and Neumann boundary conditions on global boundary Γ in a manner similar to the NDI statement of (19).

112

For $(\phi, K) \equiv (\phi^e, K^e)$ in Ω^e during a small timestep Δt where ϕ^e is an assumed linear trial function for ϕ in Ω^e, (28) simplifies to the Galerkin finite element statement

$$0 \equiv K^e \frac{\partial \phi^e}{\partial R} \int_{\Omega^e} R \frac{dL_j}{dR} dR + S \frac{\partial}{\partial t} \int_{\Omega^e} R\phi^e L_j \, dR \tag{29}$$

where

$$K^e \frac{\partial \phi^e}{\partial R} \equiv K^e (\phi_{e+1} - \phi_e)/(r_{e+1} - r_e) \tag{30}$$

Integrating (29) determines the Galerkin finite element matrix system for the approximation of (1) on Ω^e

$$\underline{S}^e \, \underline{\phi}^e + \underline{P}^e(2)\dot{\underline{\phi}}^e + \underline{Q}^e(2)\dot{\underline{\phi}}^e \equiv \{0\} \tag{31}$$

where

$$\underline{S}^e \equiv \frac{K^e}{2\ell^e} \left(r_e + r_{e+1} \right) \begin{bmatrix} 1 & -1 \\ -1 & 1 \end{bmatrix} \tag{32}$$

$$\underline{P}^e(2) \equiv \frac{S_e \ell^e}{6} \begin{bmatrix} 2 & 1 \\ 1 & 2 \end{bmatrix} \tag{33}$$

$$\underline{Q}^e(2) \equiv \frac{S(\ell^e)^2}{12} \begin{bmatrix} 1 & 1 \\ 1 & 3 \end{bmatrix} \tag{34}$$

and where $\ell^e \equiv (r_{e+1} - r_e)$; and $(\underline{\phi}^e, \dot{\underline{\phi}}^e)$ are vectors of the nodal values and time derivative of nodal values of finite element e.

113

Subdomain Integration

A cover of finite element Ω^e is given by the union of nodal domains Ω_j^e, $j \in S_e$. The subdomain integration version of the weighted residuals process approximates (1) in each subdomain R_j by

$$\int_{R_j} \phi \, W_j \, dR \equiv 0 \tag{35}$$

where

$$W_j \equiv \begin{cases} 1 \, , \, R \in R_j \\ \\ 0 \, , \, \text{otherwise} \end{cases} \tag{36}$$

But

$$\int_{R_j} \phi \, W_m \, dR = \int_{\Omega_j^j} \phi \, dR + \int_{\Omega_j^{j-1}} \phi \, dR \tag{37}$$

Thus a finite element matrix system is generated by the subdomain integration method for finite element Ω^e by

$$\left\{ \int_{\Omega_j^e} \phi \, dR \right\} \equiv \{0\}, \; j \in S_e \tag{38}$$

From (25),

$$\left\{ \int_{\Omega_j^e} \phi \, dR \right\} = \left\{ \left(RK \frac{\partial \phi}{\partial R} \right) \bigg|_{\Gamma_j^e - \Gamma_j^e \cap \Gamma^e} - \int_{\Omega_j^e} RS \frac{\partial \phi}{\partial t} \, dR \right\} , \; j \in S_e \tag{39}$$

Using $(K,\phi) \equiv (K^e, \phi^e)$

$$\left\{ \int_{\Omega_j^e} \phi \, dR \right\} \equiv \left\{ \left(K^e \frac{\partial \phi^e}{\partial R} \right) R \Bigg|_{\Gamma_j^e - \Gamma_j^e \cap \Gamma_j^e} - S \frac{\partial}{\partial t} \int_{\Omega_j^e} R\phi^e \, dR \right\}, \quad j \in S_e \qquad (40)$$

Integrating (40) gives the finite element statement of a subdomain integration approximation of (1) on finite element Ω^e

$$\underline{S}^e \, \underline{\phi}^e + \underline{P}^e (3) \, \underline{\dot{\phi}}^e + \underline{Q}^e(3)\underline{\dot{\phi}}^e \equiv \{0\} \qquad (41)$$

where $\underline{S}^e$ is given by the Galerkin element matrix of (32), and

$$\underline{P}^e(3) \equiv \frac{S_e \ell^e}{8} \begin{bmatrix} 3 & 1 \\ 1 & 3 \end{bmatrix} \qquad (42)$$

$$\underline{Q}^e(3) \equiv \frac{S(\ell^e)^2}{24} \begin{bmatrix} 2 & 1 \\ 2 & 7 \end{bmatrix} \qquad (43)$$

and where vectors $(\underline{\phi}^e, \underline{\dot{\phi}}^e)$ are as defined previously.

From (40), the global finite element matrix system determined by the appropriate summation of each Ω^e matrix system satisfies Dirichlet and Neumann boundary conditions in a manner similar to the global Galerkin matrix system.

Additionally, the capability of representing an inhomogeneous medium by specifying different parameters in each finite element Ω^e is similar to the usual Galerkin finite element approach, although from (40) the conduction parameters are necessarily evaluated at the midpoint of the finite element and capacitance parameters need to represent a mean value in the control volume associated to the particular nodal point. These advantages normally associated to the Galerkin finite element approach can also be developed for an integrated finite-difference numerical analog for the approximation of (1) on Ω^e.

115

Integrated Finite Difference

The integrated finite-difference approach (Spalding, 1972) can be extended to the solution of (1) on appropriately defined control volumes. The usual control volume definition, however, is identical to the subdomain definition cover R_j of global domain Ω given by (21). Thus, an integrated finite-difference approximation for solution of (1) on Ω^e where the trial function ϕ^e is assumed to be linear in each Ω^e is given by

$$\left\{ \left(K^e \frac{\partial \phi^e}{\partial R} \right) R \Big|_{\Gamma_j^e - \Gamma_j^e \bigcap \Gamma^e} \right\} = \left\{ S \frac{\partial}{\partial t} \int_{\Omega_j^e} R \, \phi^e \, dR \right\}, \ j \in S_e \qquad (44)$$

But the integrated finite-difference approach equates

$$\int_{\Omega_j^e} \phi^e \, dR \equiv \phi_j \int_{\Omega_j^e} dR \qquad (45)$$

Thus, the finite element matrix system is given by

$$S^e \, \phi^e + P^e(\infty) \, \dot{\phi}^e + Q^e(\infty) \, \ddot{\phi}^e \equiv \{0\} \qquad (46)$$

where S^e is once more given by (32); and

$$P^e(\infty) \equiv \frac{S_e \ell^e}{2} \begin{bmatrix} 1 & 0 \\ 0 & 1 \end{bmatrix} \qquad (47)$$

$$Q^e(\infty) \equiv \frac{S(\ell^e)^2}{8} \begin{bmatrix} 1 & 0 \\ 0 & 3 \end{bmatrix} \qquad (48)$$

116

From (40), the global finite element matrix system determined by the appropriate summation of each Ω^e matrix system of (46) satisfies Neumann and Dirichlet boundary conditions in a manner generally associated with the Galerkin approach. Additionally, anisotropic inhomogeneous mediums are similarly accommodated as with a Galerkin or a subdomain integration analog previously derived.

Due to the similarity of the three numerical approximations, a single element matrix system for the approximation of (1) on Ω^e can be written by

$$S^e \, \underline{\phi}^e + P^e(\eta) \, \ddot{\underline{\phi}}^e + Q^e(\eta) \, \dot{\underline{\phi}}^e = \{0\} \tag{49}$$

where $\underline{S}^e$ is given by (32); and

$$\underline{P}^e(\eta) \equiv \frac{S_e \ell^e}{2(\eta+1)} \begin{bmatrix} \eta & 1 \\ 1 & \eta \end{bmatrix} \tag{50}$$

$$\underline{Q}^e(\eta) \equiv \frac{S(\ell^e)^2}{4(2\eta^2-\eta+3)} \begin{bmatrix} (\eta^2 - 2\eta + 3) & 3 \\ (3\eta - 3) & (3\eta^2 - 3\eta + 3) \end{bmatrix} \tag{51}$$

The Galerkin finite element, subdomain integration, and integrated finite-difference numerical analogs of (31), (41), and (46) are given by (49) for $\eta = (2,3,\infty)$ respectively.

Extension of the NDI technique to cylindrical coordinates follows directly from (32), (50) and (51). The extension to spherical coordinates follows from the tetrahedron finite element determination (Hromadka and Guymon, 1983b) and the above results.

A.4 NDI MODEL ANALYSIS

The previous section unified several numerical techniques into a single finite element matrix system as a function of the degree of mass lumping, η. The question remains whether an optimum η factor exists such that the modeling integrated relative error is a minimum.

In this work, the η factor developed for one-dimensional diffusion problems (Hromadka and Guymon, 1983b) is used to test the NDI model accuracy for radial problems where analytical solutions exist. This technique is based on the Fourier series expansion of a particular solution to the one-dimensional diffusion equation in a small homogeneous control volume. That is, the radial geometric contributions are neglected in the development of η.

For a control volume R_j, the usual process of normalization reduces the one-dimensional diffusion equation to

$$\frac{\partial^2 \theta}{\partial x^2} = \frac{\partial \theta}{\partial t} \ , \ x \in [0,1] \tag{52}$$

where θ is a normalized variable for ϕ, and variables x,t are now defined as normalized space and time. It is assumed in (52) that $\theta(x=0) = \theta_{j-1}$, $\theta(x=.5) = \theta_j$, and $\theta(x=1) = \theta_{j+1}$ where θ_k are normalized nodal values.

Using the Crank-Nicolson midtimestep advancement procedure to approximate the time derivative, the nodal equation for solution of θ_j is

$$\frac{\Delta t}{2\|R_j\|} \left[\left(\theta_{j-1}^{i+1} - 2\theta_j^{i+1} + \theta_{j+1}^{i+1} \right) + \left(\theta_{j-1}^{i} - 2\theta_j^{i} + \theta_{j+1}^{i} \right) \right] =$$

$$\frac{\|R_j\|}{2(n_j+1)} \left[\left(\theta_{j-1}^{i+1} - \theta_{j-1}^{i} \right) + 2n_j \left(\theta_j^{i+1} - \theta_j^{i} \right) + \left(\theta_{j+1}^{i+1} - \theta_{j+1}^{i} \right) \right] \tag{53}$$

where the normalized length, $||R_j|| = \frac{1}{2}$; i is the timestep number; and n_j is constant during normalized timestep Δt. Equation (53) evaluates all modeled flux terms at the midtimestep. For other time derivative approximations such as forward or backward step differencing, a similar difference statement can be developed. A solution of (52) using (53) at the midtimestep is

$$\hat{\theta}(x,\epsilon) = -\frac{1}{2}\left(\bar{\theta}_{j-1} - 2\bar{\theta}_j + \bar{\theta}_{j+1}\right) \sin \pi x e^{-\pi^2 \epsilon}$$

$$+ \left(\bar{\theta}_{j+1} + \bar{\theta}_{j-1}\right) x + \bar{\theta}_{j-1} \tag{54}$$

where ϵ is normalized time measured from the midtimestep; and where $\bar{\theta} = \frac{1}{2}\left(\theta_j^i + \theta_j^{i+1}\right)$. If it is assumed that all effects of a moving boundary value at the endpoints is equivalent to holding θ constant at the midtimestep boundary values, then (54) represents an exact solution to the assumed boundary value problem.

Holding the boundary values of $\hat{\theta}$ constant at the midtimestep allows a simplification of the NDI nodal equation to

$$\frac{\Delta t}{||R_j||} \left[\left(\bar{\theta}_{j-1} + \bar{\theta}_{j+1}\right) - \left(\theta_j^i + \theta_j^{i+1}\right) \right] = \frac{||R_j||}{2(n_j+1)} \left[2n_j\left(\theta_j^{i+1} - \theta_j^i\right) \right] \tag{55}$$

Solving for θ_j^i and θ_j^{i+1} gives

$$\theta_j^i = \hat{\theta}\left(\frac{1}{2}, \frac{-\Delta t}{2}\right) = -\frac{1}{2}\left(\bar{\theta}_{j-1} - 2\bar{\theta}_j + \bar{\theta}_{j+1}\right)e^{\pi^2 \Delta t/2}$$

$$+ \frac{1}{2}\left(\bar{\theta}_{j-1} + \bar{\theta}_{j+1}\right) \tag{56a}$$

$$\theta_j^{i+1} = \hat{\theta}\left(\frac{1}{2}, \frac{\Delta t}{2}\right) = -\frac{1}{2}\left(\bar{\theta}_{j-1} - 2\bar{\theta}_j + \bar{\theta}_{j+1}\right)e^{-\pi^2 \Delta t/2} + \frac{1}{2}\left(\bar{\theta}_{j-1} + \bar{\theta}_{j+1}\right) \tag{56b}$$

119

Combining (56a,b) and (55) gives n_j as a function of the model timestep size by

$$n_j(\Delta t) = \left\{ \frac{4\Delta t (1 + e^{-\pi^2 \Delta t})}{1 - e^{-\pi^2 \Delta t} - 4\Delta t(1 + e^{-\pi^2 \Delta t})} \right\} \qquad (57)$$

where the normalized timestep Δt is related to the global model timestep Δt^* by

$$\Delta t = \frac{\Delta t^*}{4D||R_j||^2} \qquad (58)$$

where D is the mean diffusivity ($D = K/S$) for R_j.

From (57), the mass lumping factor lies within the range

$$8/(\pi^2 - 8) \leq n_j(\Delta t) < \infty \qquad (59)$$

and is seen to be a function of timestep and element size.

To test the success of the $n(\Delta t)$ selection technique, several radially symmetric heat transfer (diffusion) problems where analytic solutions are known were modeled. Additionally, the derived n factors of 2,3, and ∞ were also tested for comparison purposes. The measure of accuracy used is a form of the L_2 norm of the error given by

$$E = \left(\int_\Omega (\phi - \hat{\phi})^2 \, d\Omega \right)^{1/2} \bigg/ \int_\Omega d\Omega \qquad (60)$$

where ϕ is the test problem solution; $\hat{\phi}$ is the approximation value; and E is the error of approximation.

In this study, six different boundary value problems of the heat flow equation were tested with various values of the timestep (Crank-Nicolson method) and finite element size. For each test, nodal values are reset to the exact nodal values after each timestep advancement in order to better test the approximation error in satisfying the flow equation rather than measuring the accumulation of approximation error. After each timestep, the E error is evaluated and stored for the four considered η factor approaches, and the factor which resulted in the minimum E value (a success) is noted. Consequently, more than 150 test problems (5 timesteps and 5 element spacings for each boundary value problem) resulted in an excess of 20,000 timestep advancements. By dividing the number of successes by the total number of timestep advancements, a probability of success for a η factor is estimated. Figure 3 shows the success probability for the $\eta(\Delta t)$ approach as a function of normalized timestep size and element size.

A.5 CONCLUSIONS

1. A unifying numerical model can be developed for radially symmetric heat conduction problems. The unifying model is based on the straight forward nodal domain integration method. The resulting model is found to have the capability of representing the Galerkin finite element, subdomain integration, and integrated finite difference methods by the specification of a single mass matrix lumping factor, η.

2. The global matrix system composed of the sum of all NDI elements accommodates Dirichlet, Neumann, and mixed boundary conditions without the need for special finite differencing equations.

3. An infinity of possible domain numerical methods are possible, and can be represented by the NDI model for specific values of η.
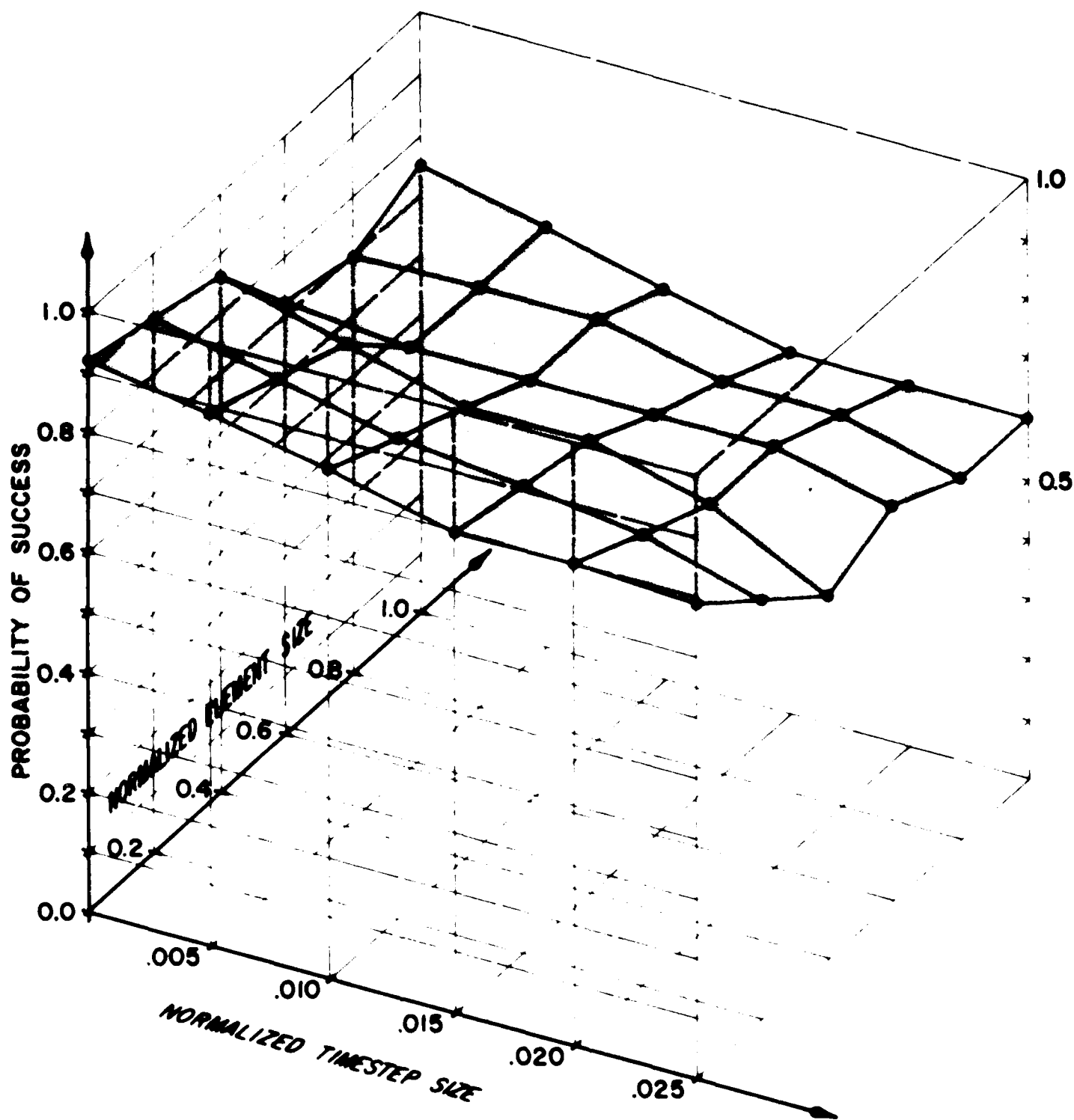
Fig. 3. Probability of Success Using Eq. 57.

122

4. A computer code based on the Galerkin finite element method can easily be modified to allow a variable mass lumped matrix system and, consequently, represent an integrated finite difference, subdomain integration, and an infinity of other domain methods.

5. An improved mass lumping factor exists (as a function of timestep and finite element size) which minimizes approximation error more often than any of the other considered domain methods. The probability of the proposed optimum mass lumping system being the best numerical method is approximately 70 percent for the normalized timestep sizes considered. The improved method is developed based on a linear trial function model and a Crank Nicolson time advancement approximation. Although only the radially symmetric problem is developed the extension of the approach to cylindrical and spherical coordinate problems is straightforward.

REFERENCES

Hromadka II, T. V. and G. L. Guymon, "Mass Lumping Models of Three-Dimensional Heat Conduction," Numerical Heat Transfer, Vol. 6, No. 3, (1983a).

Spalding, D. B., "A Novel Finite-Difference Formulation for Differential Expressions Involving Both First and Second Derivations," Int. Journal Num. Methods in Engg. (4), 551, (1972).

Zienkiewicz, O. C., "The Finite Element Method in Engineering Science," McGraw-Hill, (1977).

Hromadka II, T. V. and G. L. Guymon, "Mass Lumping Models of the Linear Diffusion Equation," Advances in Water Resources, (6), 79-87, (1983b).

END

9-87

DTIC